Influence of the soil structure interaction on the seismic response of monopile offshore wind turbines

C. A. Navarro Riveros

Master of Science Thesis

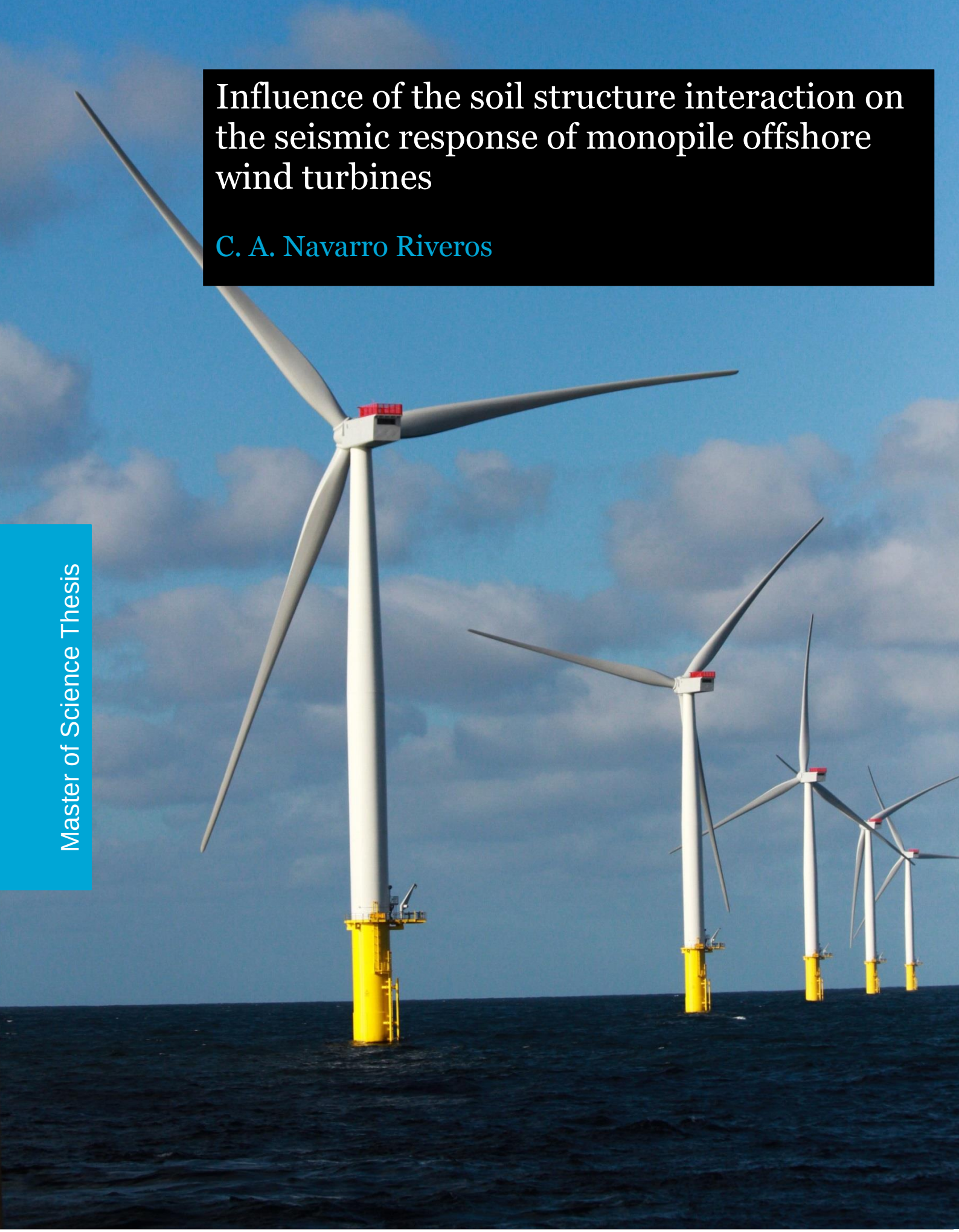

TU Delft Delft University of Technology

SIEMENS Gamesa RENEWABLE ENERGY

Challenge the future

Cover photo: Siemens Gamesa corporate web page. Available at www.siemensgamesa.com

Influence of the soil structure interaction on the seismic response of monopile offshore wind turbines

By

Claudio Andres Navarro Riveros

in partial fulfilment of the requirements for the degree of

Master of Science
in Offshore and Dredging Engineering

at the Delft University of Technology,
to be defended publicly on Wednesday August 29, 2017.

Thesis committee::	Prof. dr. ir A. V. Metrikine	TU Delft
	Dr. ir. A.Tsouvalas	TU Delft
	Dr. ir K. van Dalen	TU Delft
	Ir. W. van der Linde	Siemens Gamesa
	Ir. C. de Winter	Siemens Gamesa

This thesis is part of collaboration between:

TU Delft Delft University of Technology

SIEMENS Gamesa RENEWABLE ENERGY

Preface

This thesis marks the finish line of my studies at TU Delft, following the Bottom Founded Structures track of the Master in Offshore and Dredging Engineering. These two years have been a privilege not only from the intellectual, but also from the personal point of view.

This work represents one step forward in order to fully understand how monopile offshore wind turbines respond to seismic excitation; in particular, what is the influence of considering a frequency dependent soil structure interaction (SSI) in the analysis.

First of all, I would like to thank Dr. Apostolos Tsouvalas, Dr. Karel van Dalen and Prof. Andrei Metrikine for their interest on this project, their guidance on the process, their patience and advice, which definitely, were fundamental to achieve the goal.

I would like to thank Corine de Winter and Wouter van der Linde, for their daily support and guidance at Siemens Gamesa. Additionally I would like to thank Pim Versteijlen for sharing his knowledge with me.

Also I would like to thank the other students at Siemens Gamesa, for sharing ideas, coffee and support when it was needed. Also for the table football games!

Thanks to my parents, my family and my friends, for their endless support!

Thanks to my son Lucas (Luquitas), for being an infinite source of love and motivation. Looking at you growing up every day is the most beautiful gift I received in my life. Finally, and most important, I would like to express my eternal gratitude to my wife Cristina. She is a fundamental part of this accomplished goal, with her daily support, company and love.

Claudio Navarro
Delft, August 2018

Abstract

One of the key aspects of sustainable development is to reduce the greenhouse gas emissions. In order to achieve climate goals, it is expected that wind energy will increase its importance in the electricity production. Offshore wind energy is expected to triple its installed capacity between 2020 and 2025. Several countries have expressed plans to add this kind of energy to their energy matrix. Many of these countries are located in seismic active regions, such as China, Japan and the United States of America (USA).

Given that traditionally this kind of projects have been developed in non-seismic regions, there is a general lack of knowledge about how monopile offshore wind turbines (OWT) respond to seismic excitation. Two main properties of these structures play an important role on it response to seismic loads: 1) the large pile diameter embedded in the soil and 2) the nonlinear behavior during the operational stage.

The analysis of this kind of structures is commonly performed in the time domain, simulating operational and idling conditions. It is known that the soil structure interaction (SSI) is frequency dependent, and therefore, it is not a straightforward task to include this dependency in a time domain analysis. Previous research developed at Siemens Gamesa, performed in the time domain (and therefore neglecting frequency dependency of the SSI), suggests that seismic loads can become design driving.

This work focuses on estimating the influence of the frequency dependent SSI on the seismic response of monopile OWT. The analysis is performed in the frequency domain; therefore only idling states of the turbine is included, and aerodynamic damping is neglected. Furthermore, the structural components of the system (e.g. structural material, soil) are assumed to be linear.

A Beam on Dynamic Winkler Foundation (BDWF) model is developed to determine the seismic response of the structure including the frequency dependent SSI. The monopile and tower are modelled as a Timoshenko beam, and the Rotor Nacelle Assembly (RNA) as a lumped mass (including its rotational inertia) at the tower top. The soil structure interaction is defined by a set of PY curves along the embedded part of the monopile, considering the initial stiffness of the curves, and a dashpot coefficient proportional to the stiffness to include the soil damping.

The seismic excitation is calculated assuming an idealized uniform soil stratum from the mudline to the bedrock. It is assumed that the seismic waves arrive to the bedrock (from the hypocenter or focus) as perfectly vertical. These waves are propagated vertically from the bedrock to the mudline. Secondary waves are assumed to be the most relevant for structural design, since they produce a ground motion (horizontal motions in this case), which is transversal to the direction of propagation. This free field motion interacts with the embedded monopile through soil-structure interaction, which results in seismic loads on the structure.

The seismic response of the structure and the influence of frequency dependent SSI is calculated by considering a proposed Single Node SSI Methodology, which is a form of the Substructure Method Analysis. It consists of three main steps: 1) Estimation of the equivalent seismic lateral force and moment at the mudline, 2) Estimation of the impedances at the mudline level, 3) Solving the coupled problem by model the superstructure founded on the impedances and subjected to the equivalent seismic force and moment at the node located at the mudline. To validate this methodology, the same problem is solved by applying a Full Pile SSI Methodology, in which the solution is obtained at once, omitting the substructure step. As the focus of this study is to determine the influence of SSI, a comparison is made to a model that does not include SSI. For this model, the monopile is clamped at mudline and the lateral free field ground motion (evaluated at the mudline) is applied directly to the structure at mudline.

The responses for the model including and excluding frequency dependent SSI are compared considering relevant seismic design metrics: tower top lateral deformation and acceleration, cross sectional rotation, and bending moments evaluated at the tower top and at the tower midpoint. The results show that the deformations and bending moments are higher when considering the SSI. Additionally, the natural frequencies are compared. As it is expected, when including SSI, these frequencies tend to be lower than for the clamped case.

The obtained results, which are summarized as follows, show the relevance of including the SSI when analyzing the seismic response of monopile OWT:

- Including foundation stiffness leads to a more accurate calculation of the natural frequencies of the structure. For the analyzed case, a decrease in the first natural frequency close to 28% is obtained.
- Since the seismic load strongly depends on the natural frequencies of the structure and the frequency content of the earthquake, the seismic load is more accurately calculated
- The action of the seismic waves through the complete embedded monopile is estimated. This means that even when the seismic motion is perfectly horizontal, a rotational load is produced at the mudline.
- For the analyzed case, when including the SSI the seismic response in terms of deformation, acceleration and bending moments are larger than when the SSI is neglected.

However, this cannot be extrapolated to all the cases, since the results depend on several factors like the soil column properties, the frequency content of the earthquake and the structural properties of the OWT. The recommendation for a real project is, therefore, to consider the soil structure interaction when performing a seismic design. The methodologies described on this work (Single Node SSI Method and Full Pile SSI Method) can be used for this purpose.

Contents

List of tables

List of figures

1. Introduction

This chapter contains the background of this work, starting with an overview of the offshore wind industry and the geographic correlation between the potential project locations and the seismic active regions around the globe. A brief recap of previous research developed at Siemens – Gamesa is included. The motivations behind this work and how the problem and objectives are defined are also included. Finally, the limitations of the work developed, and the outline of the thesis is detailed.

1.1. Energy demand and offshore wind energy

Reducing greenhouse gas emissions and other pollutants is one of the keys aspects to achieve a sustainable development. International Energy Agency (IEA) reported that by 2016, more than 20% of the electricity would be originated from wind in order to achieve climate goals [1]. Additionally, between 2020 and 2025, it is expected that the offshore wind energy would need to triple its capacity to achieve the specific goal of limiting the global warming process to two degrees (°C). Figure 1-1 shows how, since 2011, the offshore wind energy has remarkably increased its installed capacity around the world. Additionally, many countries like Belgium, China, France, Germany, Japan, the Netherlands, the United Kingdom and the United States of America (USA) have informed plans to add offshore wind energy to their energy matrix [1].

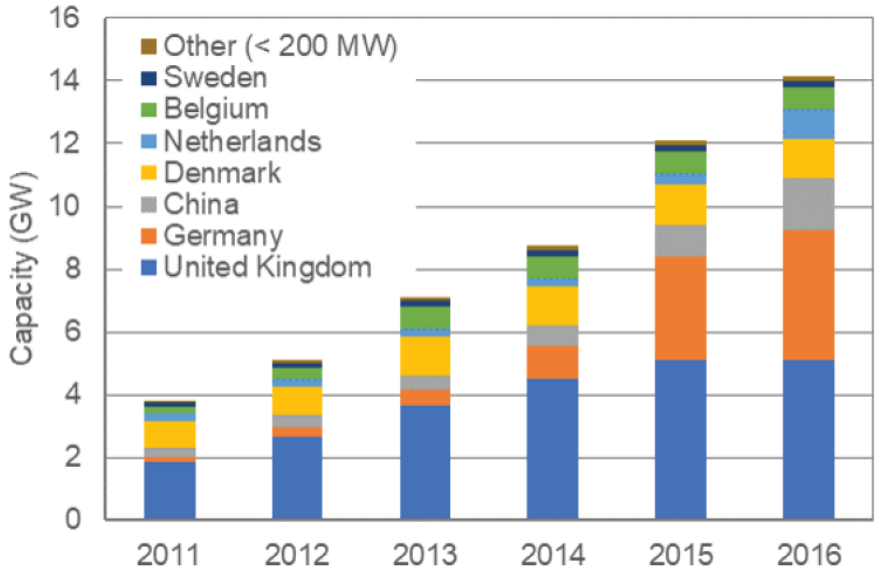

Figure 1-1: Offshore wind installed capacity evolution [1].

Historically, offshore wind energy has been developed in countries with no (or minimum) seismic activity, like in the North Sea. This tendency is changing, and this can be confirmed by checking the list of countries with plans for expanding (or initiate) their offshore wind capacity, China, Japan and the USA are countries with high seismic activity [2]. In the same line, de Risi [3] superposed three maps to visualize the correlation between seismic regions and potential offshore energy locations: first identified the countries which are investing in offshore wind energy, then the areas where subduction activity is relevant, and finally the regions where the seismic hazard is important. The outcome is shown in Figure 1-2.

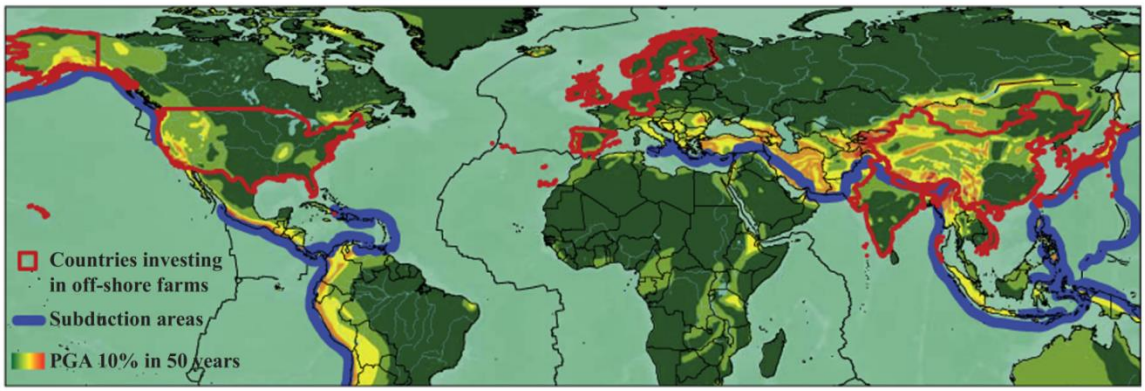

Figure 1-2: Countries investing in offshore wind energy (red), subduction zones (blue) and seismic hazard [3].

The preferred solution for this kind of projects is to consider a monopile embedded into the soil [1], [4]. Due to the specific characteristics of these monopile offshore wind turbines (OWT), it has been concluded that they cannot be seismically analyzed following the same classic procedure as regular structures [5]. These main characteristics are:

a) The large pile diameter and embedded depth originate a special soil structure interaction (SSI) system which interacts with the seismic waves in the soil.
b) The particular operational states of the turbine create non trivial damping conditions.

There have been efforts to model the seismic behavior of monopile OWT; developed both in the academic field and in the industry. The fact that so far there is a limited amount of monopile OWT which have experienced earthquake, causes a lack of empirical data to validate such efforts. This is one of the reasons why it is said that exists a general lack of understanding on the seismic response of OWT [6].

1.2. Research motivation and problem definition

Siemens Gamesa has a clear vision: *"To be the global leader in the renewable energy industry driving the transition towards a sustainable world* [7]*"*. Considering the expected increment of offshore wind energy projects in active seismic regions, especially in the Asian market, the understanding of the behavior of monopile OWT excited by earthquake loads becomes fundamental. The reason is simple: the structures should be projected to properly withstand these loads; therefore a detailed understanding of the behavior is a key aspect to achieve an efficient and competitive design.

The Company uses a powerful in – house code called BHawC (Bonus Horizontal axis wind turbine Code) to perform nonlinear analysis in the time domain. This code has the capability to perform batch simulations including wind, waves, operational and seismic loads. However, as it works in

the time domain, it is not capable to catch the frequency dependency of the soil structure interaction (SSI) in the simulations.

Siemens Gamesa elaborated a detailed roadmap to continuously develop its methodology for seismic design of OWT. In that sense, previous research works related with the seismic design of monopile OWT have been developed. In 2016, Rosales [6] performed a detailed analysis to determine the response of a 4[MW] monopile OWT. For this purpose, BHawC simulations were performed considering different operational states and soil properties. Simulations were performed in the time domain, therefore the dependency on the frequency of the SSI was not considered. Results obtained shows that the seismic load can become a design –driving for the tower.

The challenge of analyzing the seismic response of a monopile OWT considering the frequency dependent SSI represents a non-trivial problem for the engineers. Two aspect of this, which defines the main problem of this research, is related to the frequency dependency itself, and the fact that it influences the seismic load. Seismic waves travel through the soil and when they are close to the pile, they are affected by its presence (mainly because of the difference in the rigidity of the pile and the soil), creating a complex wave field which interact with the pile. This wave field activates the SSI system (pile – soil interaction) originating the seismic load which then excites the structure. In this context, and considering the previous research developed at Siemens Gamesa, this work represents a step forward in order to understand the influence of this frequency dependent SSI in the seismic performance of monopile OWT.

1.3. Goals and limitations of the thesis

The main goal of this work is linked directly to its title, and is to answer the question:

- **What is the influence of the frequency dependent SSI on the seismic response of a monopile OWT?**

To achieve this goal, and based on the problem definition, three main intermediate objectives need to be accomplished:

- Since the seismic excitation is defined in the soil, originated by seismic waves travelling through the soil: What is the influence of the soil on the definition of the load?

- Considering that the seismic load is the product of a wave field interacting with the SSI system between the pile and the soil: What is the influence of the SSI on the definition of the loads?

- Create a methodology to model a monopile OWT which is able to catch the frequency dependent SSI when performing a seismic analysis.

Given the time framework and the complexity of the problem analyzed, this work has some limitations. Since the model has to be able to catch the dependence on the frequency of the SSI, it performs a frequency domain analysis to estimate the response of the structure. This is considered as a limitation because the earthquake can occur when the turbine is operating. In

operation state, it is known that some nonlinearities are originated, which cannot be captured through a frequency domain analysis.

Another limitation is aligned with the type of analysis performed (frequency domain analysis), since only linear properties at different components of the problem analyzed are allowed. This means that non nonlinearities in the structural materials, and especially in the soil, cannot be considered.

1.4. Scope, applicability and approach

Considering the goals and limitations stated before, the scope of this work covers the analysis, in the frequency domain, of the influence of the SSI on the seismic response of a monopile OWT. In this context, the applicability of this work relies in the fact that design codes requires not only seismic – operational analyses, but also analyses in the parked or idling state. If the nonlinearities at these states can be neglected, then the methodology defined in this work is applicable.

The approach to accomplish the intermediate objectives, and therefore to answer the question defining the goal of this thesis, can be summarized in the following points, which are expanded at every section of this document.

- Based on the timeframe and the complexity of the problem, determine a method to model the monopile OWT considering the frequency dependent SSI.
- Once the model is created, validate it by solving a base problem but considering another method.
- Once the model is validated, compare the response of the model including SSI against the responses obtained when the SSI is not considered.

1.5. Thesis outline

The report follows the same structure defined for the approach, which is described as follows:

This **Introduction** chapter aims to give the reader a general overview about the energy problem, and the role offshore wind energy will play in the future years, especially considering the forecasted development in seismic active regions. It also gives an overview of the problem studied, and based on this; it states the goal and intermediate objectives of this work. Additionally the limitations are clearly stated, as well as the scope and the applicability of this work. Finally, the approach considered to accomplish the goal previously defined is included.

The second chapter consists of a **Literature Review and Theoretical Background**. It gives the reader an overview of the design guides and regulations which are commonly used in the industry to perform a seismic design of OWT, including the recommendations related to the definition of the SSI. After that, a recap about the main two approaches about how to model a structure including SSI is described, focusing on embedded pile foundations. Since the focus of this work is on monopile OWT, a state of the art review about how previous research include SSI and how do they perform seismic analysis (for these structures) is included. Also a review about how to model the pile foundation (not only for monopile OWT) response against seismic excitations is included. After the literature review, a theoretical review of the main techniques considered on this work is included.

The third chapter contains the **Problem Definition**, in which the aspects and mechanism governing the seismic excitation on a monopile OWT are described.

Based on the concepts and models described in chapter two, and given the problem described in chapter three, chapter four contains the **Methodology** proposed to accomplish the goal: a Single Node SSI Method (based on the substructure method analysis) to estimate the seismic response of a monopile OWT including frequency dependent SSI is described. Additionally, another approach to solve the same problem is included: the Full Pile SSI Method. This approach is used afterwards to validate the Single Node SSI Method. As the interest is on comparing the response of a monopile OWT when considering / neglecting SSI, a model to perform a classis seismic analysis is detailed, which neglects the influence of the SSI.

Chapter five contains the **Analysis and Discussion**, and it consists in two parts. The first contains the estimation of the seismic response of a monopile OWT considering the Single Node SSI Method and the Full Pile SSI Method. A control point is defined at the tower top, and the results are compared. Since they are equivalent, the Single Node SSI Method is validated. The second part contains a comparison between the case when including SSI and when it is neglected. The responses are compared in terms of lateral deformations and accelerations, and bending moments along the structure. Also the shift in the natural frequencies is estimated using the Peak Picking Method. The influence of including the SSI is evaluated qualitatively in the frequency domain.

Finally, chapter six contains a set of **Conclusions and Further Research**, which are obtained based on the investigation performed and the results obtained.

2. Literature review and theoretical background

This chapter starts with a literature review. An overview of the different seismic resistant design guidelines for wind turbine projects is included. Secondly, a review of the soil structure interaction (SSI) problem is described, focusing on the main two approaches to solve it: the direct and the substructure approach. Then the pile – soil interaction problem is studied, identifying the approaches to solve it, and the one selected to develop this work. After that, an overview of the recent research on seismic analysis and how to consider SSI for monopile OWT is presented. Then some features of the pile-soil interaction model considered are detailed, including an overview of the seismic wave propagation theory. Finally, the state space representation technique is explained.

2.1. Regulations and design codes

There is an important difference on the amount of detailed seismic resistant design guidelines for regular buildings and for wind turbines. Specific design code for regular buildings at the region where a given project is being developed is common. Daniell [8] reviewed many of the over 160 design codes (or a form of it) around the world. He concluded that the quality, extent of application and methodologies differ importantly. Analyze these guidelines is out of the scope of this work, however, the interested reader can find more information in the literature [8], [9]. For the seismic design of wind turbine (onshore or offshore) the situation is completely different, since only a few seismic design codes are available around the world. According to the literature reviewed, the most relevant are:

- Guidelines for Design of Wind Turbines by Det Norske Veritas and Risø National laboratory [5].
- Guideline for the Certification of Wind Turbines by Germanischer Lloyd (GL) [10].
- International Electrotechnical Commission's IEC 61400-1: Wind turbines - Part 1: Design requirements [11]

Each of them has their own characteristics and considerations, which are covered in the following sections.

2.1.1. DNV/Risø guidelines

The objective of this design guideline is to provide an introduction to the most important topics in wind turbine engineering [5]. According to this, the suggestions regarding seismic design is general. The code prescribes that the seismic effects should be considered for OWT installed in

zones which are considered as active (based on previous earthquake activity registered). When there is not enough information to characterize the seismicity, it recommends the evaluation of the regional and local geology and a seismic hazard study.

Regarding the load combinations, it is not clear about how to combine the different loads (wind, waves, earthquake, among others). However it is prescribed that the structure should be designed to withstand the seismic loads at any event. Therefore it is implicit that the loads combinations should at least include: a) earthquake loads and operational wind loads, b) earthquake loads and emergency stop loads and c) earthquake loads occurring in an idling state [8].

The analysis can be performed as time domain simulations or considering a response spectrum analysis. It only provides brief suggestions for the response spectrum analysis. In particular, it recommends the use of a single degree of freedom (SDOF) system to obtain the seismic load. The model should consider a lumped mass at the tower top (including the RNA and one fourth of the tower mass). It is prescribed that the fundamental period of vibration of this SDOF system should be used together with a design acceleration response spectrum to determine the loads. It recommends considering both the horizontal and the vertical directions of analysis [5].

No explicit recommendations are given for the damping ratio to be considered. In many cases, engineers consider the standard design spectrum described in the International Building Code [12]. It has to be clear that the 5% damping ratio which is implicit in this standard design spectrum, is appropriate for the case when the turbine is operating (and for the fore aft direction). However it overestimates considerably the damping for the idling state or for the side-side direction of analysis.

Regarding the structural model, it recommends to pay attention to include an accurate model of the supporting soil structure interaction (SSI). For this purpose, it recommends the use of nonlinear and frequency dependent models, and it allows the use of appropriate linearize models (depending of course, on the strain level of the soil) [8].

2.1.2. GL guideline

The objective of this guideline is to set the requirements for the certification of wind turbine projects. For this reason, it is more detailed about the information provided for seismic design.

As well as DNV/GL, it prescribes that seismic analysis should be performed for projects located in seismically active regions. A design earthquake event of 475 years return period should be considered. To define the seismic load, it recommends the use of the local seismic resistant design guidelines, and if it is not available, it suggests to consider or Eurocode 8 [13] or American Petroleum Institute (API) guidelines [14].

It prescribes a set of loads combinations, which are included in the so called extended design considerations. It recommends that the seismic loads should be combined with a normal wind load both in the operational and in the idling state. Also suggests considering the activation of the emergency shutdown activated by the earthquake.

Regarding the methods of analysis, it allows both, a fully coupled or a decoupled analysis, with the restriction of considering at least three (most important) modes of vibration in both cases. Regarding the time domain simulations, at least six simulations per load case should be

considered. As well as DNV/GL, no guidelines about the damping is given, therefore caution should be taken about how much damping needs to be considered for a given scenario (regarding operational/idling state and fore-aft/side-side direction of analysis).

Regarding the structural model, as it prescribes at least three modes of vibration, it is implicit that the model should be a multi degree of freedom (MDOF) system. Interesting is the fact that it assumes a linear elastic behavior, and the fact that it allows a ductile response (inclusion of a q factor according to Eurocode 8 [13]) if the support structure has appropriate static redundancy. If ductile behavior is considered, then it demands the inspection of the structure after the occurrence of a seismic event.

2.1.3. IEC standards

The objective of this code is to ensure the structural integrity of the OWT. For seismically active regions, it recommends to perform a seismic analysis. If the local seismic resistant design guidelines exclude the particular region, then it is not required to perform the seismic assessment. A design earthquake event of 475 years return period should be considered and taking into account a ground motion or a response spectrum according to the local seismic resistant design guidelines.

Regarding the load combinations, it recommends to combine the seismic load with other frequent operational loads. In particular it prescribes to combine with the higher of the following operational loads: a) loads during normal power production, and b) Loads during emergency shutdown, for a wind speed defined so that the loads level before the shutdown is equal to the case described in a). However, no explicit recommendation is given for the earthquake loads exciting the structure for the idling state.

Fully coupled or decoupled analyses are allowed. For time domain analyses, the number of simulations has to be enough to ensure that the operational load is statistically illustrative. Regarding the modes of vibration to include, it allows to consider the recommendation of a recognized design code. Otherwise, it allows considering consecutive modes with a total modal mass equal to the 85% of the total mass of the structure.

Regarding the model, it is implicit that a MDOF system shall be considered (which is able to consider to at least 85% of the total mass of the structure). In general, it recommends assuming a linear elastic response. The seismic load should be estimated by considering a concentrated mass (equal to the RNA plus the half of the mass of the tower) at the tower top, under the acceleration described in the local design code response design spectrum considering a 1% damping, for the first tower bending natural frequency. The code is aware that considering only the first natural frequency to define the seismic load is a non-conservative approach. It is said that is compensated by including the half of mass of the tower as a point mass at the tower top.

2.1.1. JSCE

It was not possible for the author to get access to the English version of this guideline; however, Rosales [6] listed many of its interesting recommendations, which are listed as follows:

- Analysis has to be performed in the time domain, to ensure that high order modes are taken into account.

- Requires the structure to be analyzed for both cases: operational and non-operational states. This is achieved by combining the seismic load to the corresponding wind velocity load case.
- To take into account the interaction with the soil, it is recommended to perform the time history analysis based on a rocking-swaying motion model. This means that the structure is supported by swaying / rocking springs and dashpots.
- Different target response spectra are defined depending on the nature of the seismic solicitation considered. Two levels are described:
    - Level 1: for an earthquake event of 50 years return period, defines a target response spectrum of 0.16g.
    - Level 2: for an earthquake event of 500 years return period, defines a target response spectrum of 0.32g.
- Vertical seismic load need to be considered.
- Since the analysis has to be performed in the time domain, it is allowed the use of an artificial motion matching the corresponding target response spectrum, or the use of observed motions with frequency content adequate to match the corresponding target response spectrum.

2.1.2. Remarks

It is clear that different guidelines have different objectives and requirements. It is responsibility of the engineer to apply them correctly. The following points are considered as important in this aspect:

- When no guidance for damping, strong caution should be taken since commonly, an acceleration design spectrum is computed for 5% damping ratio. It has to be clear that the damping in the side-side vibration is generally in the range of 0.5% to 1% [15], and that the damping in the fore-aft vibration can reach values of 5% or more during operation, due to aerodynamic effects [15].
- Elastic behavior assumption is the common recommendation.
- MDOF systems which are able to consider an important percentage of the total mass of the structure are recommended.
- Fully coupled and uncoupled analyses are, in general, accepted. For time domain analysis, it is recommended to run several simulations, and for response spectrum analysis, it is recommended to select adequately the damping, consider elastic behavior, and to be aligned with the local seismic design guidelines.
- It was found that in many cases it is not required to include accurate SSI. Only two of the guidelines reviewed (DNV/GL and JSCE) are explicit in this point, giving recommendations on how to include this feature to the model.

2.2. Soil structure interaction

2.2.1. General

The goal of an analysis which includes the SSI is to determine the response of the structure when the interaction with the surrounding soil is taken into account. For a seismic analysis, the excitation is introduced to the structure through the soil, and because of this, the behavior of the structure cannot be analyzed without considering the seismic wave propagation into the soil. When the seismic wave reaches the structure, a part of the energy is transferred to the structure,

and another part is scattered away [16]. The part that is transferred to the structure can re-enter into the soil or be dissipated through the damping mechanism of the structure.

One of the most important tasks of a foundation is to transmit dynamic loads (wind, earthquake or machinery loads) from the structure to the soil and vice versa. In general, there are two main approaches to solve dynamic SSI problems [17]: the "Direct method analysis" and the "Substructure method analysis".

2.2.2. Approaches to SSI

2.2.2.1. Direct method analysis

The direct method analysis requires both the soil and the structure to be modelled (in the time domain and considering a 2D or 3D approach) using an adequate method (a finite element method, or a finite differences method). This combined modeling allows introducing inelastic behavior at any component of the model (structure and/or soil). Usually the model is solved using a numerical integration (step by step) algorithm. However, even when the model can be meticulously detailed, it is necessary to prescribe the ground motion (commonly at the base of the model), where it is unknown [8].

The main benefit is at the same time a drawback because including the structure and the soil in the model is very time demanding and not well suited for design, especially in 3D [18]. However, it has the main advantage of being able to capture non-linear effects [17]. A simple visualization of this method is shown in Figure 2-1, where the structure, the soil and the interface are modelled. The seismic input is prescribed at the bottom as waves. The larger the soil domain modelled, the more accurate results are expected [17].

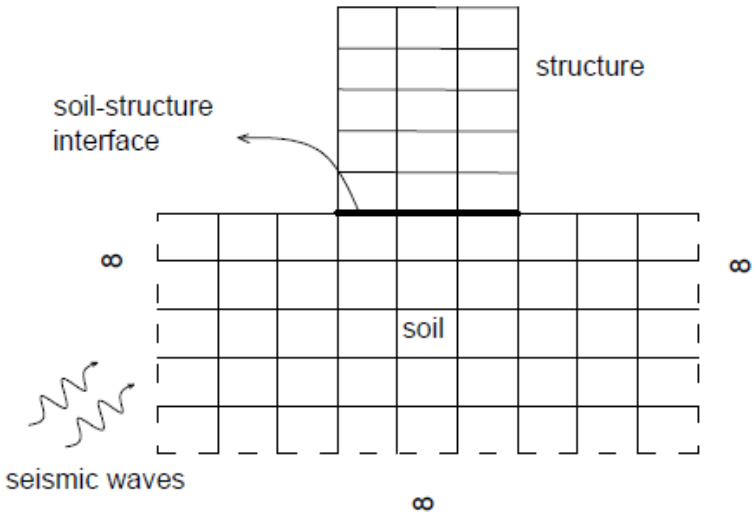

Figure 2-1: Visualization o the SSI direct method [17].

2.2.2.2. Substructure method analysis

Another approach can be considered to incorporate the influence of the SSI in the response of the structure. In the substructure method analysis, the full coupled system is represented as a set of two separate systems, joined at a common interface (soil-structure), by imposing two conditions at all times [17]:

- Force equilibrium and,
- Kinematic compatibility.

It is known that the substructure method analysis is not able to catch non-linear responses, but it has the capability of being much faster than the direct approach. Another benefit of this method is to allow a more clear separation of the role of the geotechnical engineer from the role of the structural engineer [18].

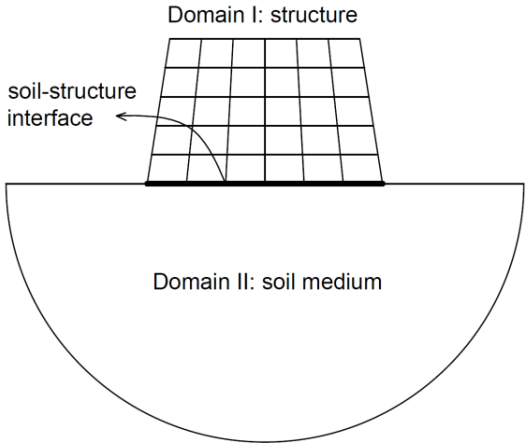

Figure 2-2: Visualization of the substructure method analysis [17].

Several approaches can be developed considering the substructure method of analysis when accomplishing the conditions described. Based on the superposition theorem and on the substructure method analysis, Kausel [16] proposed an approach to analyze the SSI of nuclear energy facilities. These structures are usually robust and projected with thick reinforced concrete walls. The approach postulates that when the foundation – structure system can be considered to be rigid, then the solution can be obtained by performing the three steps visualized in Figure 2-3.

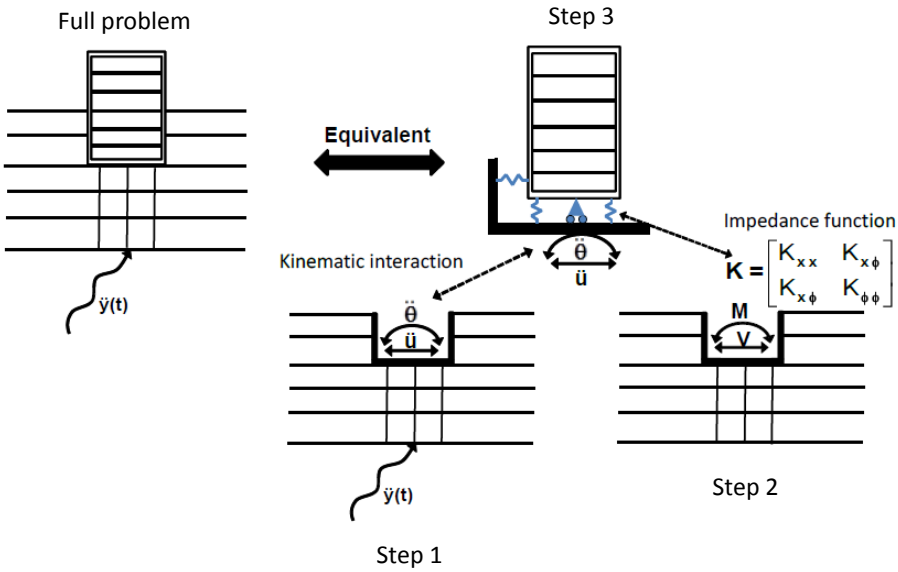

Figure 2-3: Three steps approach to solve SSI problems [18].

The full problem consists on a structure which is connected to the ground considering an embedded foundation, and each of the three steps states:

- Step one: Calculate the kinematic interaction motion at the pile head, as the response to base acceleration of a system which differs from the original by assuming the mass of the superstructure as zero. For a pile foundation, this step yields, in general, translations and rotations at the pile head.
- Step two: Calculate the frequency dependent dynamic impedances matrix at the pile head level. This matrix is composed of a real (stiffness related) component and an imaginary (damping related) component.
- Step three: Calculate the dynamic response of the real structure being supported on the frequency dependent dynamic impedances calculated in b) and excited, at the base, by the kinematic interaction motion calculated in a), and including the mass of the embedded pile.

Note that the only approximation involved in this approach is related to the deformability of the structural foundation. If it can be assumed as rigid, then the solution found would be identical to that of the direct method analysis [16]. This approximation can be realistic for robust structures (reinforce concrete nuclear facilities for instance), but not entirely correct for a monopile OWT. Detailed explanation about this approach are out of the scope of this work, however, interested reader can find more information in the literature [16], [18], [19], [20].

The focus in the next sections is on the state of the art of the specific problem analyzed in this work: the SSI for piled foundation structures, and the particular application to wind turbines projects.

2.3. Pile soil interaction

This work focuses on the SSI of laterally loaded monopile OWT, specifically in the pile soil interaction against seismic loads.

As an introduction, let us think on the response of a pile embedded in a soil stratum and being excited by seismic waves travelling through the soil. If the situation is idealized, and focus on the response to incident vertical shear waves only, one will realize that this response depends on several factors, but maybe the most important is the flexural rigidity of the pile in relation to the stiffness of the surrounding soil [8]. The incoming wave field is modified due to the presence of the pile, and therefore the displacement at the pile head (that can be considered at the surface level) is different from that of the free field (measured at the surface level). Additionally, a rotation at the pile head is induced. The displacement at the pile head depends on the ratio of the pile modulus to soil modulus, the slenderness o the pile and the frequency of the excitation. Commonly, the high frequency components of the excitation are filtered out, in special for relative short and rigid piles [21].

This is one of the aspects the pile – soil interaction has to solve. Over the past few decades, various analytical methods (approaches) have been developed in order to predict the response of a pile-soil system subjected to a dynamic load. The majority of these methods are based on the idealization of the soil behavior. These methods propose models that can vary in terms of complexity and features, which can be classified in main four groups [17]:

a) Beam-on-Dynamic-Winkler-Foundation (BDWF) or Kelvin – Voigt model [22].
b) Analytical (or semi analytical) models.
c) Finite elements or Finite Elements/Boundary Elements formulations.

d) Analytical or semi-analytical for dynamic impedance matrix at the level of the pile-head.

The following sections focus on a) and b). Regarding the other approaches, d) is commonly used for early stages of design [23], [17], and c) is maybe the most popular tool used for engineers to analyze this topic.

2.3.1. Beam-on-Dynamic-Winkler-Foundation model

The idea is to model the soil as a series of discretized springs and dashpots, where the stiffness of each of the springs defines the soil strength, and the dashpots define the soil damping. At the same time, the pile is modeled as a flexible beam. The base of this model is on the idea proposed by Winkler [24]: the lateral resistance is directly proportional to the ground deformation. By the inclusion of the dashpot, the dynamic response of the soil-pile interaction can be calculated over the frequencies [25]. It is well known that the soil usually experiments non-linear deformations. To include this effect, one way is to divide the soil media in two regions i.e., a near field and a far field element. The idea is that the near field elements reproduce the nonlinearities of the soil, and that the far field elements represents govern the elastic behavior [26]. These two elements can be used to take into account another two phenomena occurring in the pile – soil interaction: the soil-pile gapping and soil slippage.

An improved version of this approach is the denominated “p-y” method. Here the pile is again modeled as a beam element, and the surrounding soil is modeled as springs. The soil resistance is defined by “p”, and the pile deflection is defined as “y”, originating the so called “p-y” curves. Nonlinearities of the soil can be introduced con considering inelastic p-y curves, which can be obtained from a hysteretic curve [27]. Some other important parameters like the 3D soil-pile interaction, soil continuity, the degradation of stiffness, cyclic strength, soil gapping and slippage are taken into account with the introduction of the strain wedge method proposed by Ashour and Norris [28]. Details about this method are out of the scope of this work; however, the interested reader can find more information in the literature [28], [29]. A visualization of this model, including dashpots, is shown in Figure 2-4.

The soil dissipates energy (material and geometrical damping) when it is subjected to a dynamic load, therefore the model can be improved by the introduction of dashpots in addition to springs, as it is shown in Figure 2-4. When including the damping, the model is called Beam-on-Dynamic-Winkler-Foundation (BDWF) model [22].

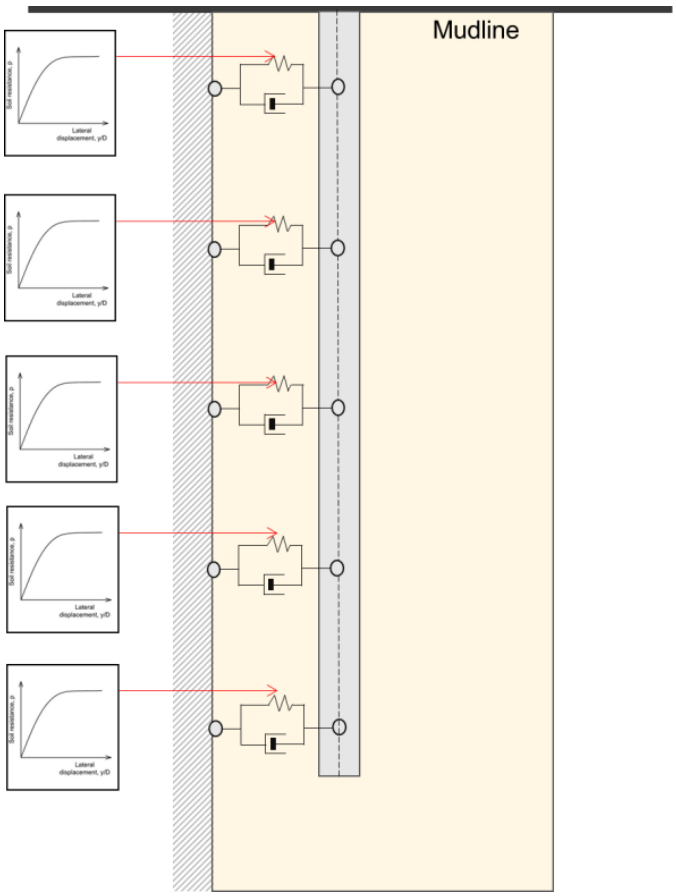

Figure 2-4: Beam supported by non-linear distributed springs (derived on the basis of P-Y curves) and dashpots.

2.3.2. Analytical (semi analytical) models

The idea of this approach is to analyze the response of a pile embedded in the soil by assuming the soil as a (homogenous) elastic or viscoelastic continuum [30], [17]. This feature overtakes the original restriction of the beam on foundation approach, meaning that the soil deformation can be analyzed not only immediately next to the loaded zone, but also within some limited regions outside the loaded zone. In order to take into account the continuous behavior, commonly the soil is idealized as a 3D continuous solid, represented as a half space. However, it has limitations, since is difficult to determine accurate soil properties for the half space, and the fact that the application of the continuum theory [30] of classical elasticity to SSI situations leads to a non-trivial and complicated mathematical problem.

In 2009, Basu [31] proposed a procedure to calculate the response of a pile embedded in a layered elastic soil and excited by a horizontal force and a moment at the pile head. The energy principle was considered to determine the differential equations governing the soil displacements and the pile deflections. A set of equations governing the pile deflection were obtained, and the results were comparable against a 3D finite elements model simulation.

Another way is to model the soil and the pile as continua, to then apply a model decomposition method to represent the soil reaction. By doing this, it is possible to obtain complex dynamic stiffness at the pile head or along the pile surface. The soil reaction depends on the modes of the structure, the excitation frequency and on the modes of the soil. Tsouvalas and Metrikine [32] presented an analytical derivation for a layered soil of finite depth [17].

2.4. Pile soil interaction in wind turbines

The focus of this work is on the seismic response of monopile OWT. This section covers previous research on this topic, starting with the analysis for onshore/shallow founded structures, to then review projects in the offshore environment, which considers a piled foundation.

In 2002, Bazeos [33] studied the seismic response of an (relatively small) onshore prototype wind turbine steel tower. The structure considered was a shallow foundation (not an embedded pile), and he introduced the SSI by considering a set of discrete springs and dashpots at the soil – foundation interface. The soil was a representative semi rock soil. Under this scenario, it was concluded that the SSI has a strong influence on the modes of vibration (shift to lower eigenfrequencies), in spite of the relatively stiff soil conditions considered. Additionally, it was concluded that the seismic loads produced low level of stresses in the structure compared to the design driving case: the aerodynamic loads under survival conditions [33].

In 2012, Hongwang [34] studied the seismic performance of lager (1.65[MW] and 3.0[MW]) onshore, shallow foundation, wind turbine. The structure considered a lumped mass at the tower top to model the RNA. He introduced the SSI by considering a set of discrete springs and dashpots at the soil – foundation interface, based on assumed soil properties. The seismic load considered included six historical earthquake records. It was concluded that the SSI was to show a 7% decrease in the first natural frequency, an approximately 10% decrease at the tower top horizontal acceleration, an approximately 10% decrease at the tower base horizontal moment and an approximately 5% decrease at the tower base shear load. In average, the inclusion of SSI was beneficial for the scenarios analyzed [34].

In the offshore environment, in 2015, Sapountzakis [35] analyzed the nonlinear response of a 5[MW] monopile OWT under wind and seismic excitation including SSI. A beam formulation based on the boundary element method (BEM) was implemented. The SSI considered was a set of frequency independent springs and dashpots based on the work performed by Kampitsis [36]. From the scenario analyzed, it was concluded that the influence of the SSI is of great importance, since it leads to a more flexible structure, and a smaller values of stresses along the structure [35].

Later, in 2018, Alamo [37] studied the SSI effects on the dynamic properties of monopile OWT. To do so, he analyzed a three DOF sub structured model based on modal parameters, meaning that he considered the complete superstructure as a point mass using its fundamental modal mass and height, whereas the pile-soil dynamic stiffness was considered by the corresponding impedance functions. The impedances functions were obtained considering a model developed by the same author based on the integral formulation of the elastic problem and the use of Green's functions for the soil medium [38]. He found that when including the SSI, variations in the fundamental frequency close to 15% can be obtained (more flexible). Additionally, he concluded that the superficial layers of the soil play an important role in the estimation of the natural frequencies and the damping of the structure.

In 2018, De Risi [3] investigated the seismic performance of monopile OWT using non-scaled natural earthquake records. Various types of earthquakes were considered (crustal, inslab and interface). The structure was modeled using the finite elements method. The SSI is captured through impedance functions which are frequency independent. Regarding the seismic load, he neglected the influence of the pile-soil interaction in the definition of the seismic motion exciting the structure (since the passage of the seismic waves through the surrounding soil close to the

pile creates curvatures along the pile, and therefore an additional 'kinematic' bending moment). The reason to because this influence is that the embedded portion of the pile is short and it was studied that for aspect ratios less than 5, this kinematic contribution can be neglected [39]. The results show that monopile OWT are vulnerable to extreme crustal and interface earthquakes, especially when the she structure is founded on soft soils deposits.

In 2018, Zuo [40] evaluated the dynamic operational (and in parked condition) response of a monopile OWT including SSI. The structure was excited to a combined wind and waves loading configuration, the blades were explicitly modelled, and the model was created using the finite elements code ABAQUS. The structure analyzed was a 5[MW] OWT; the SSI undrained clay) was introduced as a set of nonlinear springs using p-y curves from literature [14].The results shows that the eigenfrequencies of the structure are considerably decreased when SSI is taken into account. Additionally, it was found the SSI marginally influences the natural frequencies of the blades.

2.5. Seismic response of embedded piles

A key part of this work is to define a procedure to model how the earthquake affects the pile. This is not a straight forward procedure; therefore it is analyzed in the following sections.

2.5.1. Ground response

A general overview of the situation analyzed is shown if Figure 2-5.

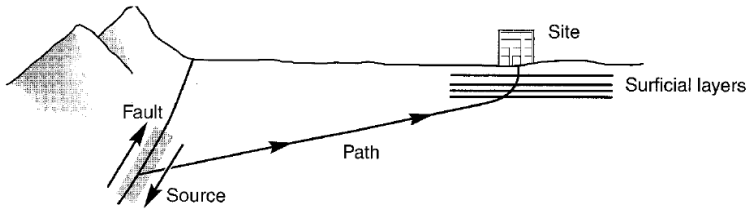

Figure 2-5: Refraction mechanism producing nearly vertical wave propagation near the ground surface [41]

The problem starts when a fault ruptures below the surface of the earth, producing body waves, which travel away in all directions. In earthquake resistant design, body waves are considering the most relevant, being classified in main two types of waves: P – waves and S – waves. P – Waves receive the name from "primary", meaning that they are the fastest waves, arriving first to the site. For these waves, the direction of propagation and the direction of the vibration are parallel. Due to this property, they are commonly called longitudinal waves. They are also called compression (compressional) wave. S –waves receive the name from "secondary", meaning that they are slower than the P – waves, arriving secondly to the site (after the P –waves). For these waves, the direction of the propagation is perpendicular to the vibration, causing shear deformation in the medium. This is the reason they are termed as shear waves. When the vibration of the soil particles are in the plane of the wave propagation, the S – waves are called SV waves, and when the soil particles vibrate out of the plane, they are called SH waves. This classification is briefly visualized in Figure 2-6.

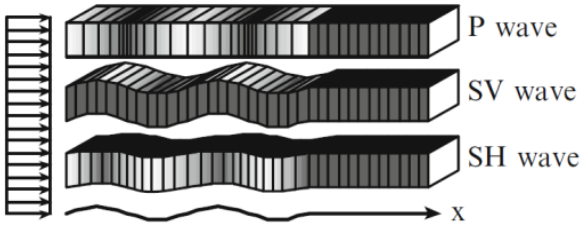

Figure 2-6: Types of earthquake waves (body waves) [42].

When boundaries between different materials are reached by the seismic waves, they are refracted and reflected. Commonly, the wave propagation velocity is lower as the material is closer to the surface; producing that inclined rays striking horizontal layer boundaries are reflected to a more vertical direction. This mechanism takes place several times before arriving to the surficial layers, bending the rays to an approximately vertical direction. This process allows engineers dealing with structural –seismic problems, to consider a one dimensional ground response analysis. The main conditions required to assume this behavior are clearly described and detailed in the literature [41], [42]:

- All boundaries along the path of the rays are horizontal
- The response of the soil deposit is mainly dominated by SH waves, which are propagated vertically from the bedrock underneath the site.
- The soil at the site and the bedrock underneath it are assumed to extend infinitely in the horizontal direction.

Even when these conditions are common for the kind of projects this work is dealing with (monopile OWT), it is important to clearly visualize when it is not possible to assume a one dimensional ground response, and therefore it is required to use a two dimensional or maybe even a three dimensional analysis [41]. Some examples of it are situations are: Ground with sloping / irregular ground surfaces, the presence of heavy, stiff or embedded structures, or projects involving walls and tunnels. In these cases, an analytical approach can be performed to find a closed form solution, or an approximate method can be implemented. The most common one is a finite elements method [41].

2.5.2. Pile response against SH waves

Once the vertical SH waves dominate the response of the soil profile where the structure is founded, they produce a horizontal oscillation motion at some “free field” location of the soil medium. This location is therefore not affected by the existence of the pile. Close to the pile, the waves are “perturbed”, creating a field which is a combination of mainly three waves: the diffracted by the pile and primarily propagated in the horizontal behavior, the reflected at the mudline waves (propagating downwards) and the incident waves (propagating upwards) [43]. In 1982, Kaynia and Kausel [44] developed a solution method to this dynamic boundary value three dimensional problem. This method “is in essence a boundary-integral-type formulation in which the Green's functions, defining the displacement fields due to uniform unit loads acting on an elemental cylindrical surface and on a circular disk, are computed by solving the wave equations through Fourier and Hankel transformations” [43], [44]. This approach is out of the scope of this work; however, the interested reader can find more information in the literature.

This work considers an approximate solution to this problem, proposed in 1992 by Makris and Gazetas [45]. This approach assumes that for a flexible pile excited by incoming relatively low frequency (large wavelength) waves, the pile closely follows the oscillating free field motion.

Therefore the excitation on the pile can be assumed to be equal to the free field motion [45], [46], [47]. This is visualized in Figure 2-7.

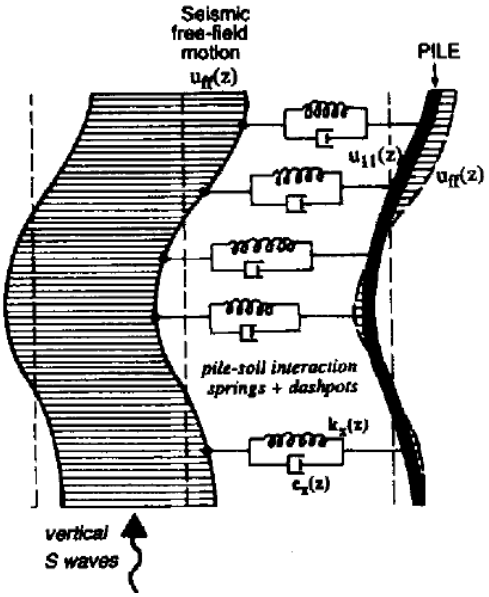

Figure 2-7: Pile deforming under seismic type excitation [45].

2.6. Free field motion

This section contains the theoretical calculation of the free field motion described in Section 2.5.1. As it is explained in that section, a one dimensional ground response analysis is performed. The soil analyzed, according to Kramer [41], is described as a "uniform, damped soil on rigid rock", meaning that the following assumptions are considered [8], [41], [42], [48]:

- The soil profile can be modeled as several layers, but for this work, a uniform single layer is considered. This means complete soil column dynamic behavior is governed by a set of constant parameters. These parameters, in reality, should be calibrated with experimental measurements at a given project location. These parameters are: the uniform density ρ_s, an equivalent Young modulus E_s, an equivalent shear modulus G_s, and the material damping coefficient η_s.
- The free surface (the mudline for this case) and the boundary between the soil layer and the bedrock are horizontal.
- SH waves are governing the response of the soil stratum, and they propagate vertically from the bedrock to the mudline
- This mechanism can be modeled considering the shear wave propagation concept.
- The bedrock and the soil stratum are wide enough to be considered as infinite, meaning that no interferences are in the path to avoid the bending of the rays to an approximately vertical direction, and that influence of the surface waves have can be neglected.
- The soil stratum is modeled considering damping or dissipation of energy, through material damping.
- The horizontal seismic input motion is assumed to be known at the bedrock underneath the soil profile.

The seismic input motion is prescribed at the bedrock and it is assumed to be known. It is defined as an acceleration signal (in the time domain). This signal is transferred to the frequency domain by calculating its Fourier transform.

The signal is received in the time domain and assumed to be correct, meaning [49]:

- At the beginning of the signal, ground acceleration, velocity and displacement must be zero.
- At the end of the ground shaking caused by an earthquake, the ground velocity must return to zero.
- At the end of the signal, some residual displacements can be present.

These conditions are not always met when measuring a signal from a real earthquake. If this is the case, some filtering process can be considered. This topic is out of the scope of this work; however, the interested reader can find more information in the literature [49], [17].

The signal received in the time domain can be transferred to the frequency domain by calculating its Fourier transform:

$$A_g(\omega) = \int_{-\infty}^{\infty} a_g(t) e^{-i\omega t} dt \tag{2-1}$$

Therefore the velocity and the displacement signal can also be transferred to the frequency domain:

$$V_g(\omega) = \frac{1}{i\omega} A_g(\omega) \tag{2-2}$$

$$U_g(\omega) = -\frac{1}{\omega^2} A_g(\omega) \tag{2-3}$$

This bedrock seismic input motion excites the complete soil profile, where an S wave from the bedrock to the mudline is propagated. This propagation is assumed to be ideally vertical [8]. The vertical propagation of the S wave causes a denominated free field motion along the soil profile.

The free field motion can be calculated by writing down the equation of motion (EOM) governing this shear wave propagation along the soil profile [41] [48]. For a small element like the one shown in Figure 2-8 the situation reads:

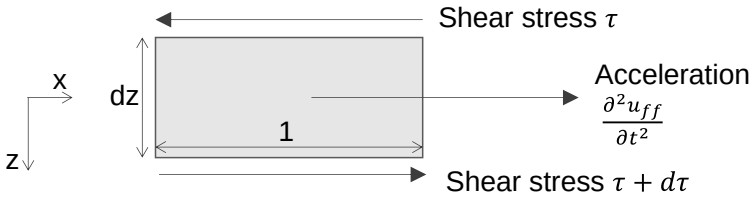

Figure 2-8: Portion of soil to model the S-wave propagation.

$$\rho \frac{\partial^2 u_{ff}}{\partial t^2} = \frac{\partial \tau}{\partial z} \tag{2-4}$$

Where u_{ff} is the horizontal displacement, ρ represents the mass density of the soil, τ is the shear stress in a horizontal plane at the top and bottom of the analyzed soil element. Note that lateral normal stresses are not included. This is due to the assumption of an idealized vertical propagation creating a constant stress in the x direction; therefore the normal stresses that are present at both sides of the element cancel each other.

The linear kinematic relation is defines the shear strain by:

$$\gamma = \frac{\partial u_{ff}}{\partial z} \tag{2-5}$$

A linear constitutive law including material damping η_s (Kelvin-Voigt model) can be written as:

$$\tau = G_s\gamma + \eta_s \frac{\partial \gamma}{\partial t} \tag{2-6}$$

It is possible to write the EOM of the displacement caused by the shear wave being propagated in the vertical direction by combining Eq. (2-4), Eq. (2-5) and Eq. (2-6).

$$\rho_s \frac{\partial^2 u_{ff}}{\partial t^2} = G_s \frac{\partial^2 u_{ff}}{\partial z^2} + \eta_s \frac{\partial^3 u_{ff}}{\partial z^2 \partial t} \tag{2-7}$$

Two boundary conditions are assumed for this problem:

1) Zero shear stress at the mudline (z=0):

$$\tau(0,t) = 0 \tag{2-8}$$

2) Acceleration compatibility at soil bedrock interface (z=H):

$$\left.\frac{\partial^2 u_{ff}}{\partial t^2}\right|_{z=H} = a_g(t) \tag{2-9}$$

Assuming a harmonic solution for the lateral displacement, and a steady state regime:

$$u_{ff}(t) = U_{ff}(z,\omega)e^{i\omega t} \tag{2-10}$$

The solution to this problem is defined as follows:

$$U_{ff}(z,\omega) = U_g(\omega)\frac{\cos\left(\frac{\omega z}{c_s{}^*}\right)}{\cos\left(\frac{\omega H}{c_s{}^*}\right)} \tag{2-11}$$

And the resonance frequencies of the soil column are defined at:

$$f_n = \frac{n}{4H}\sqrt{\frac{G_s}{\rho_s}} \tag{2-12}$$

With n=1, 3, 5, 7…

The complete derivation of this propagation is included in Appendix 4.

These calculations are applicable to calculate the free field motion along the soil profile considering only a single stratum. The same calculations can be performed for a multilayer soil profile, which are out of the scope of this work. However, the interested reader can found more information in the literature [17], [50].

2.7. Beam on Dynamic Winkler Foundation model features

Based on the approach visualized in Figure 2-7, this section describes features of a Beam-on-Dynamic-Winkler-Foundation (BDWF) model considered for this work:

- Pile is modeled as Timoshenko beam. Note that for this kind of beams, the response is defined as the lateral deformation and the cross sectional rotation (Figure 2-7 only shows a lateral deformation since Makris and Gazetas [45] considered an Euler Bernoulli beam).
- Pile-soil interaction is modeled considering the linear section of a set of idealized P-Y curves obtained from an experimental- project, where the stiffness at every depth

(springs) is defined by the initial stiffness of the P-Y curve, and the damping at every depth (dashpots) is assumed to follow the shape of the stiffness [51]:

$$c_z = \alpha k_z \tag{2-13}$$

- At this point, it is assumed that all the sources of damping of the structure come from the linear interaction between the pile and the soil (geometric and material damping). This is accepted since the other sources of damping (hydrodynamics and steel hysteresis) are relatively small. Therefore it is logical to assume that the damping has the same shape as the stiffness. To be consistent, α has unit of time [s] [51].
- Other authors have developed alternatives to relate damping to stiffness [45], [52].

The main limitations of this model are listed below:

- BDWF model assumes that the springs and dashpots are independent of each other. This is not realistic since the soil mobilizes continuously and affects the behavior of the surrounding elements.
- Only the linear part of the P-Y curves is considered. This means that the deformations obtained are not entering to the plastic deformation regime.
- The damping along the embedded pile is assumed to be a fraction of the stiffness estimated from the idealized P-Y curves.
- Only horizontal motions are allowed for the structure. The pile is considered vertically restrained at the pile tip

2.8. State space representation

A structural dynamic system is described by a set of second order differential EOM. It is convenient (in terms of time and computational resources) to represent them as a set of equivalent first order differential equations (DE) in the state-space. This means that the set of first order DE relates the inputs and the outputs of the system considering an intermediate variable named state. For a single degree of freedom (SDOF) system, it is known that its motion is described by a (one) second order DE; therefore, when considering a state-space representation, the result will be a set of two first order DE [53]. Following the same logic, the motion of a MDOF system with N number of DOF can be described by a set of N second order DE, therefore it can be represented using a set of 2N first order DE in the state-space representation, [54], [53], [55].

For a better understanding of this this procedure, the spring-dashpot SDOF system shown in Figure 2-9 is considered.

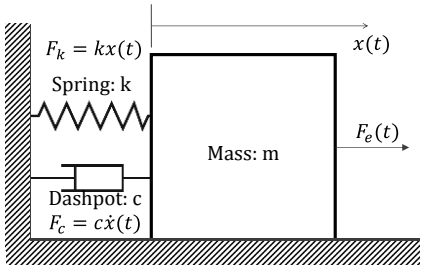

Figure 2-9: Spring-dashpot SDOF system.

The second order DE of this system reads:

$$m\ddot{x}(t) + c\dot{x}(t) + kx(t) = F_e(t) \tag{2-14}$$

It is possible to rewrite it separating the inertial forces from the other terms, and dividing by the mass m:

$$\ddot{x}(t) = -\frac{c}{m}\dot{x}(t) - \frac{k}{m}x(t) + \frac{1}{m}F_e(t) \tag{2-15}$$

The system is represented by an DE which is second order. The next step is to define two new variables, called q_1 and q_2. They are so-called state variables, and it is possible to combine them in a column state vector called $\boldsymbol{q}(t)$. Additionally, the first component of this state vector $q_1(t)$ is defined as the displacement variable $x(t)$. Additionally, the second component of this state vector $q_2(t)$ is defined as the time derivative of the displacement variable $x(t)$, meaning:

$$q(t) = \begin{bmatrix} q_1(t) \\ q_2(t) \end{bmatrix} = \begin{bmatrix} x(t) \\ \dot{x}(t) \end{bmatrix} \tag{2-16}$$

Now it is possible to define a set of two first order ODE using the state variables $q_1(t)$ and $q_2(t)$ defined in (2-16). The first order ODE states that $\dot{q}_1(t) = q_2(t)$ and the second contains the rewritten equation of motion defined in (2-15), meaning:

$$\dot{q}_1(t) = q_2(t) \tag{2-17}$$

$$\dot{q}_2(t) = -\frac{c}{m}\, q_2(t) - \frac{k}{m}\, q_1(t) + \frac{1}{m}F_e(t) \tag{2-18}$$

The representation defined in (2-17) and (2-18) contains the same information as the original system described in (2-15), but considering a set of two first order DE.

When a dynamic motion problem is modeled using the state-space representation (set of first order DE), it can be solved by including the adequate conditions (BC, IC). This work considers the Matlab® based “bvp5c” tool, which solves a boundary value problem for ordinary differential equations.

3. Problem definition

This chapter contains a detailed explanation of the problem analyzed. It starts with the monopile OWT characteristics, such as the pile-tower diameter / thickness and the RNA dynamic properties. The soil profile is characterized, including the pile-soil interaction. Additionally, the seismic motion properties and the ground motion excitation characteristics are included.

A general overview of the problem analyzed is shown in Figure 3-1

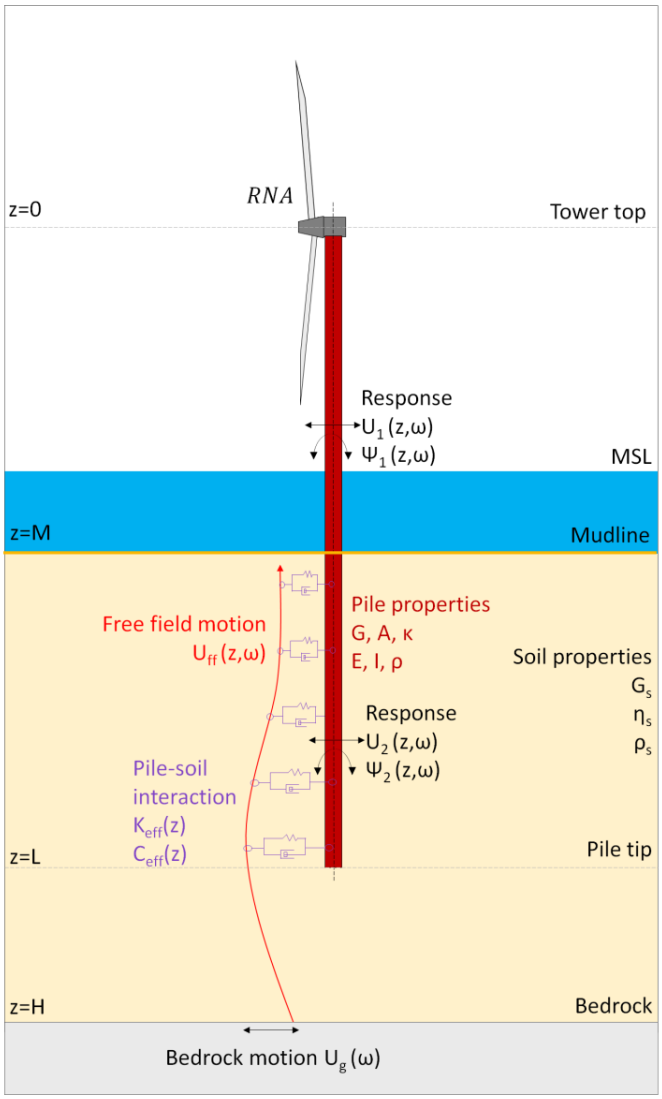

Figure 3-1: Visualization of the problem analyzed.

The problem consists of a monopile OWT. As it is shown in Figure 3-1, the superstructure consists of the RNA installed at the tower top level. This RNA system is supported by a steel tower. Since this work focuses on a methodology to study the influence of the SSI on the seismic performance of the structure, the tower is defined as a uniform diameter/thickness cylindrical element. When penetrating into the soil, this cylindrical element is identified as monopile. The monopile is driven into the soil, and the distance between the pile tip and the mudline defines the embedded part of the pile. Regarding the full soil profile, the scope of this work allows for the consideration of the soil as a uniform single layer stratum. The soil stratum covers the distance between the mudline and the bedrock. The soil is characterized with 4 main properties governing its dynamic behavior: a characteristic material density, an equivalent Young and shear modulus and an equivalent material damping coefficient.

The pile and the surrounding soil interact at every moment. This interaction is defined as the pile-soil-interaction and is represented by linear springs (stiffness) and dashpots (damping). These elements are defined by considering a set of idealized P-Y curves. The spring coefficients are defined as the initial stiffness calculated from these PY curves, and the dashpots are assumed to be proportional to the springs [56] and are calibrated to represent the overall response of a real project OWT.

The ground motion describing the seismic input is assumed to be known at the bedrock underneath the soil profile. This ground motion is defined in the time domain, and provided as an adequate filtered acceleration signal [49]. Due to the assumed viscoelastic properties of the soil, the assumed long distance between the seismic source (fault) and the bedrock surface, and the assumed infinite horizontal dimension of the soil profile, the ground motion at the bedrock is (ideally) vertically propagated from the bedrock to the mudline [50]., defining a free field motion along the complete soil column [8].

The turbine is assumed to be in its idling regime, meaning that it is not operating. Due to this assumption, the aerodynamic damping can be neglected. Since the focus of this work is on the seismic performance of the monopile OWT, the influence of the water covering the distance from the mudline to the MSL, in terms of loads and damping, is neglected.

All the parameters involved in the problem are included and detailed in Table 3-1. The units and a classification regarding the element which encloses each parameter are included. Finally, a brief description is incorporated.

Table 3-1: Problem definition parameters

Group	Parameter	Unit	Description
Soil	H	$[m]$	Distance between the mudline and the bedrock
	G_s	$\left[\frac{N}{m^2}\right]$	Equivalent shear modulus of the soil
	η_s	$\left[\frac{N}{m^2}\right]$	Equivalent viscosity of the soil material
	ρ_s	$\left[\frac{kg}{m^3}\right]$	Equivalent density of the soil
Seismic input	$u_g(t)$	$\left[\frac{m}{s^2}\right]$	Lateral ground motion displacement at the bedrock (time domain)
	$U_g(\omega)$	$\left[\frac{m}{s^2}\right]$	Lateral ground motion displacement at the bedrock (frequency domain)
	$U_{ff}(z,\omega)$	$\left[\frac{m}{s^2}\right]$	Free field motion, propagated from bedrock to mudline (frequency domain)
Pile soil interaction	$k_{eff}(z)$	$\left[\frac{N}{m^2}\right]$	1D effective Winkler stiffness
	$C_z(z)$	$\left[\frac{kg}{ms}\right]$	Effective viscous soil damping
	α	$[s]$	Dependency between soil damping and stiffness
Pile/tower properties	D_p	$[m]$	Pile diameter
	t_p	$[m]$	Pile wall thickness
	L_p	$[m]$	Pile penetration
	ρ_p	$\left[\frac{kg}{m^3}\right]$	Pile density (material)
	$E_p(z)$	$\left[\frac{N}{m^2}\right]$	Young modulus of the pile
	$I_p(z)$	$[m^4]$	Cross-section second moment of inertia
	$G_p(z)$	$\left[\frac{N}{m^2}\right]$	Shear modulus of the pile (material)
	$A_p(z)$	$[m^2]$	Cross sectional area of the pile
	κ_p		Cross section-dependent Timoshenko shearing coefficient (0.5 assumed for piles)
RNA	M_{RNA}	$[kg]$	Mass of the RNA
	J_{RNA}	$[kgm^2]$	Rotational inertia of the RNA

4. Methodology

This chapter contains the methodology proposed to calculate the seismic response of a monopile OWT in its idling state: The Single Node SSI Method, which is a form of the substructure method analysis described in Chapter 2. To validate this method, a second approach to solve the same problem (but solved at once with no substructure) is proposed: the Full Pile SSI Method. Finally, as the interest is on comparing the seismic response of such structure, a model to perform a classic seismic analysis is detailed, considering the structure as clamped at the mudline and subjected to the horizontal ground motion evaluated at the mudline.

4.1. Single node SSI method

The problem described in Chapter 3 is solved by implementing a denominated Single Node SSI Method. It consists on a three steps procedure, which considers the substructure method analysis described in Section 2.2.2.2. A general overview of how the three steps methodology is defined is shown in Figure 4-1.

- Step one: Calculate the equivalent seismic load at the mudline.
- Step two: Calculate the impedances at the mudline.
- Step three: Calculate the response of the superstructure founded on impedances (Step two) and excited at the mudline node with equivalent seismic load (Step one).

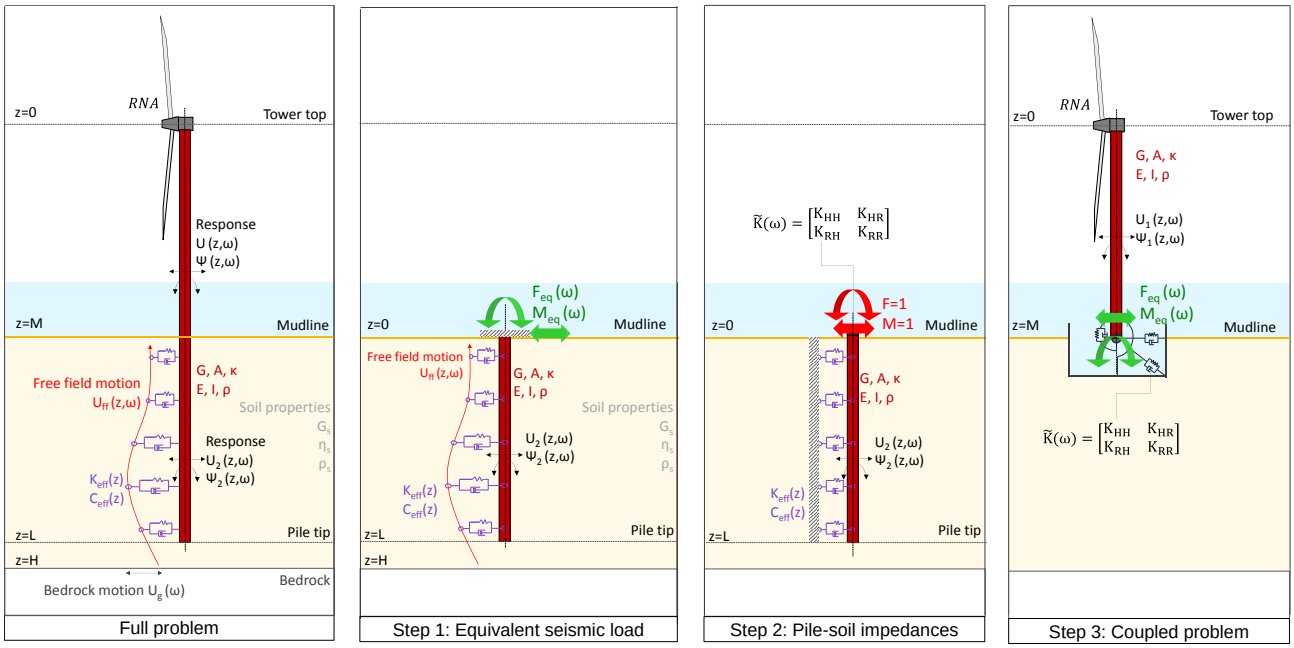

Figure 4-1: Three steps methodology proposed

A detailed explanation of each of the steps is included in the following sections.

4.1.1. Step one: Calculate the equivalent seismic loads at the mudline

As it is shown in Figure 4-2, the first step of the methodology proposed consists on the calculation of the equivalent seismic load at the mudline. This load is defined as a combination of a shear force $F_{eq}(\omega)$ and an overturning moment $M_{eq}(\omega)$, which has the same influence on the embedded part of the pile as the free field motion $U_{ff}(z,\omega)$, acting through the viscoelastic elements defining the pile-soil interaction.

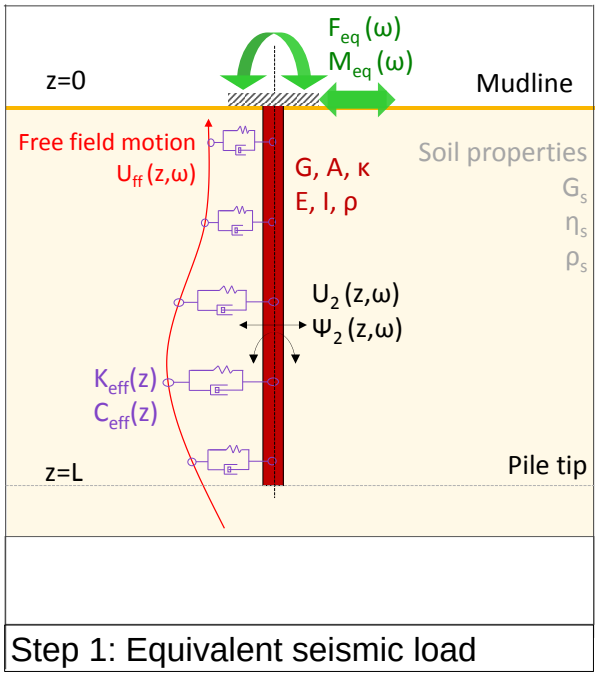

Figure 4-2: Single Node SSI Method. Step one.

The procedure to calculate this equivalent seismic load consists on:

a. Consider only the embedded part of the pile, being excited by the free field motion $U_{ff}(z,\omega)$ through the viscoelastic elements defining the pile-soil interaction.
b. Define a clamped connection at the mudline, imposing 2 boundary conditions at this point: lateral deformation and cross sectional rotation equal to zero.
c. Consider the original free end boundary conditions at the pile tip.
d. Calculate the reactions at the mudline, which define the equivalent seismic load.

As it is detailed in Section 2.5, the embedded part of the pile including the pile- soil interaction, under the seismic excitation, is modelled as a BDWF model excited at the end of the springs and dashpots by the free field motion (Figure 4-2). The EOM of this system are written in terms of the continuum lateral equilibrium of forces, Eq. (4-1), and bending moments (4-2), along the pile:

$$GA\kappa\left(\frac{d^2U_2(z,\omega)}{dz^2}-\frac{d\Psi_2(z,\omega)}{dz}\right)-(K_{eff}(z)+i\omega C_{eff}(z)-\omega^2\rho A)U_2(z,\omega)=\left(-K_{eff}(z)-i\omega C_{eff}(z)\right)U_{ff}(z,\omega) \quad (4\text{-}1)$$

$$GA\kappa\left(\frac{dU_2(z,\omega)}{dz}-\Psi_2(z,\omega)\right)+EI\frac{d^2\Psi_2(z,\omega)}{dz^2}+\omega^2\rho I\Psi_2(z,\omega)=0 \quad (4\text{-}2)$$

In these equations, the response of the structure is measured considering the deflection $U_2(z,\omega)$ and the cross sectional rotation $\Psi_2(z,\omega)$ along the pile. Regarding the pile properties, *G* and *E* represent respectively the shear and the Young's modulus of the pile material (steel). Additionally, *A* and *I* represent the area and the second moment of inertia of the cross section of the pile. The cross-section dependent Timoshenko shearing coefficient κ is considered equal to 0.53, representative for cylindrical sections, whereas the density of the steel is identified as ρ. As it was detailed in Section 2.7, the pile-soil interaction properties are defined considering 2 elements; the equivalent stiffness coefficient K_z and the effective damping coefficient C_z. Finally, $U_{ff}(z,\omega)$ represents the free field motion.

The boundary conditions for this problem are defined at the pile tip and at the mudline, and they are detailed as follows:

Free end at the pile tip:

$$GA\kappa\left(\frac{dU_2(L,\omega)}{dz}-\Psi_2(L,\omega)\right)=0 \tag{4-3}$$

$$EI\frac{d\Psi_2(L,\omega)}{dz}=0 \tag{4-4}$$

Eq. (4-3) represents the lateral equilibrium of forces, whereas Eq. (4-4) represents the equilibrium of moments.

Clamped connection at the mudline:

$$U_2(0,\omega)=0 \tag{4-5}$$

$$\Psi_2(0,\omega)=0 \tag{4-6}$$

Since it is a clamped connection, Eq. (4-5) represents the lateral displacement being equal to zero, whereas Eq. (4-6) represents the cross sectional rotation being equal to zero.

The equivalent seismic load is estimated by evaluating the shear force and the bending moment at the mudline:

$$GA\kappa\left(\frac{dU_2(0,\omega)}{dz}-\Psi_2(0,\omega)\right)=F_{eq}(\omega) \tag{4-7}$$

$$EI\frac{d\Psi_2(0,\omega)}{dz}=M_{eq}(\omega) \tag{4-8}$$

Now that the equivalent seismic load is estimated, the next section explains how to calculate the pile-soil impedances at the mudline.

4.1.2. Step two: Calculate the pile-soil impedances at the mudline

As it is shown in Figure 4-3, the second step of the methodology proposed consists on the calculation of the pile – soil impedances at the mudline. These impedances represent the dynamic stiffness of the embedded part of the pile including the pile-soil interaction system. This means that it includes a real part related to the stiffness, and an imaginary part related to the damping. Due to the embedded length of the pile, four impedances catch the pile – soil interaction defined at a single point at the mudline. They are composed by a swaying component (K_{HH}), a rocking component (K_{RR}), and a set of 2 coupled swaying-rocking components (K_{HR}, K_{RH}).

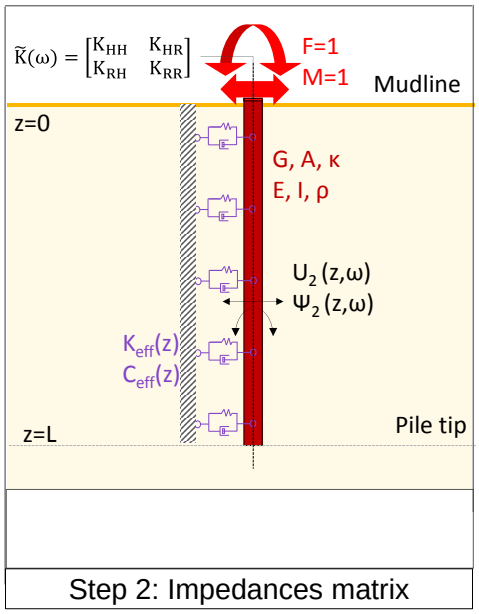

Figure 4-3: Single Node SSI Method. Step two.

The procedure to calculate these impedances consists on:

a. Recall the EOM defined in Eq. (4-1)and in Eq. (4-2)), but now without the influence of an incident free field motion $U_{ff}(z,\omega)$. Again, they are written in term of the continuum lateral equilibrium of forces (Eq.(4-9)) and bending moments (Eq. (4-10)):

$$GA\kappa\left(\frac{d^2U_2(z,\omega)}{dz^2}-\frac{d\Psi_2(z,\omega)}{dz}\right)-\left(k_{eff}(z)+i\omega C_{eff}(z)-\omega^2\rho A\right)U_2(z,\omega)=0 \qquad (4\text{-}9)$$

$$GA\kappa\left(\frac{dU_2(z,\omega)}{dz}-\Psi_2(z,\omega)\right)+EI\frac{d^2\Psi_2(z,\omega)}{dz^2}+\omega^2\rho I\Psi_2(z,\omega)=0 \qquad (4\text{-}10)$$

b. Define a set of force and overturning moment at the mudline level, to compute the corresponding lateral displacements and rotations, as it is shown in Figure 4-4.

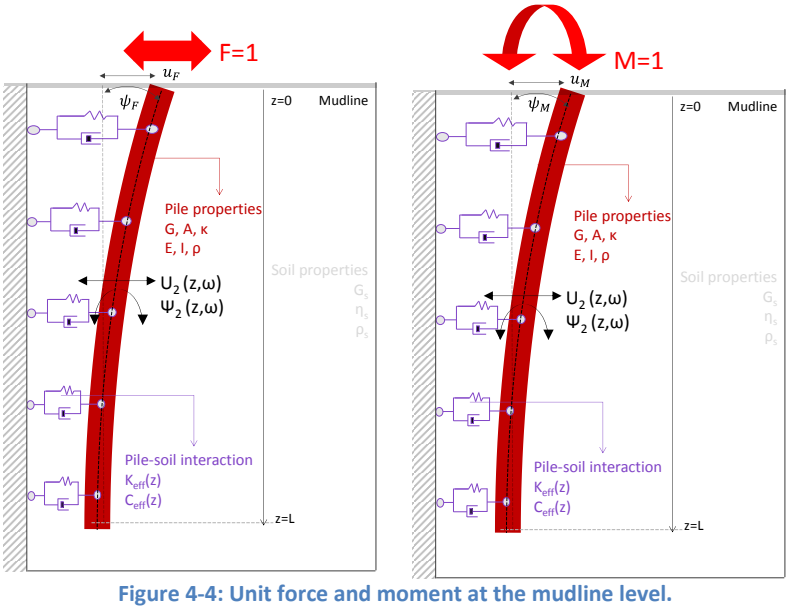

Figure 4-4: Unit force and moment at the mudline level.

This unit force and moment are stored in a unit force matrix:

$$\tilde{\mathrm{F}} = \begin{bmatrix} 1 & 0 \\ 0 & 1 \end{bmatrix} \tag{4-11}$$

c. Since this set of unit force and moment is acting at the pile head, the boundary conditions of the BDWF model are updated when it is adequate:

Unit force and moment applied at the mudline level:

$$GA\kappa\left(\frac{dU_2(0,\omega)}{dz} - \Psi_2(0,\omega)\right) = 1 \tag{4-12}$$

$$EI\frac{d\Psi_2(0,\omega)}{dz} = 1 \tag{4-13}$$

Free end at the pile tip:

$$GA\kappa\left(\frac{dU_2(L,\omega)}{dz} - \Psi_2(\mathrm{L},\omega)\right) = 0 \tag{4-14}$$

$$EI\frac{d\Psi(\mathrm{L},\omega)}{dz} = 0 \tag{4-15}$$

d. For this unit force/moment, the lateral displacement and rotations are evaluated at the mudline level, and stored in a displacement matrix:

$$\tilde{\mathrm{u}}(\omega) = \begin{bmatrix} \mathrm{u_F} & \mathrm{u_M} \\ \psi_\mathrm{F} & \psi_\mathrm{M} \end{bmatrix} \tag{4-16}$$

e. The flexibility matrix is calculated by inverting the forces vector and multiplying it by the calculated displacement matrix:

$$\tilde{\mathrm{f}}(\omega) = \tilde{\mathrm{F}}^{-1}\tilde{\mathrm{u}}(\omega) \tag{4-17}$$

f. Now the dynamic stiffness matrix is calculated as the inverse of the flexibility matrix previously found:

$$\tilde{\mathrm{K}}(\omega) = \tilde{\mathrm{f}}^{-1} \tag{4-18}$$

g. The components of the dynamic stiffness matrix are defined as the pile – soil impedances at the mudline, and considering the notation described at the beginning of this section:

$$\tilde{\mathrm{K}}(\omega) = \begin{bmatrix} \mathrm{K_{HH}} & \mathrm{K_{HR}} \\ \mathrm{K_{RH}} & \mathrm{K_{RR}} \end{bmatrix} \tag{4-19}$$

h. This dynamic stiffness matrix is a complex valued matrix, which can be expressed as:

$$\tilde{\mathrm{K}}(\omega) = \mathrm{Re}\left(\tilde{\mathrm{K}}(\omega)\right) + \mathrm{iIm}\left(\tilde{\mathrm{K}}(\omega)\right) \tag{4-20}$$

$$\tilde{\mathrm{K}}(\omega) = \hat{\mathrm{K}}(\omega) + \mathrm{i}\omega\tilde{\mathrm{C}}\,(\omega) \tag{4-21}$$

Where $\mathrm{K_{HH}}$, $\mathrm{K_{RR}}$ and $\mathrm{K_{HR}} = \mathrm{K_{RH}}$ represent the stiffness in the swaying, rocking and coupled swaying/rocking mode. Note that each of these terms is complex valued. The real part reflects the stiffness and inertia, and its frequency dependency is associated only to the influence of the inertia. In the other hand, the imaginary part reflects the damping [17].

Now that the pile –head impedances are estimated, the next section explains how to calculate the response of the coupled problem, defined as the third step of the methodology proposed.

4.1.3. Step three: Solve the coupled problem

As it is shown in Figure 4-5, the step three of the methodology proposed consists of solving the coupled problem, meaning that the superstructure is founded on the impedance elements calculated in step two, and being excited at the mudline node by the equivalent seismic load calculated in step one.

The EOM of this system is obtained by recalling the EOM of a BDWF model but neglecting the terms related to the SSI, and of course without the influence of an incident free field motion $U_{ff}(z,\omega)$. For this case the continuous lateral equilibrium of forces (Eq. (4-22)) and bending moments (Eq.(4-23)) can be written as:

$$GA\kappa\left(\frac{d^2U_1(z,\omega)}{dz^2}-\frac{d\Psi_1(z,\omega)}{dz}\right)-(\omega^2\rho A)U_1(z,\omega)=0 \tag{4-22}$$

$$GA\kappa\left(\frac{dU_1(z,\omega)}{dz}-\Psi_1(z,\omega)\right)+EI\frac{d^2\Psi_1(z,\omega)}{dz^2}+\omega^2\rho I\Psi_1(z,\omega)=0 \tag{4-23}$$

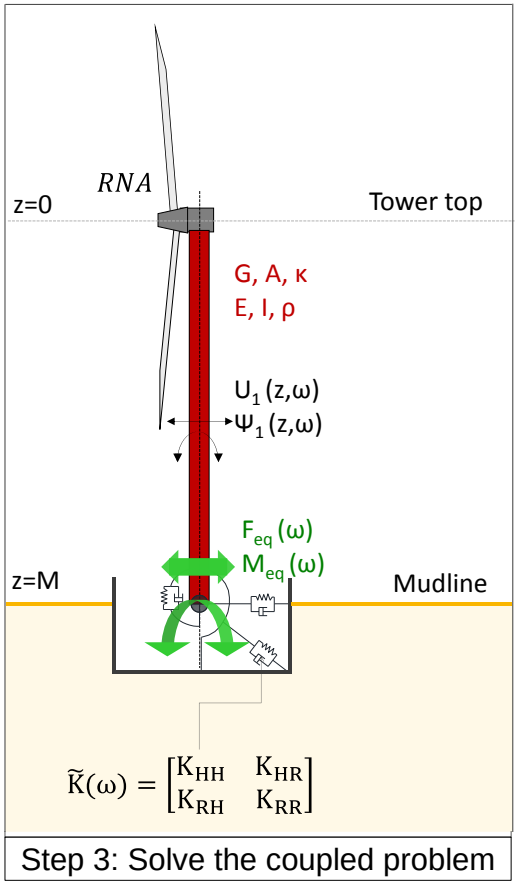

Figure 4-5: Single Node SSI Method. Step three.

The boundary conditions for this problem are defined at the tower top and at the mudline node, and they are detailed as follows:

At the tower top the equilibrium of forces and moments should be achieved. Eq. (4-24) represents the equilibrium of lateral forces; therefore the inertial force related to the acceleration of the RNA mass is included. Eq. (4-25) represents the equilibrium of moments, therefore the inertial moment related to the rotational acceleration of the RNA mass is included (considering the rotational inertial of the RNA, J_{RNA}).

$$GA\kappa\left(\frac{dU_1(0,\omega)}{dz}-\Psi_1(0,\omega)\right)-\omega^2 M_{RNA}U_1(0,\omega)=0 \tag{4-24}$$

$$EI\frac{d\Psi_1(0,\omega)}{dz}-\omega^2 J_{RNA}\Psi_1(0,\omega)=0 \tag{4-25}$$

At the mudline node:

$$GA\kappa\left(\frac{dU_1(0,\omega)}{dz}-\Psi_1(0,\omega)\right)+\mathrm{K_{HH}}(\omega)U_1(0,\omega)+\mathrm{K_{HR}}(\omega)\Psi_1(0,\omega)+F_{eq}=0 \tag{4-26}$$

$$EI\frac{d\Psi_1(0,\omega)}{dz}+\mathrm{K}_{RR}(\omega)\Psi_1(0,\omega)+\mathrm{K}_{RH}(\omega)U_1(0,\omega)+M_{eq}=0 \tag{4-27}$$

Eq. (4-26) represents the lateral equilibrium of forces at the mudline level; therefore the force caused by the activation of the swaying impedance due to the lateral deformation of the beam at that level is included. Additionally, the lateral force created by the activation of the coupled swaying-rocking due to the cross sectional rotation of the beam at the mudline level is included. Finally, the equivalent seismic shear force calculated in step 2 acting at the mudline node is included. In the same line, Eq. (4-27) represents the equilibrium of moments at the mudline level, therefore the bending moment caused by the activation of the rocking impedance due to the cross section rotation of the beam is included, the same for the bending moment caused by the activation of the coupled rocking-swaying impedance due to the lateral deformation of the beam. Finally, the equivalent seismic moment calculated in the step 2 is also included in the equilibrium equation.

The problem is defined as a set of two EOM (each of them are second order differential equations), and a set of four BC defined at the mudline node and the tower top. This system has a solution and it is calculated by following the procedure:

- Rewrite the continuous two EOM as a set of four first order ODEs using the state space representation described in Section 2.8.
- Solve this set of four first order ODEs (with the four BC) using a finite difference solver implemented in Matlab®. The tool considered in this work is the “bvp5c”, which solves a boundary value problem for boundary value problems for ODE.

Once the three steps previously detailed are performed, it is possible to estimate the seismic response of the superstructure including the SSI, as the lateral deflection $U_1(z,\omega)$ and the cross sectional rotation $\Psi_1(z,\omega)$.

4.2. Full Pile SSI Method

Another approach to calculate the seismic response of a monopile OWT considering SSI, as it is detailed in Section 3, is to solve the full model at once, without defining a substructure procedure. This approach is called Full Pile SSI Method. A visualization of the problem is shown in Figure 4-6. The key aspects of this procedure are:

- Define a set of two EOM for the embedded part of the pile (which covers from the pile tip to the mudline) and a set of two EOM for the part of upper part of the structure (which covers from the mudline to the tower top).
- Define a set of two BC at the pile tip and at the tower top.
- Define a set of four IC at the mudline, defining the continuity of the structure.

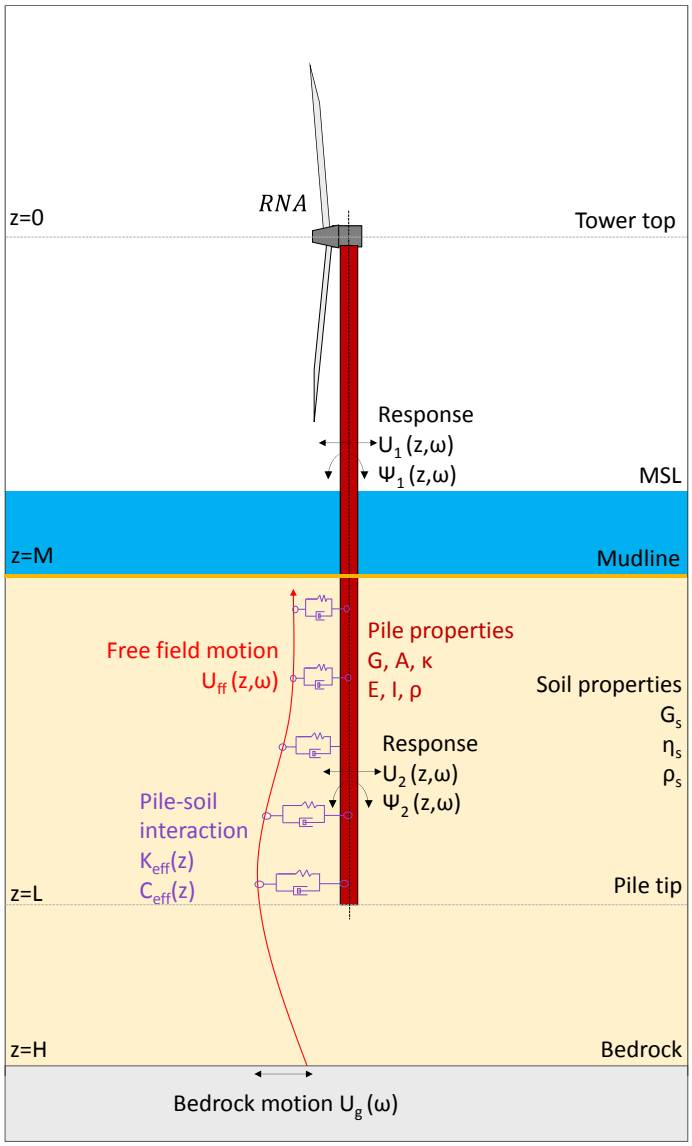

Figure 4-6: Full Pile SSI Method.

From the tower top to the mudline level, the structure can be represented using the same model described in Section 4.1.3. Recalling Eq. (4-22) and Eq. (4-23):

$$GA\kappa\left(\frac{d^2U_1(z,\omega)}{dz^2}-\frac{d\Psi_1(z,\omega)}{dz}\right)-(\omega^2\rho A)U_1(z,\omega)=0 \tag{4-28}$$

$$GA\kappa\left(\frac{dU_1(z,\omega)}{dz}-\Psi_1(z,\omega)\right)+EI\frac{d^2\Psi_1(z,\omega)}{dz^2}+\omega^2\rho I\Psi_1(z,\omega)=0 \tag{4-29}$$

From the mudline to the pile tip (substructure), the structure can be represented using the same BDWF model described in Section 4.1.1. Recalling Eq. (4-1)and Eq. (4-2):

$$GA\kappa\left(\frac{d^2U_2(z,\omega)}{dz^2}-\frac{d\Psi_2(z,\omega)}{dz}\right)-\left(K_{eff}(z)+i\omega C_{eff}(z)-\omega^2\rho A\right)U_2(z,\omega)=\left(-K_{eff}(z)-i\omega C_{eff}(z)\right)U_{ff}(z,\omega) \tag{4-30}$$

$$GA\kappa\left(\frac{dU_2(z,\omega)}{dz}-\Psi_2(z,\omega)\right)+EI\frac{d^2\Psi_2(z,\omega)}{dz^2}+\omega^2\rho I\Psi_2(z,\omega)=0 \tag{4-31}$$

The boundary conditions for this problem are defined at the tower top and at the pile tip, and they are detailed as follows:
Free end at the pile tip:

$$GA\kappa\left(\frac{dU_2(L,\omega)}{dz}-\Psi_2(L,\omega)\right)=0 \tag{4-32}$$

$$EI\frac{d\Psi_2(L,\omega)}{dz}=0 \tag{4-33}$$

At the tower top:

$$GA\kappa\left(\frac{dU_1(0,\omega)}{dz}-\Psi_1(0,\omega)\right)-\omega^2M_{RNA}U_1(0,\omega)=0 \tag{4-34}$$

$$EI\frac{d\Psi_1(0,\omega)}{dz}-\omega^2J_{RNA}\Psi_1(0,\omega)=0 \tag{4-35}$$

Eq. (4-32) and Eq. (4-33) represent the lateral force and the bending moment at the pile tip being equal to zero, respectively. Additionally, Eq. (4-34) and Eq. (4-35) represents the same condition but for the tower top. Note that for this case the situation is slightly different, since the inertial forces of the point mass representing the RNA need to be included. The lateral inertial force is calculated as the acceleration (lateral) times the mass of the mass of the RNA, and the rotational inertial force is calculated as the acceleration (rotational) times the rotational inertia of the RNA.

Additionally, the four interface conditions are defined at the mudline level in order to ensure the continuity of displacements (Eq.(4-36)) and slope (Eq. (4-37)), a dynamic shear balance (Eq.(4-38)), and the continuity of bending moments ((4-39)):

$$U_1(M,\omega)=U_2(M,\omega) \tag{4-36}$$

$$\frac{dU_1(M,\omega)}{dz}=\frac{dU_2(M,\omega)}{dz} \tag{4-37}$$

$$GA\kappa\left(\frac{dU_1(M,\omega)}{dz}-\Psi_1(M,\omega)\right)=GA\kappa\left(\frac{dU_2(M,\omega)}{dz}-\Psi_2(M,\omega)\right) \tag{4-38}$$

$$\frac{d\Psi_1(M,\omega)}{dz}=\frac{d\Psi_2(M,\omega)}{dz} \tag{4-39}$$

The problem is defined as a pair of two EOM (each of them are second order differential equations), a set of four BC defined at the mudline node and the tower top, and a set of four IC at the mudline level. This system has a solution and it is calculated by following the procedure:

- Rewrite each set of two continuous EOM as a set of four first order ODEs using the state space representation described in Section 2.8. This has to be done for the embedded part of the structure and for the superstructure. The outcome of this step is a set of eight first order ODEs.
- Solve this set of eight first order ODEs (with the four BC and the four IC) using a finite difference solver implemented in Matlab®. The tool considered in this work is the "bvp5c", which solves a boundary value problem for boundary value problems for ODE.

Once the single step previously detailed is performed, it is possible to estimate the seismic response of the superstructure including the SSI, as the lateral deflection $U_1(z,\omega)$ and the cross sectional rotation $\Psi_1(z,\omega)$ for the superstructure, and the lateral deflection $U_2(z,\omega)$ and the cross sectional rotation $\Psi_2(z,\omega)$ for the substructure.

The reason behind developing this solution is to be able to compare and to validate the three steps methodology proposed. The next chapter explains how a representative problem is solved by implementing the two approaches described, and how the response is compared for validation purposes.

4.3. Classic seismic analysis (clamped model)

A common and classic approach to perform seismic analysis of a monopile OWT is to consider the structure as clamped at the mudline, neglecting the embedded part of the pile, and excite the superstructure to a lateral acceleration defined as the free field motion evaluated at the mudline. This approach is visualized in Figure 4-7. The model developed to perform the classic seismic analysis is called "Clamped Model".

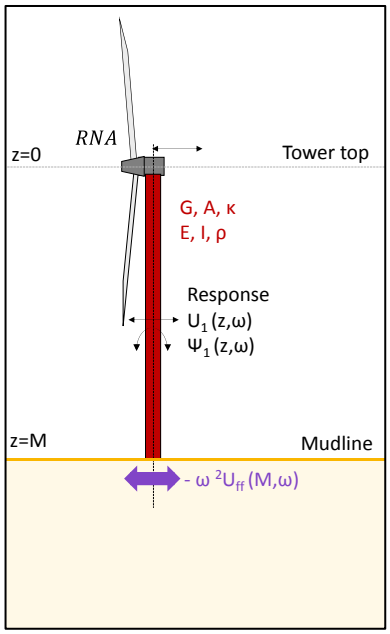

Figure 4-7: Classic seismic analysis using a clamped model.

In this classic approach for seismic analysis, the ground motion at the surface is usually obtained considering the definition contained in a design code specially developed for the project. These design codes contain the influence of the soil stratum on the properties of the seismic load. Another way is by performing a seismic hazard study. In both cases, the information is usually obtained as a lateral excitation at the mudline, neglecting the influence of the embedded part of the structure on the properties of the seismic load. As the goal of this work is to analyze the influence of the SSI in the seismic response of OWT, the results from this classic approach can be used to compare the results when considering the SSI.

The EOM of this Clamped Model reads:

$$GA\kappa\left(\frac{d^2U_1(z,\omega)}{dz^2}-\frac{d\Psi_1(z,\omega)}{dz}\right)-(\omega^2\rho A)U_1(z,\omega)=0 \tag{4-40}$$

$$GA\kappa\left(\frac{dU_1(z,\omega)}{dz}-\Psi_1(z,\omega)\right)+EI\frac{d^2\Psi_1(z,\omega)}{dz^2}+\omega^2\rho I\Psi_1(z,\omega)=0 \tag{4-41}$$

The boundary conditions for this problem are defined at the tower top and at the mudline node, and they are detailed as follows:

At the tower top:

$$GA\kappa\left(\frac{dU_1(0,\omega)}{dz}-\Psi_1(0,\omega)\right)-\omega^2M_{RNA}U_1(0,\omega)=0 \tag{4-42}$$

$$EI\frac{d\Psi_1(0,\omega)}{dz}-\omega^2J_{RNA}\Psi_1(0,\omega)=0 \tag{4-43}$$

Eq. (4-42) represents the equilibrium of lateral forces; therefore the inertial force related to the acceleration of the RNA mass is included. Eq. (4-43) represents the equilibrium of moments, therefore the inertial moment related to the rotational acceleration of the RNA mass is included (considering the rotational inertial of the RNA, J_{RNA}).

At the mudline node:

$$U_1(0,\omega)=U_{ff}(mudline,\omega) \tag{4-44}$$

$$\Psi_1(0,\omega)=0 \tag{4-45}$$

Eq. (4-44) represents the kinematic condition imposed by the seismic input motion. The acceleration of the mudline node is equal to the acceleration component of free field motion evaluated at the mudline. Eq. (4-45) represents the cross section rotation being equal to zero (clamped connection).

4.4. Remarks

Based on the definition of the two approaches to determine the seismic response of a monopile OWT, it in t is possible to analyze some pros and cons of each of them.

- The Full Pile SSI Method is direct and therefore faster than the Single Node SSI Method. The reason is evident since for the latter method; the model of the embedded part of the

pile has to be run two times: one to obtain the equivalent seismic loads, and another one to obtain the impedances.

- The Full Pile SSI Method can be implemented to consider nonlinearities at different components of the system. The Single Node SSI Method, since it is based on substructuring, is valid only when considering linear properties of the system.

5. Analysis and discussion

This chapter consists in main two parts. The first contains the estimation of the seismic response of a monopile OWT using the Single Node SSI Method and the Full Pile SSI Method defined in Chapter 4. A control point is defined at the tower top, and the results are compared. Since they are equivalent, the Single Node SSI Method is validated. The second part contains a comparison between the case when including SSI and when it is neglected. The responses are compared in terms of lateral deformations and accelerations, and bending moments along the structure. The influence of the SSI is evaluated qualitatively in the frequency domain.

5.1. Base case

5.1.1. Overview

For a real project, the monopile diameter/thickness is variable along the height and a set of secondary structures (connection flanges, service platform, among others) are present along the structure. This work focuses on the methodology to determine the seismic response and not on perform a detailed model of the structure, and therefore an idealized model is implemented to perform the simulations. Table 5-1 contains detailed information of the base case analyzed.

Table 5-1: Monopile OWT properties.

Variable	Value	Unit	Overview
Level tower top	120	[m]	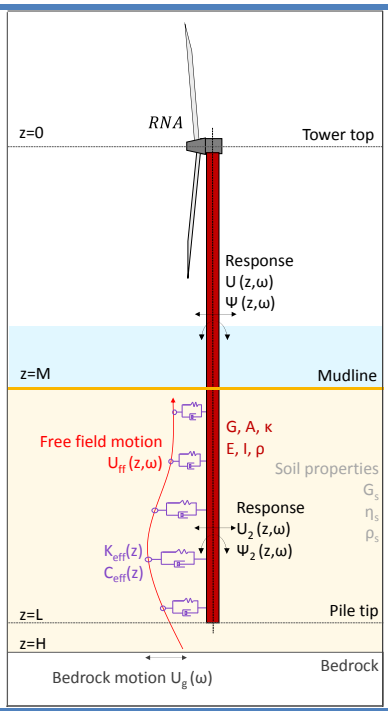
Mean sea level (MSL)	0	[m]	
Level mudline	-30	[m]	
Level Pile tip	-80	[m]	
Diameter at tower top	10	[m]	
Diameter at pile tip	10	[m]	
Thickness at tower top	100	[mm]	
Thickness at pile tip	100	[mm]	
Steel Young modulus Es	210	[GPa]	
Steel shear modulus Gs	80	[GPa]	
RNA mass at the tower top	400000	[kg]	
RNA rotational inertia at the tower top	40000000	[kgm^2]	
Soil profile depth (bedrock to mudline)	150	[m]	
Unit weight of soil γ	15	[kN/m^3]	
Soil Poisson ratio μ	0.4		
Soil damping ξ	5%		
Soil representative Young modulus E	60	[MPa]	
Soil representative shear modulus G: E/2(1+mu)	21	[MPa]	

5.1.2. Pile – soil interaction

As it is explained in Section 2.7, the properties of the pile – soil interaction are defined by a set of spring (stiffness) and dashpots (damping) along the embedded part of the pile. The springs are defined with stiffness equal to the initial stiffness obtained from a set of idealized PY curves along the embedded part of the pile, whereas the dashpots coefficients are defined as a fraction of the stiffness at the same depth. For this work, a real project PY curve has been idealized in order to be representative of a uniform medium sand profile.

Figure 5-1(left) shows the evolution of the linear part of the PY curve with the depth, meaning the lateral stiffness. For instance, at a depth of 15m measured from the mudline, the initial soil stiffness is approximately $1x10^8[N/m]$. Figure 5-1(right) shows the evolution of the dashpot coefficient as a proportion of the stiffness, according to Eq. (2-13). For instance, at a depth of 25[m] measured form the mudline, the dashpot coefficient is approximately $1.5x10^4[Ns/m]$

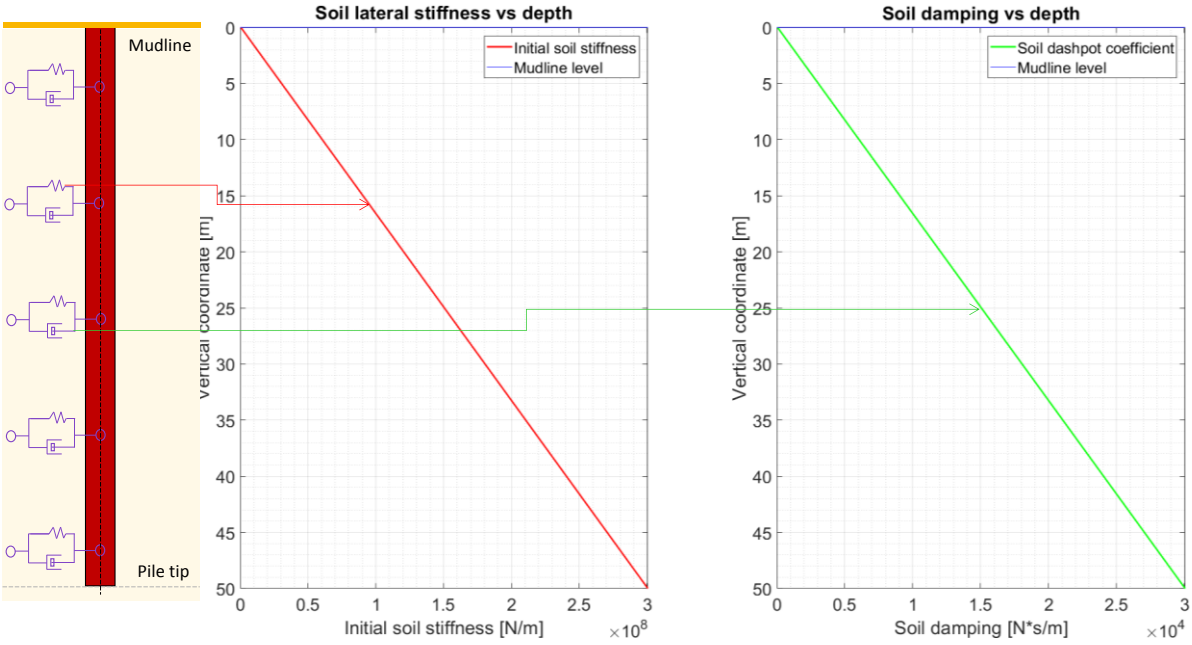

Figure 5-1: Pile-soil interaction along the depth.

5.1.3. Ground motion at the bedrock

The seismic excitation considered for this work corresponds to a ground motion which is scaled to a response spectrum based on the Taiwanese Building Code (Building Code Design Spectrum) considering a time domain spectral matching [57]. Details about this procedure are omitted for confidentiality reasons.

The seismic input motion is in the time domain, defined at the bedrock, and in terms of the horizontal motion. The acceleration (blue), velocity (red) and the displacement (magenta) signals are included and shown in Figure 5-2. The signal shows a maximum acceleration of $2.25[\mathrm{m/s2}]$, a maximum velocity of $0.24[\mathrm{m/s}]$, and a maximum displacement of $0.042[\mathrm{m}]$. The most important part of the motion approximately starts at t=20[s] and ends at t=50[s].

Analyzing the beginning of the signal, there is no observed initial motion (acceleration, velocity and displacement). Regarding the end of the signal, no residual acceleration or velocities are present. Considering this, it is possible to conclude that the signal is adequate [49].

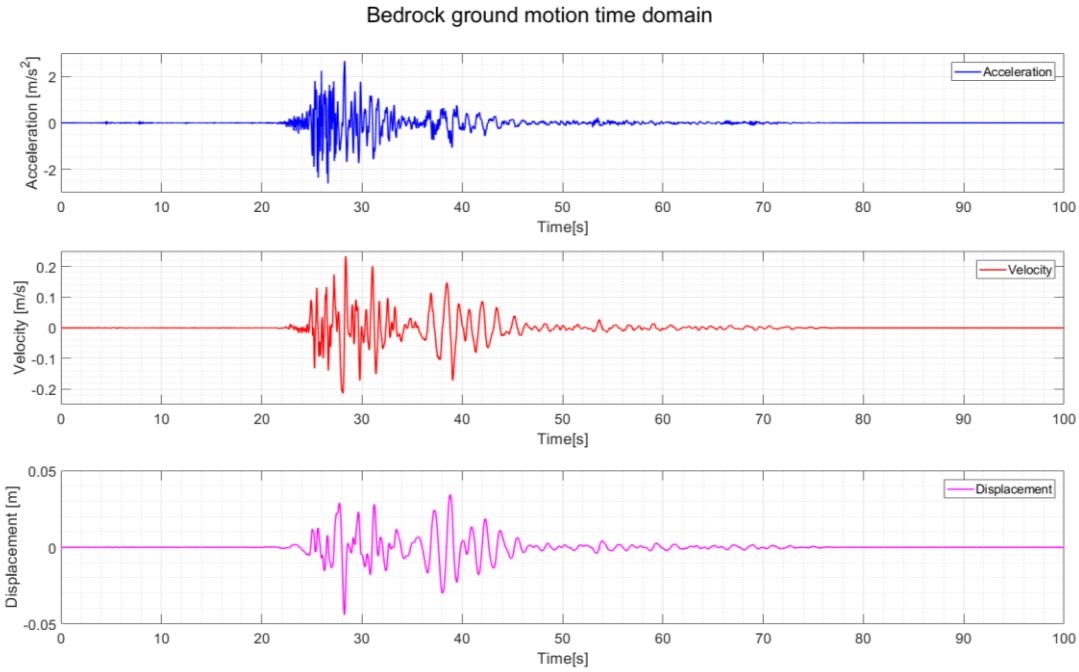

Figure 5-2: Bedrock ground motion (time domain).

The seismic input motion at the bedrock in the frequency domain, expressed as the Fourier transform of each signal is shown in Figure 5-3. For a better visualization of the plots, the x axis (frequency) is defined using a logarithmic scale.

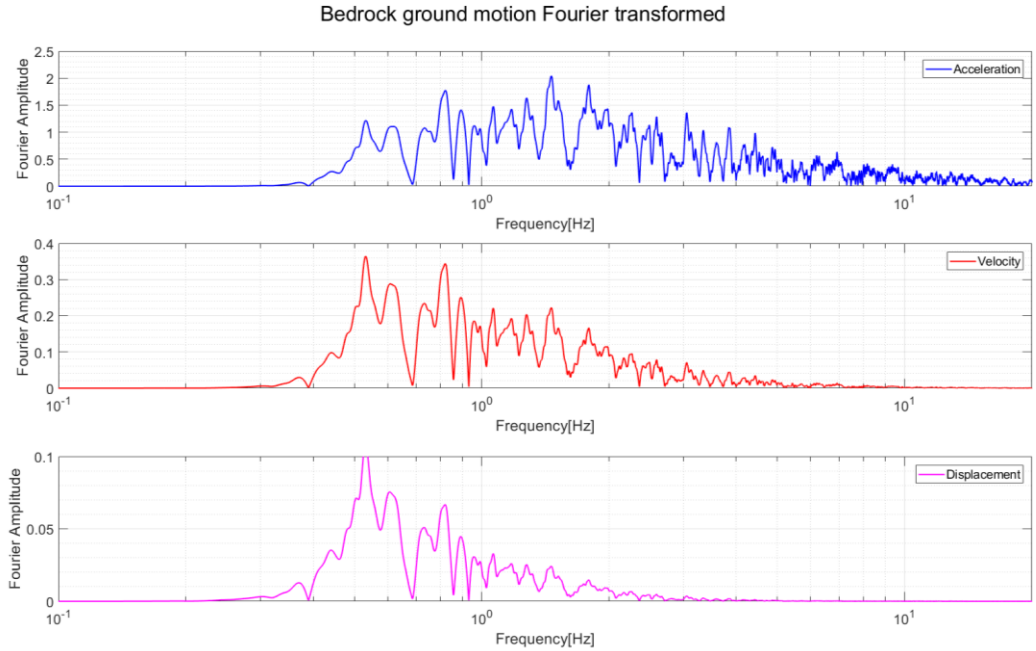

Figure 5-3: Bedrock ground motion (frequency domain).

The acceleration (blue), velocity (red) and the displacement (magenta) components of the signal are included. It can be observed that the frequency content of the earthquake is mainly contained

between 0.2[Hz] and 5[Hz]. Outside this range, the energy content decreases significantly, especially for the velocity and the displacement component, therefore the analysis is performed up to this 5[Hz] frequency.

5.1.4. Free field motion

Following the procedure described in Section 2.6, the evolution of the free field motion $U_{ff}(z,\omega)$ along the soil stratum is calculated. The first relevant information is the set of natural frequencies of the soil stratum considered, which is calculated by using Eq. (2-12). The values obtained are shown in Table 5-2, and are based on the properties listed in Table 5-1, including a soil damping ratio ξ = 5%.

Table 5-2: Natural frequencies of the soil profile

Natural frequency of the soil profile	Value [Hz]
1st	0.19
2nd	0.59
3rd	0.98
4th	1.38
5th	1.77

The frequencies displayed in Table 5-2 represent the frequencies where the soil stratum experiences resonance, meaning that it is expected for the free field motion to be amplified at these frequencies.

Considering the procedure described in Chapter 4, the focus is on the evolution of the displacement component of the signal, since it is the one that is considered in all the calculations in the frequency domain. Figure 5-4 shows the evolution of the free field motion (in the frequency domain) in terms of displacement, starting at the bedrock (blue), passing through the pile tip (green) and at the mudline (red). The top plot shows the evolution including the full range of the Fourier amplitude, and the bottom plot shows details of the behavior of the propagation for small amplitudes.

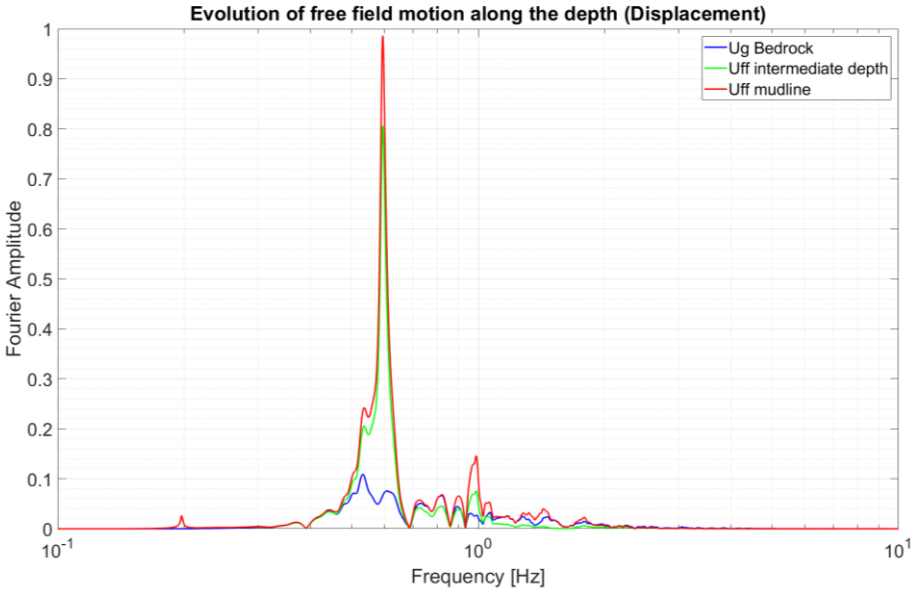

Figure 5-4: Evolution of the free field motion $U_{ff}(z,\omega)$ from bedrock to mudline.

As it is expected, an amplification of the motion is increasing as the S wave travels upwards. It can be observed that the bedrock motion (blue) has the smallest amplitude, which is amplified as the motion is approaching the mudline (red), passing through the pile tip level (green). This amplification is especially important at the natural frequencies of the soil stratum (0.2[Hz], 0.59[Hz], 0.98[Hz]), and this is visualized as peaks at these frequencies. For higher frequencies, above 1.5[Hz], the amplification is not readable, since the displacement component of the bedrock ground motion tends to be zero.

This free field motion $U_{ff}(z,\omega)$ contains a real part and an imaginary part, and they evolve in depth, and in frequency. As it was detailed in Chapter 4, it excites the embedded pile by activating the springs and dashpots as it propagates upwards, and evolves with the frequency. To visualize this propagation/evolution, Figure 5-5 shows the complete soil profile, including the non-deformation line (green), the shape of the real (blue) and the imaginary (red) part of $U_{ff}(z,\omega)$, evaluated for several frequencies.

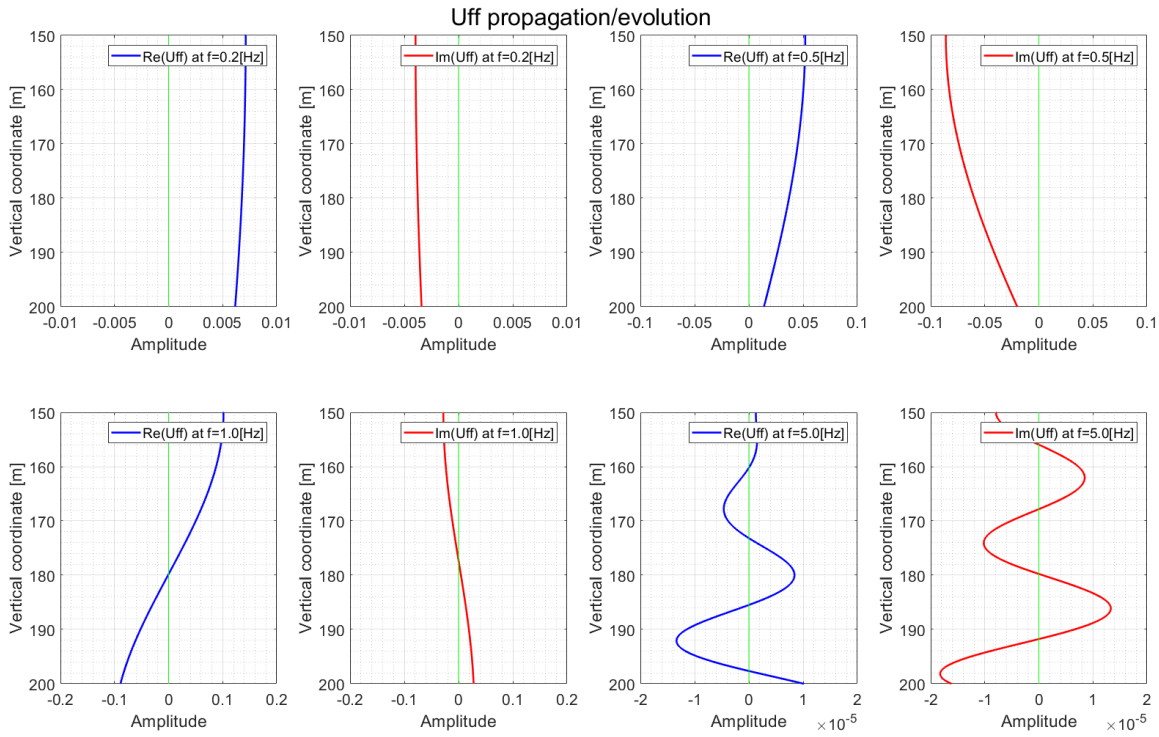

Figure 5-5: Propagation/evolution of the free field motion $U_{ff}(z,\omega)$.

Analyzing Figure 5-5, it is possible to visualize how, for different frequencies, the real part activates the springs and the imaginary part the dashpot. At f=0.2[Hz] (top left), the real part of $U_{ff}(z,\omega)$ is positive, meaning that it is imposing a compression to the springs. The imaginary part is negative, meaning that it is imposing an extension to the dashpots. The situation is similar at f=0.5[Hz]. At f=1[Hz] and at f=5[Hz] it is possible to visualize that both amplitudes (real and Imaginary) oscillates around the non-deformed condition, producing compressions and extensions to the viscoelastic elements.

5.2. Solving the base case with the three steps methodology

5.2.1. Step one: Calculating the equivalent seismic loads at the mudline

As it is detailed in Section 4.1.1, to calculate the equivalent seismic loads at the mudline ($F_{eq}(\omega)$and $M_{eq}(\omega)$), only the embedded part of the pile being excited by the free field motion $U_{ff}(z,\omega)$ is considered, and a clamped connection is introduced at the mudline. Figure 5-6 and Figure 5-7 show the evolution (in the frequency) of these equivalent seismic loads.

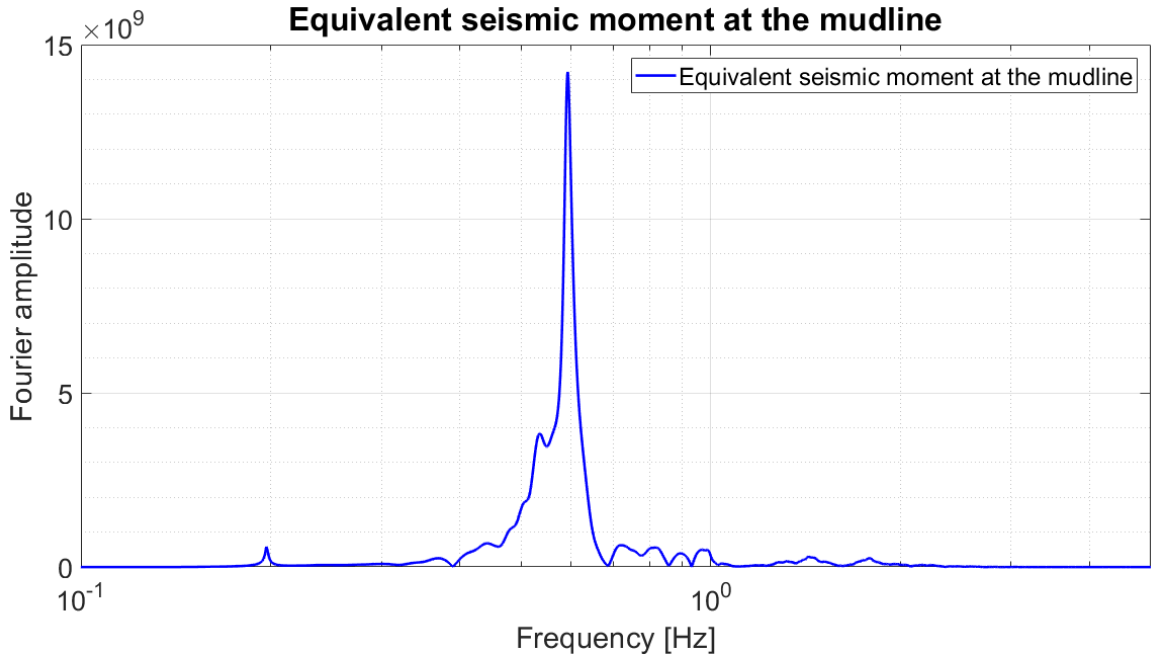

Figure 5-6: Equivalent seismic moment at the mudline.

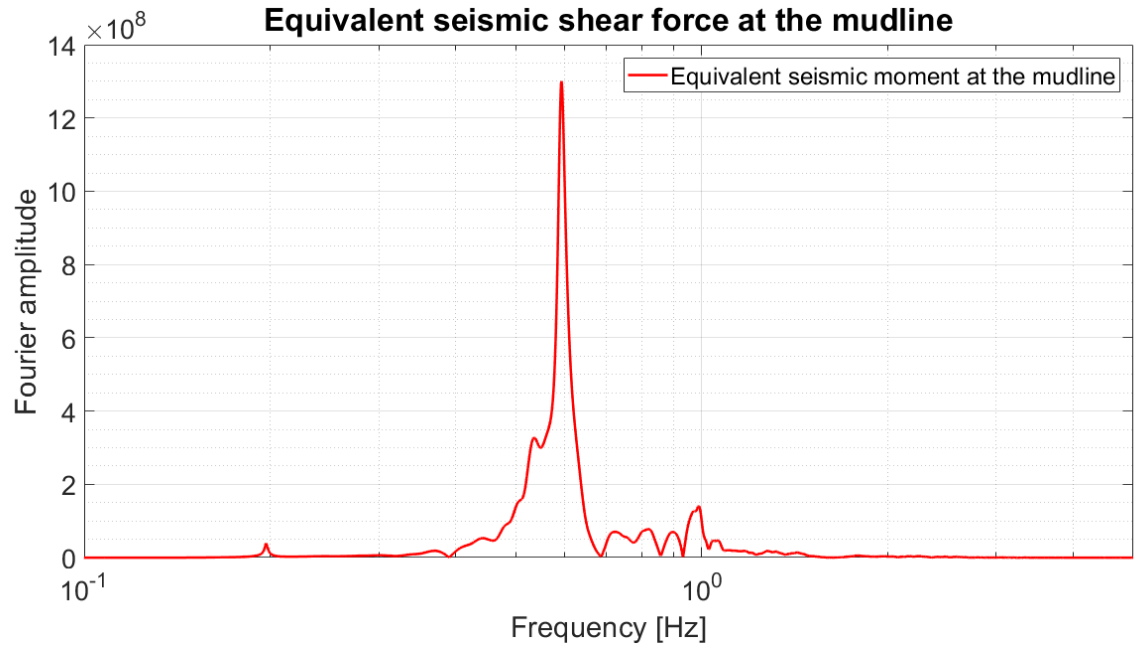

Figure 5-7: Equivalent seismic shear force at the mudline.

As it is expected, both components follow the evolution of the free field motion $U_{ff}(z,\omega)$. How important is the modification of the free field depends mainly on how flexible / rigid is the embedded structure (compared to the soil). When the structure is flexible, then it tends to follow the free field motion around it. This result shows that the pile is not that flexible or rigid, because it alters the free field motion, but not importantly [45]. Additionally, it is possible to visualize the importance of the natural frequencies of the soil profile, since at that frequencies, the equivalent loads show important peaks.

5.2.2. Step two: Pile-soil impedances at the mudline

According to Section 4.1.2, the next step is to calculate the pile – soil impedances at the mudline. After performing the calculations detailed, the results are analyzed in terms of the swaying, rocking and couple swaying/rocking impedance. For the three cases, the real and the imaginary parts are analyzed. Figure 5-8, Figure 5-9 and Figure 5-10 shows the evolution of the swaying, rocking and coupled impedances along the frequency, respectively.

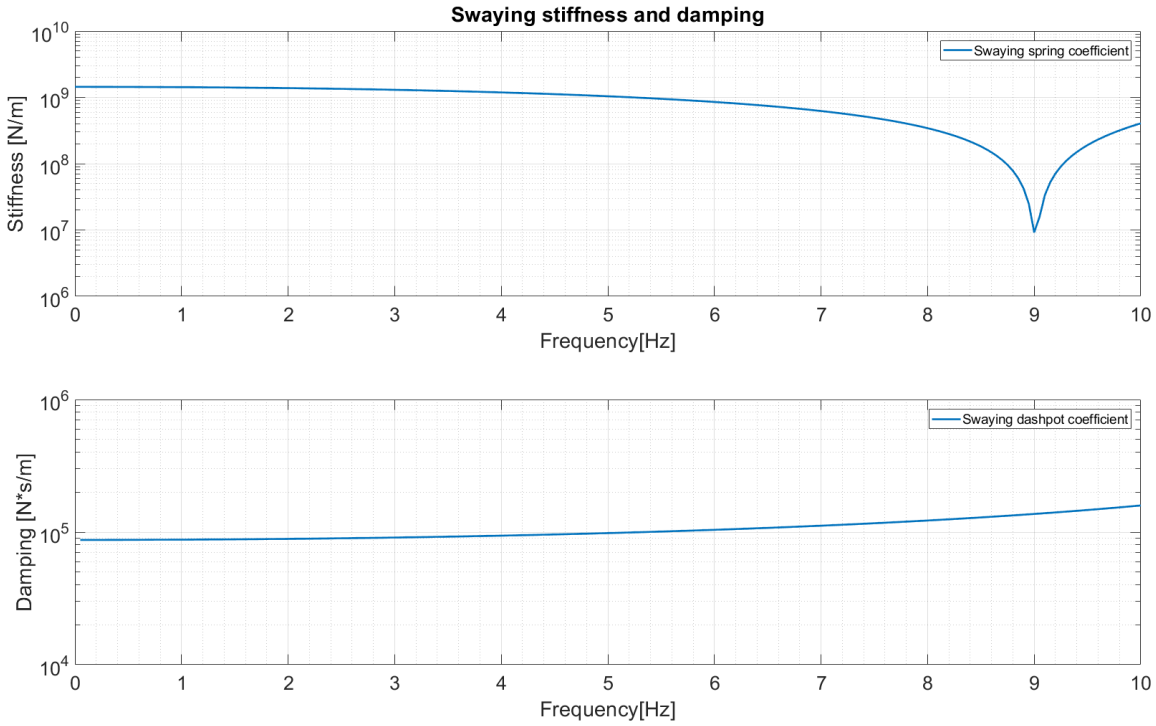

Figure 5-8: Swaying impedances.

The swaying stiffness and dashpot coefficient evolution with the frequency is shown in Figure 5-8. For the stiffness a dependency on the frequency is evident, showing a decrement from the quasi-static case to the resonance case (at frequency equals to 8.92[Hz]). After that frequency there is an increment of the stiffness to decay once again, at the second resonance frequency. For the dashpot coefficient the behavior shows a monotonic increment until the frequency analyzed, meaning that the higher the frequency analyzed, the higher the damping of the system.

The rocking stiffness and dashpot coefficient evolution with the frequency is shown in Figure 5-9. The behavior is similar than the one calculated for the swaying impedances, with the stiffness showing a decrease from the quasi-static condition to the rocking resonance frequency (which is

found at 13.8[Hz], being significantly higher than the swaying one). This is because a pile is much more rigid (larger stiffness), relatively speaking, when subjected to a moment than to a lateral force. This is caused by the important moment of inertia of a pile. This means that the rocking natural frequencies will be higher than the lateral ones.

The dashpot coefficient also shows a monotonic increment from quasi-static condition to higher frequencies.

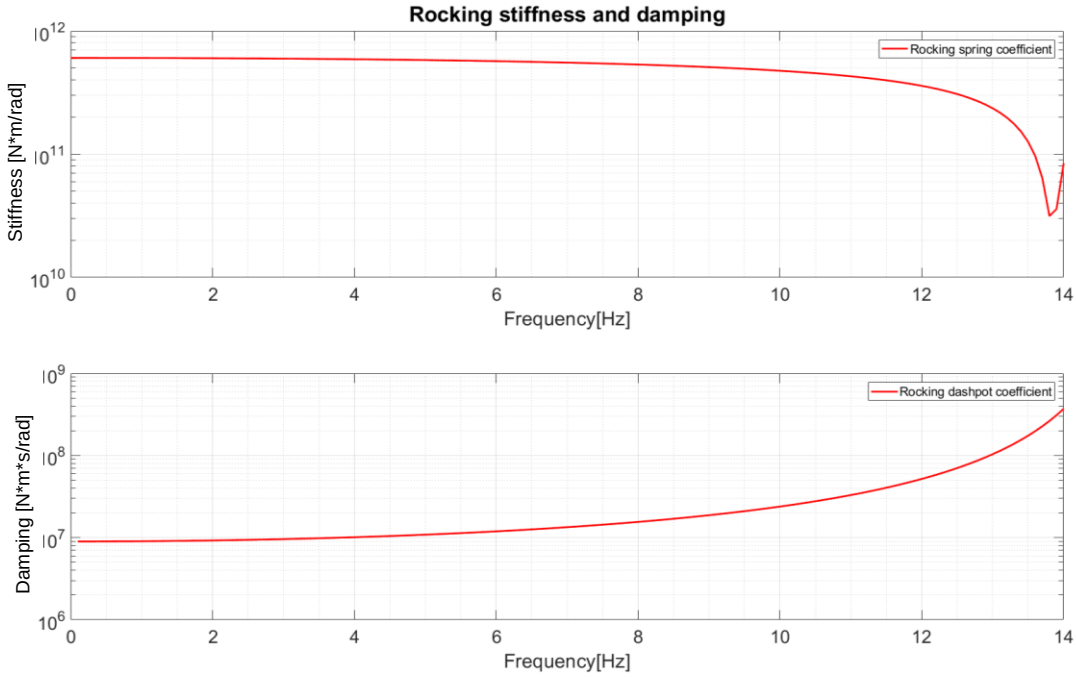

Figure 5-9: Rocking impedances.

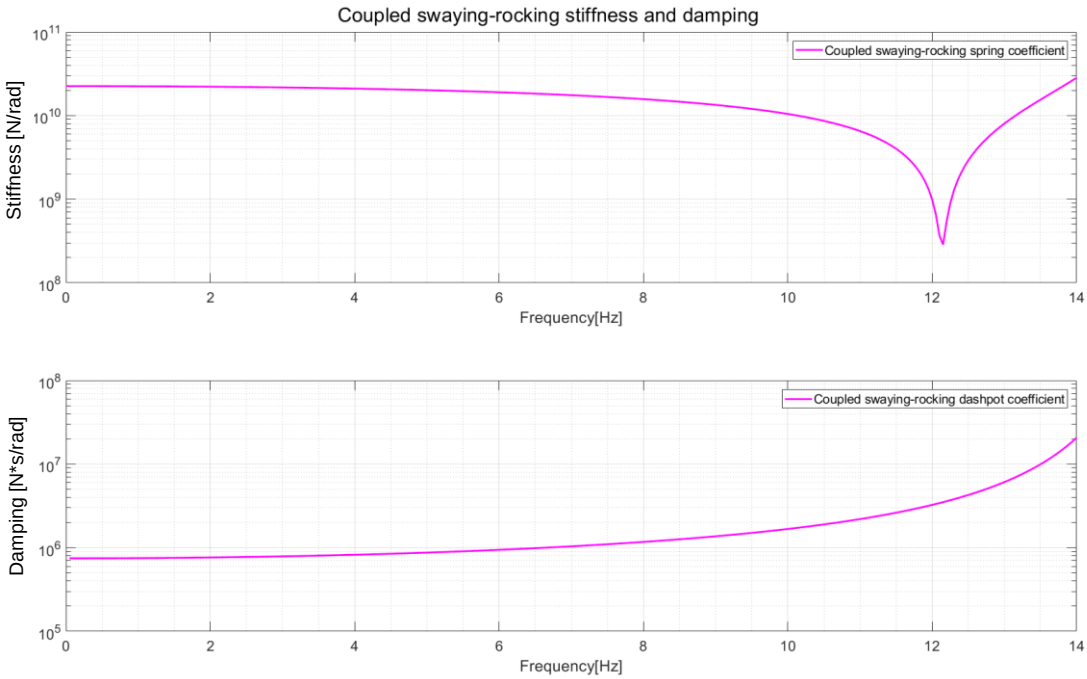

Figure 5-10: Coupled swaying/rocking impedances.

The coupled swaying/rocking stiffness and dashpot coefficient evolution with the frequency are shown in Figure 5-10. The behavior is similar than the one calculated for the swaying and rocking impedances, with the stiffness showing a decrease from the quasi-static condition to the coupled resonance frequency (which is found at 12.15[Hz], being significantly higher than the swaying one). The dashpot coefficient also shows a monotonic increment from quasi-static condition to higher frequencies.

5.2.3. Step three: Solving the coupled problem

Once the steps one and two of the methodology proposed are accomplished, the final step is to solve the coupled problem, meaning that the superstructure is modeled as founded on the impedances calculated in step two, and excited at the mudline node with the equivalent seismic loads calculated in the step one. This model is called the "Coupled Model". An overview of this step is shown in Figure 4-5, where for this particular base case, the equivalent seismic loads at the mudline are obtained in Section 5.2.1, whereas the dynamic impedances are obtained in Section 5.2.2.

5.3. Validating the Single Node SSI Method

The first task after solving the base case problem using the Single Node SSI Method is to validate the solution obtained. With this in mind, the same base case is solved by considering the single step approach described in Section 4.2. When considering this approach, the solution is direct, meaning that no intermediate steps related to a sub structuring procedure are considered. A control point is defined at the tower top of the structure, and the lateral deformation is measured there for both approaches. The properties of these responses are compared in order to validate the three steps method. If they are equivalent, then the methodology proposed is correct. A visualization of the comparison is shown in Figure 5-11.

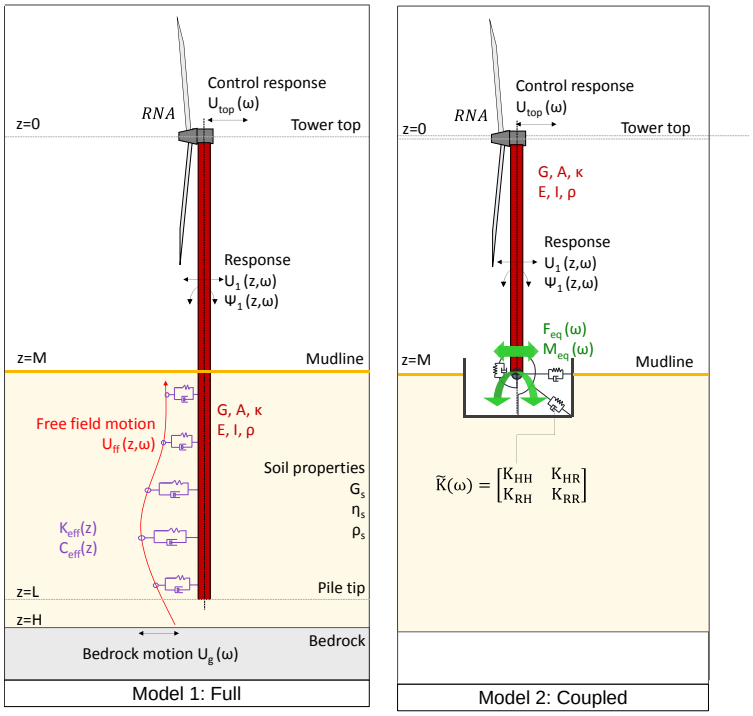

Figure 5-11: Full and coupled model comparison overview.

For the comparison, the full model is identified as Model 1, and the coupled model is identified as Model 2. The control output is defined as the lateral deformation at the tower top, identified as $U_{T1}(\omega)$ for Model 1, and $U_{T2}(\omega)$ for Model 2. As the control output is complex valued, it is adequate to compare every component of it, meaning the real and the imaginary part. It is clear that including the absolute value of the response add no extra information, but it is included for formality reasons.

Figure 5-12 contains the results obtained for the lateral deformation at the tower top in the frequency domain (Fourier-transformed signal). To compare them, they are plotted in the same graph. The top plot contains the real part of the response, the middle plot contains the imaginary part of the response, and the bottom plot contains the absolute value of the response. It can be seen that they match for every frequency analyzed.

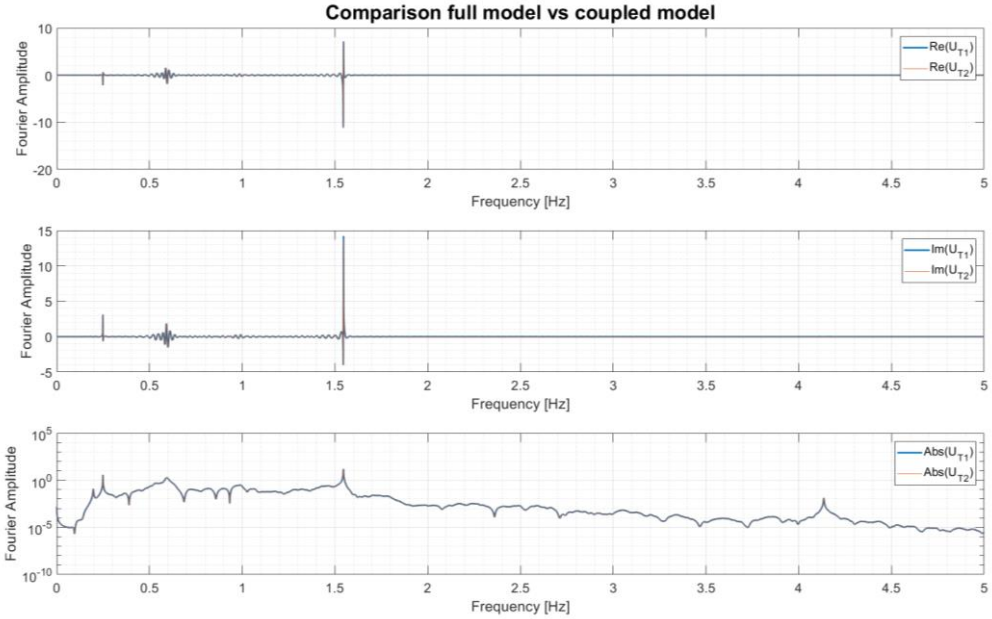

Figure 5-12: Full and coupled model comparison (1)

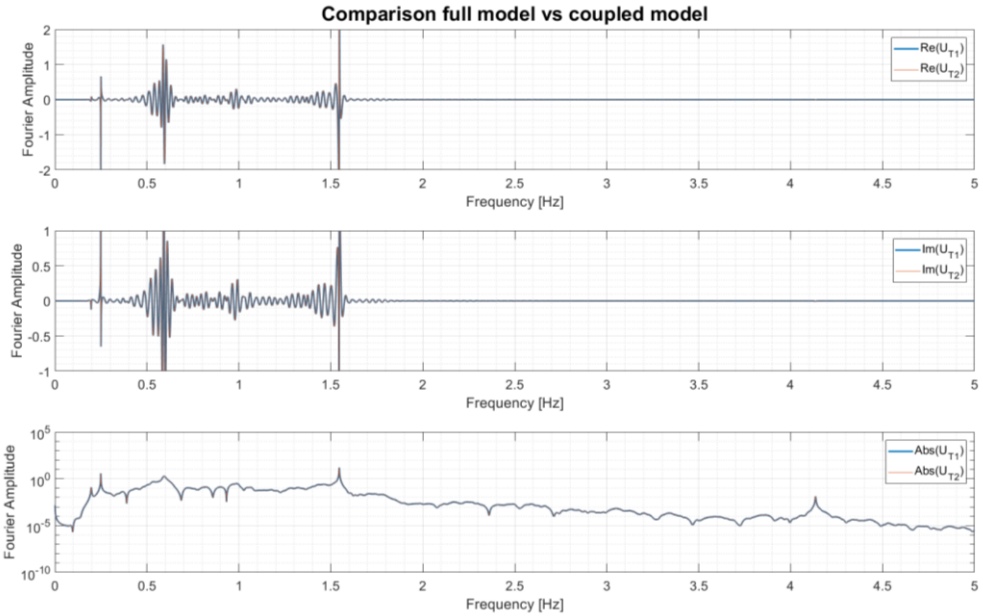

Figure 5-13: Full and coupled model comparison (2)

Figure 5-13 contains the same information, but neglecting the resonances peaks to check small amplitudes. It is clear that the responses are identical. Note that for a Timoshenko beam, the response is measured considering both the lateral deformation and the cross sectional rotation. Therefore it is adequate to compare the responses measuring the cross sectional rotations to confirm that the responses are equivalent.

Figure 5-14 contains the results obtained for the cross sectional rotation at the tower top in the frequency domain (Fourier-transformed signal). To compare them, they are plotted in the same graph. The top plot contains the real part of the response, the middle plot contains the imaginary part of the response, and the bottom plot contains the absolute value of the response. It can be seen that they match for every frequency analyzed.

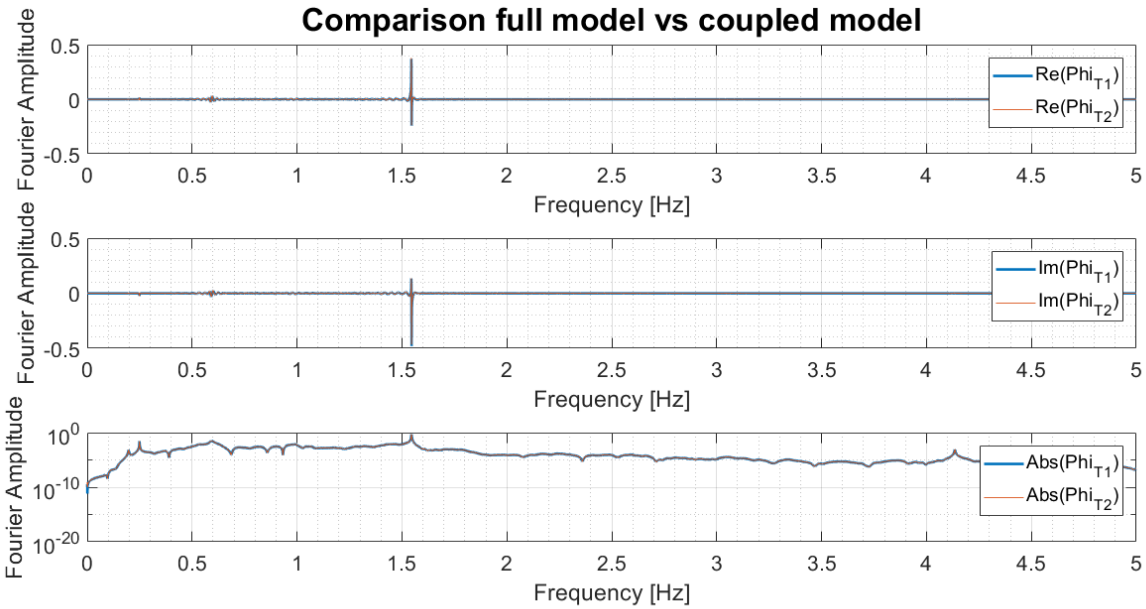

Figure 5-14: Full and coupled model cross sectional rotation comparison.

Now that the three steps methodology proposed is validated, it is adequate to study the results obtained.

5.4. Influence of the SSI on the seismic response

This work focuses on study what is the implication of including the SSI when analyzing the seismic response of a monopile OWT. This section contains the results obtained when comparing the base case solved using the Single Node SSI Method (Section 4.1) and the Classic Method (Section 4.3). Note that the Single node SSI Method is validated in Section 5.3, where it is shown that the response obtained is equivalent than the obtained using the Full Pile SSI Method (4.2). Two models are developed to perform the comparison, one including SSI (Model SSI), and the other one as clamped at the mudline (Model Clamped).

5.4.1. Natural frequencies

The system analyzed (monopile OWT considering SSI) is a non-classical damped system. Therefore it has complex valued eigenfrequencies and eigenmodes. Regarding the eigenfrequencies, the

real part defines the corresponding natural frequency, and the imaginary contains information related to the damping of the corresponding mode. For the eigenmode, the displacements at different locations of the structure are not in phase (as for classical damped systems). The imaginary part contains the information of this phase [58].

An eigenvalue analysis is not included in this work, since the focus is not on evaluating the modal properties of the structures, but to estimate what is the influence of including the SSI in the seismic response. To obtain the natural frequencies of the structure, the Peak Picking Method is considered. This method postulates that close to a resonance frequency, the response (in the frequency domain) is mainly dominated by the contribution of that particular vibration mode, and the contribution of the other vibration modes can be considered as negligible. This method is commonly used in identification of structural systems, and it has strengths and limitations, which are not in the scope of this work, but the interested reader can find more information in the literature [59] [60].

For a better visualization of the peaks in the response in the frequency domain, and therefore for a better estimation of the natural frequencies, a lateral pulse load is applied at the tower top. The responses (measured as the lateral deformation at the tower top) for the two cases analyzed, the base case considering a) the clamped model representing he classic seismic approach and b) the Single Node SSI method, are visualized in Figure 5-15.

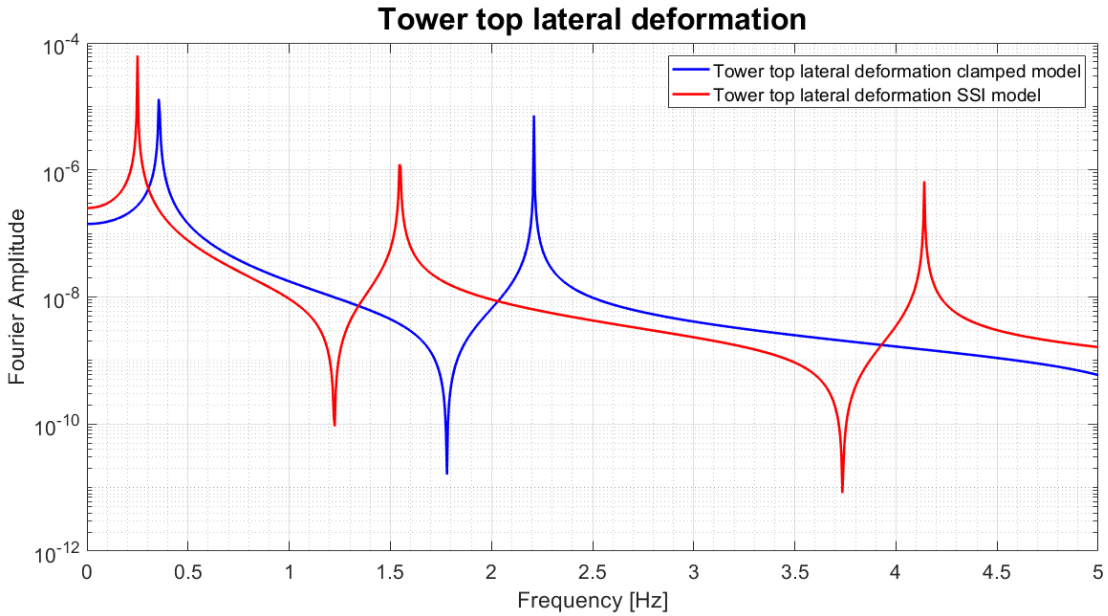

Figure 5-15: Tower top deformation in frequency domain for pulse load (Clamped model and SSI model).

It is possible to visualize the lateral deformation at the tower top for the two models. In blue the clamped model and in red the model including SSI. The first three natural frequencies of the clamped model are located at 0.35[Hz] at 2.21[Hz] and at 4.14[Hz]. For the SSI model the first two of them are located at 0.25[Hz] and at 1.5[Hz]. The third natural frequency is not present at the frequency range analyzed. It is clear that there is a shift to more flexible natural frequencies when incorporating the SSI. This is caused by the inclusion of the impedances at the mudline node of the Coupled Model. Since this impedance contains a spring and a dashpot, it is expected for the system to be more flexible than considering a fixed connection. This elongation in the natural periods of vibration can influence importantly the seismic performance of the structure, since the seismic input generally depends on how stiff/flexible is the structure analyzed.

5.4.2. Tower top displacement / acceleration

Key metrics of the response of a monopile OWT are the tower top displacements and accelerations. The equipment installed at this point is particularly sensible to motions; therefore it is adequate to compare these values measured performing the classical seismic analysis (clamped model neglecting the SSI) and the seismic analysis including SSI. The lateral deformation at the tower top is shown in Figure 5-16:

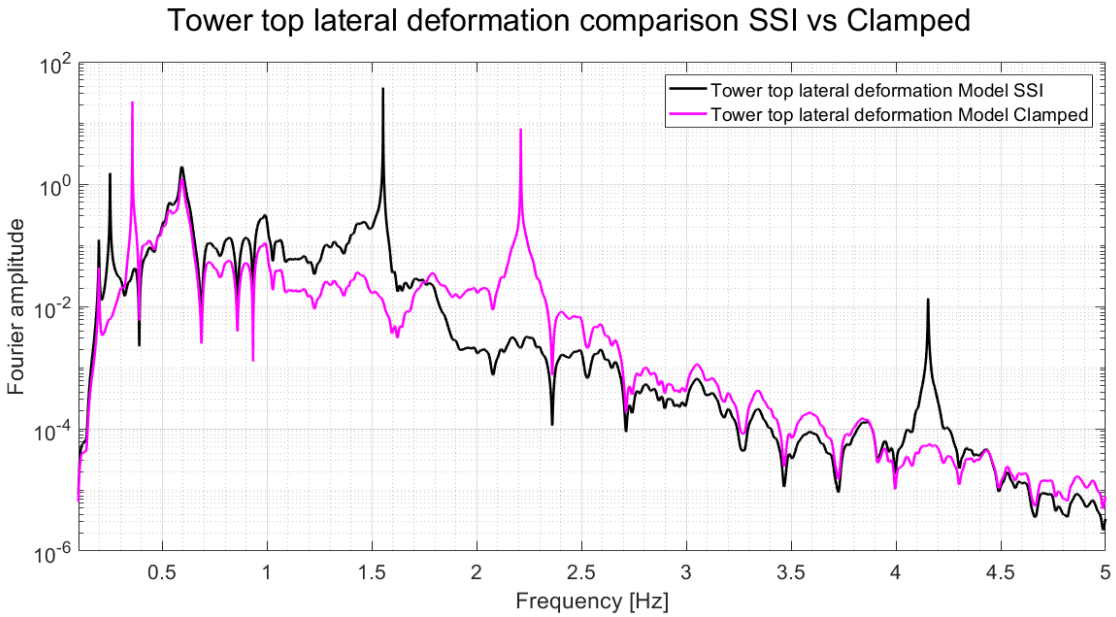

Figure 5-16: Tower top deformation in frequency domain (Clamped model and SSI model).

It can be observed that the natural frequencies of the Model SSI are located (as expected) at 0.25[Hz], 1.55[Hz] and 4.14[Hz]). Now the amplitude of the vibration at the first mode is no longer larger than the vibration in the second mode (as it was the case for the pulse excitation). This is caused by earthquake excitation (described by the equivalent seismic lateral force and moment). Figure 5-6 and Figure 5-7 shows that at 0.25[Hz] its influence is lower compared to the influence at 1.55[Hz]. For the Model Clamped, the natural frequencies are 0.35[Hz] and 2.21[Hz]. For this case, the amplitude of the vibration at the first mode is larger than the one at the second mode. This is due to the influence of the seismic loads, since at 0.35[Hz] it is more important compared to the influence at 2.21[Hz].

The accelerations of both models measured at the tower top are shown in Figure 5-17. The natural frequencies are clearly (and correctly) identified. Regarding the amplitudes of the response, it is possible to visualize that for the Model SSI, the most important vibration is at the second natural frequency (the same as for the deformations). For the Model Clamped, however, it is possible to visualize that the vibration at the first natural frequency is no longer the most important, being the most relevant one at the vibration at the second natural frequency.

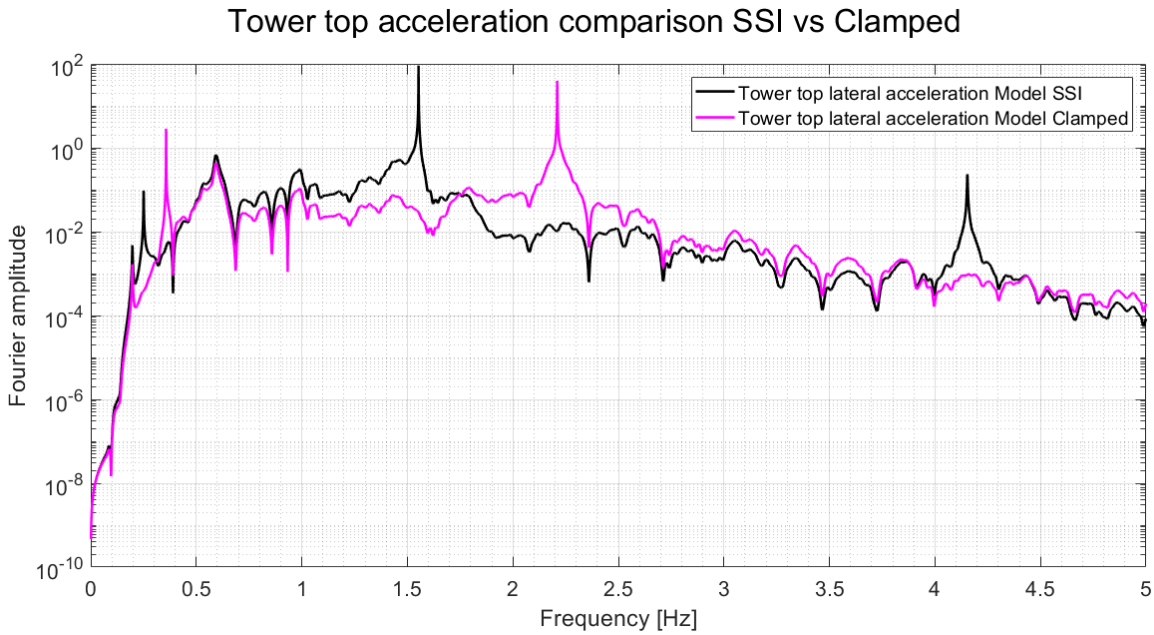

Figure 5-17: Tower top acceleration in frequency domain (Clamped model and SSI model).

It can be seen that the influence of the equivalent seismic load is strong in the spectra (displacement and accelerations). The presence of the earthquake can be observed not only in the magnitude, but also in several peaks along the signal. A small peak is observed at 0.19[Hz], related to the first natural frequency of the soil stratum (contained in the equivalent seismic load). The first natural frequency of the Model SSI appears at 0.25[Hz], to then evidence another two peaks at 0.59[Hz] and at 0.98[Hz] (related to a resonance frequency of the soil stratum). At 1.55[Hz] and at 4.15[Hz], the second and third natural frequencies of the Coupled Model are present. The natural frequencies of the soil profile can be consulted in Table 5-2.

When comparing Figure 5-16 and Figure 5-17, one can visualize the influence of the SSI in the seismic performance of the monopile OWT. For this case, larger deformations are expected at the tower top when considering the SSI since its response measured as the lateral deformation is slightly larger for the relevant frequency range. Additionally, larger accelerations are expected at the tower top when including the SSI since the response is slightly larger in the relevant frequency range..

5.4.1. Bending moment at the tower top and at the tower midpoint

Another relevant metric of the seismic response of the structure is the distribution of bending moments along the tower. Two control points are selected to visualize the influence of the SSI: the tower top and the tower midpoint.

Figure 5-18 shows the bending moment at the tower top for the Model SSI and the Model Clamped. Again the importance of the natural frequencies of the structures in the response is evident. For the Model SSI the vibration at the second natural frequency dominates the response. For the Model Clamped, the contribution of the vibration at the first and second natural frequencies is comparable. Figure 5-19 shows the bending moment at the tower midpoint for both models. As it is expected, the values are larger than at the tower top. Comparing Figure 5-18

and Figure 5-19 it is possible to visualize a tendency showing that the bending moments, for this particular case, are larger when including the SSI.

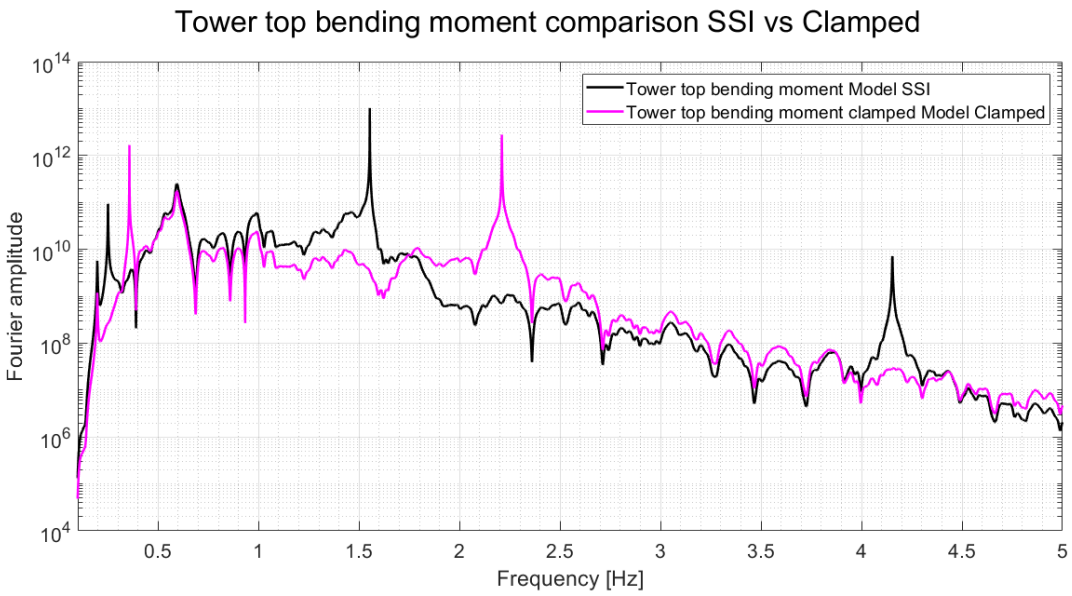

Figure 5-18: Tower top bending moment in frequency domain (Clamped model and SSI model).

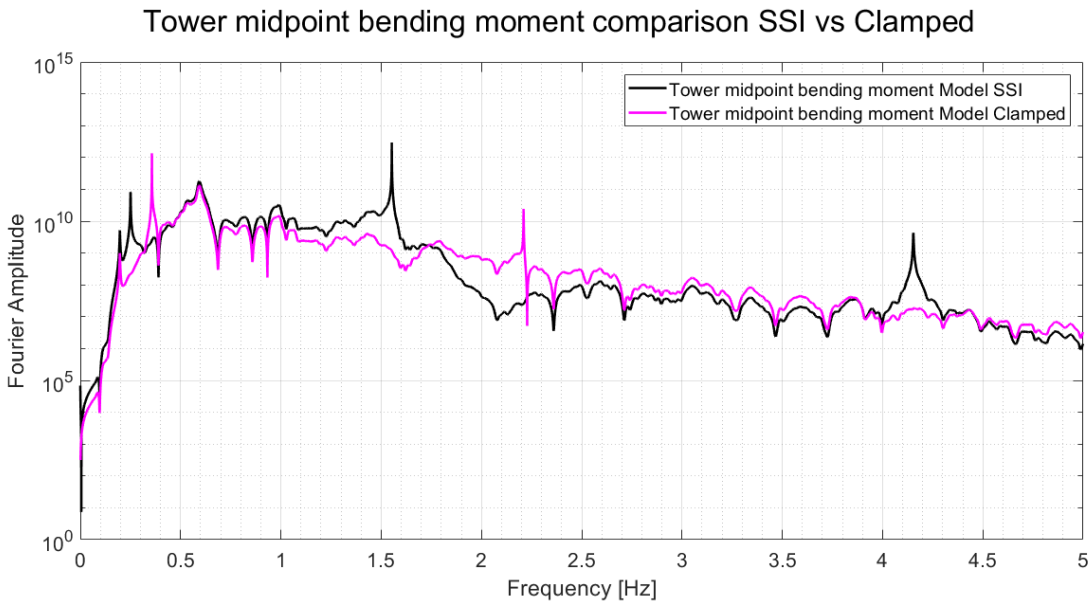

Figure 5-19: Tower midpoint bending moment in frequency domain (Clamped model and SSI model).

5.5. Extrapolating the Single Node SSI Methodology to 3D case

An additional application of the Single Node SSI Methodology proposed can be analyzed: Its application to a generic three dimensional case. For this purpose, a basic 3D model is shown in Figure 5-20. The soil is modelled as a volume (blue) and the pile is embedded in the soil (red). From the mudline to the tower top, the superstructure is modelled as a beam element, including a concentrated mass (it can also include the rotational inertia) at the tower top, representing the RNA. The seismic ground motion is assumed to be known at the bedrock, and the waves are being propagated in the soil volume, represented as red arrows.

This section contains a brief explanation about how the Single Node SSI can be applied to this generic case.

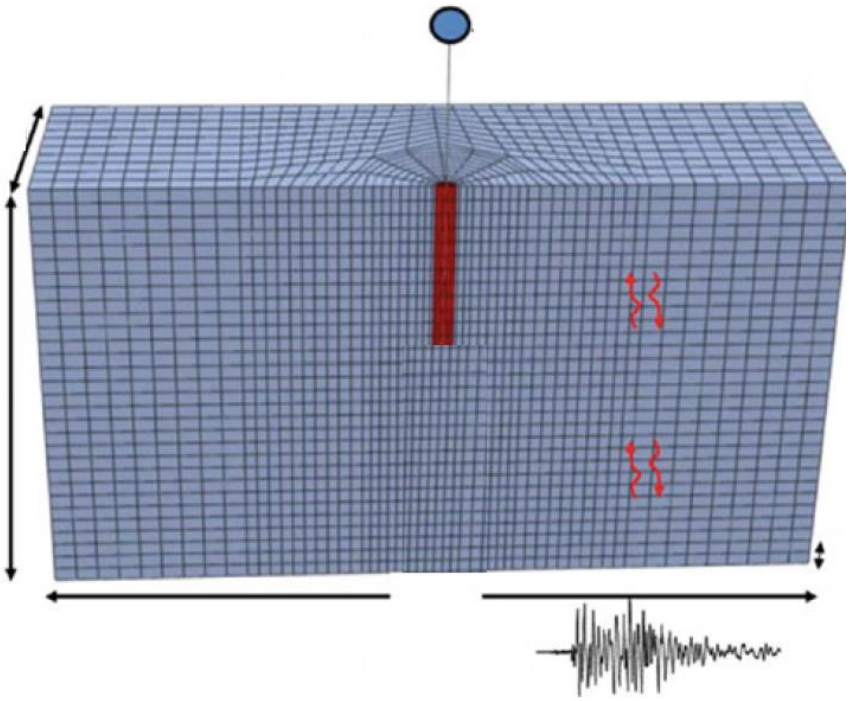

Figure 5-20: Generic 3D case [20].

A key aspect about this procedure is how to determine the propagation of the seismic waves into the soil volume. As it is explained in Chapter 2, this can be done through more than one way (analytical or approximate using for instance, a finite elements model). The alternative selected to perform this is not relevant for the extrapolation of the proposed methodology for the three dimensional case. One can assume, for instance, that an adequate finite elements model is implemented.

As it is detailed in Section 4.1, the first step is to calculate the equivalent seismic forces at the mudline level. To do so, a clamped connection for the pile is defined at that level, as it is visualized in Figure 5-21. When solving this problem, meaning that the seismic motion at the bedrock generates waves being propagating into the soil volume, these waves interact with the pile, and then the reactions at the mudline due to the presence of clamped connection are identified as the equivalent seismic forces (green arrows). Note that in this case, these equivalent

seismic forces have six components: three forces in the x, y and z direction, Fx, Fy and Fz respectively; and three moments around each axis, Mx, My, Mz.

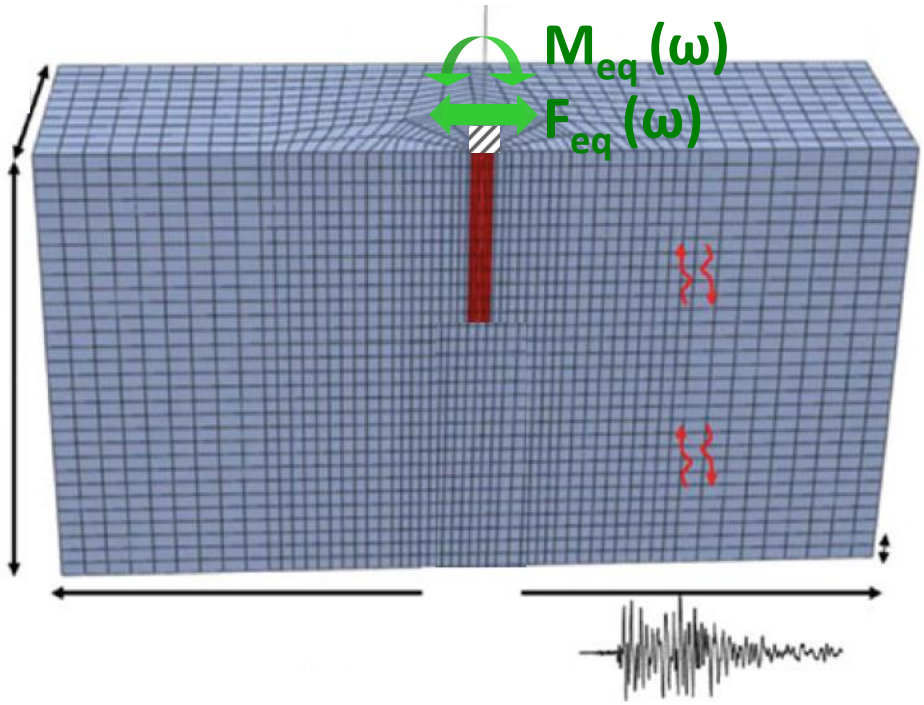

Figure 5-21: Generic 3D case [20].

The second step is to calculate the dynamic impedances. To do so, the basic same procedure described in Section 4.1.2 has to be followed, meaning that a unit displacement and rotation is applied at the mudline, following each of the directions/rotations (displacement along x, y, z; and rotation around x, y and z). The reactions obtained after performing this procedure, are defined as the impedances at the mudline.

The third step is equivalent to the procedure described in Section 4.1.3, meaning that the superstructure can be modelled founded on these impedances calculated in the second step, and excited by the equivalent seismic forces calculated in the first step.

If all the properties on the model are linear, then it will be equivalent to solve the full three dimensional problem, or the problem considering the Single Node SSI Model extrapolated to the 3D case.

6. Conclusions and further research

This chapter includes the main conclusions of this research, as well as a brief discussion on each of them. Finally, recommendations and potential future research topics are included.

6.1. Conclusions

The goals and objectives defined at the beginning of this work are recalled at this point:

The goal is to answer the question:

- **What is the influence of the frequency dependent SSI on the seismic response of a monopile OWT"**

And the three intermediate objectives:

1. Create a methodology to model a monopile OWT which is able to catch the frequency dependent SSI when performing a seismic analysis.

2. Since the seismic load is defined in the soil, originated by seismic waves travelling through the soil: What is the influence of the soil column in the definition of the load?

3. Considering that the seismic load is the product of a wave field interacting with the SSI system between the pile and the soil: What is the influence of the SSI in the definition of the loads?

Regarding the objective 1, a Single Node SSI Method is implemented. This methodology is an approach of the substructure method analysis and it can be described as:

- Step one: Estimate the equivalent seismic loads at the mudline level.
- Step two: Calculate the frequency dependent pile-soil impedances (dynamic stiffness matrix) at the mudline level.
- Step three: Solve coupled problem, by calculating the dynamic response of the superstructure being founded on the frequency dependent dynamic impedances calculated in step 2, and excited by the equivalent seismic loads calculated in step 1, being applied at the mudline node.

To validate the methodology, a representative base case was solved by implementing it. The solution was then compared against the one obtained for the same case, but considering another described method: the Full Pile SSI Method. The two solutions obtained are equivalent; therefore the three steps methodology and its implementation are validated.

Regarding objectives 2 and 3, it is concluded that the dynamic behavior of the complete soil column plays an important role in the seismic response of the monopile OWT. It was found that close to the soil column natural frequencies, the equivalent seismic loads (shear force and overturning moment) present important peaks. Based on this, a recommendation for designers of this kind of projects, is that the soil properties governing the dynamic behavior of it (shear modulus, density, damping coefficient and profile depth from bedrock to mudline) should be known.

Additionally, it was found that the seismic waves interact with the embedded pile when exciting it. Even when original signal (bedrock motion and free field motion) are perfectly lateral, the equivalent seismic load at the mudline contains an important overturning moment. Considering the nature of the equipment installed at the tower top, this overturning moment can play an important role in the design/operation of the structure, since strict restrictions related to the motion at the tower top are requested by the different design codes.

Together with the calculation of the equivalent seismic loads at the mudline, the impedances at the same level were calculated. These impedances contain a real part (related to the dynamic stiffness, frequency dependent) and an imaginary part (related to the damping). They are modeled as a set of springs and dashpots, covering the swaying, rocking and coupled swaying rocking directions. Including the springs lead to an elongation of the natural vibration period of the system analyzed and the dashpots is traduced as an extra source of damping in the system.

The case analyzed confirms that the impedances calculated at the mudline representing the (springs and dashpots) are frequency dependent. The springs elements reduce their stiffness from the quasi – static (frequency equals to zero) to their own natural vibration frequencies. However, these natural vibration frequencies are observed to be far from the rest of the important frequencies governing the seismic problem (soil stratum natural frequencies, fundamental frequencies of the structure and energy content of the earthquake. However, this cannot be generalized, and it should be evaluated case by case. For instance, it can occur that the natural frequencies of the pile-soil system move to the relevant frequency range (in case of liquefaction of the surrounding soil). If that is the case, then the stiffness and dashpots can modify their properties drastically, therefore the frequency dependency becomes relevant.

The Single Node SSI Methodology can be extrapolated to a three dimensional case, meaning that all the properties of the pile – soil interaction can be represented using a set of impedances at the mudline level. Additionally, it is possible to determine the equivalent seismic forces at the mudline level. Then the superstructure can be analyzed as founded on the impedances and excited by these equivalent seismic forces at the node defined at the mudline level. If the properties of the system are linear, then this is equivalent to solve the full three dimensional problem at once.

6.1. Recommendations and further research

There is a long way to fully determine, implement and understand the influence of the SSI in the seismic performance of a monopile OWT. In that sense, this work can be considered as a step in that direction. As a part of this knowledge trip, it is possible to visualize a set of recommendations when facing a project of this kind.

It was concluded that soil column and the pile soil interaction system have a strong influence on the seismic response of the structure, not only due to the amplification of the S waves, but also due to the inclusion of an overturning moment at the mudline. In many cases, the design codes do not consider this component and allow the seismic analysis to neglect it; however the recommendation is to verify the influence of this component on the structural response.

It was found that the soil column strongly influences the seismic response at mudline. Therefore, it is recommended to include the local soil profile to determine the seismic input for a project.

Since it was found that the inclusion of the SSI in the allows a more accurate calculation of the natural frequencies of the structure, another recommendation is to pay special attention to the elongation of the natural vibration period and how similar can it be compared to the natural vibration period of the other dynamic components of the system (soil column and frequency content of the). If they are close enough, resonances can occur, leading to amplifications in the deformations and stresses along the structure.

Since the Single Node SSI Methodology proposed is based on the substructure method analysis, only linear properties at every component of the model can be considered. Therefore, a future line of investigation should be related to how to include non-linear properties when including SSI in the evaluation of the seismic performance of a monopile OWT, including aerodynamic damping, hysteretic behavior of the soil and liquefaction around the monopile.

A model is an abstraction of the reality, and the one developed in this work simplifies some aspects of it. Another possible future research is related to the improvement of the model considered in the three steps methodology proposed. The good news is that the method will be valid when a more sophisticated model is included. The key aspect is to define the new properties in the fundamental EOM, BC and IC described in this work. An improvement in the model can be incorporated by considering elements of the structure itself (additional masses along the monopile, damping at the tower top or extra restriction due to friction at the pile tip), or in the definition of the pile – soil interaction properties.

Due to the strong correlation between potential offshore wind locations and seismic regions around the globe, it is expected that new monopile OWT project are going to be developed. The challenge for the engineers involved in these projects is to fully understand the seismic response of these structures, in order to develop smart and efficient structures. The methodologies described on this work can be used as an important tool to achieve this goal.

7. Bibliography

[1] IEA, "Energy Technology Perspectives 2017," IEA, Download from: http://www.iea.org/etp2017/, 2017.

[2] USGS, "Earthquake Facts and Statistics," [Online]. Available: https://earthquake.usgs.gov/earthquakes. [Accessed 13 August 2018].

[3] R. de Risi, "Seismic performance assessment of monopile-supported offshore wind turbines using unscaled natural earthquake records," *Soil Dynamics and Earthquake Engineering,* vol. 109, pp. 154-172, 2018.

[4] EWEA, "The European Offshore Industry-Key Trends and Statistics 2015," EWEA, 2015.

[5] DNV/Risø, "Guidelines for design of wind turbines," Det Norske Veritas/Wind Energy Department, Risø, Copenhagen/Roskilde, 2002.

[6] L. Rosales, "Seismic analysis on mopolile based offshore wind turbines including aero-elasticity and soil-structure interaction," TU Delft - Siemens, Delft, The Netherlands, 2016.

[7] Siemens Gamesa, "Siemens Gamesa corporate website," 2018. [Online]. Available: https://www.siemensgamesa.com. [Accessed 10 August 2018].

[8] M. Beer, Encyclopedia of earthquake engineering, Heidelberg: Springer, 2015.

[9] Y. Ishiyama, "Introduction to earthquake engineering and seismic codes in the world," Hokkaido University, Sapporo, 2011.

[10] GL, "Guideline for the certification of wind turbines," Germanischer Lloyd, Hamburg, 2010.

[11] IEC, "IEC 61400 Ed. 3: Wind turbines - Part 1: Design requirements," International Electrotechnical Comission, 2005.

[12] ICC, "International building code," International Code Council, Country Club Hills, 2012.

[13] British Standards Institution, Eurocode 8 Design of structures for earthquake resistance, London: British Standards Institution, 2004.

[14] API, "Recommended practice for planning, designing and constructing fixed offshore platforms, API," American Petroleum Institute, Washington, DC, 2000.

[15] V. Valamanesh, "Aerodynamic Damping and Seismic Response of Horizontal Axis Wind Turbine Towers," *Journal of Structural Engineering, 140 (11),* p. 04014090, 2014.

[16] Kausel, Advanced Structural Dynamics, Cambridge: Cambridge University Press, 2017.

[17] A. Tsouvalas, "CIE5260 Structural response to earthquakes: Lecture notes," Delft University of Technology, Delft, 2016.

[18] Pecker, "Seismic Analyses and Design of Foundation Soil Structure Interaction," in *Perspectives on European Earthquake Engineering and Seismology. Geotechnical, Geological and Earthquake Engineering, vol 2*, Springer, Cham, 2015, pp. 153-162.

[19] E. a. R. J. Kausel, "Soil Structure Interaction for Nuclear Containment Structures," in *ASCE, Power Division Specialty Conference*, Boulder, 1974.

[20] J. Jia, Soil Dynamics and Foundation Modeling: Offshore and Earthquake Engienering, Cham: Springer, 2018.

[21] I. Chowdhury, Dynamics of structure and foundation - A unified approach, Taylor & Francis Group: London, 2009.

[22] G. Gazetas, "Seismic response of end-bearing single piles," *Soil Dynamics and Earthquake Engineering Vol. 3,* pp. 82-93, 1984.

[23] G. Gazetas, Foundation Vibration, pages 553 -593, Boston, MA: Springer US, 1991.

[24] E. Winkler, "Die Lehre Von Elasticitaet Und Festigkeit 1st edn," *H. Dominicus Prague,* 1867.

[25] T. Nogami, "Time domain flexural response of dynamically loaded single pile," *Journal of Engineering Mechanics,* vol. 114, no. 9, pp. 1512-1525, 1989.

[26] Nogami, "Nonlinear soil-pile interaction model for dynamic lateral motion," *Journal of Geotechnical Engineering,* vol. 118, no. 1, pp. 89-106, 1992.

[27] N. Allotey, "A numerical study into lateral cyclic nonlinear soil–pile response," *Canadian Geotechnical Journal,* vol. 45, no. 9, p. 1268–1281 , 2008.

[28] M. Ashour, "Lateral loaded pile response in liquefied soil," *Journal of Geotechnical and Geoenvironmental Engineering, ASCE,* vol. 129, no. 6, pp. 404-414, 2003.

[29] T. Abdoun, Soil dynamics and soil-Structure interaction for resilient infrastructure : Proceedings of the 1st geoMEast international congress and exhibition, egypt 2017 on sustainable civil infrastructures, Cham: Springer International Publishing, 2018.

[30] A. Selvadurai, Elastic Analysis of Soil-Foundation Interaction, Amsterdam: Elsevier Scientific Publishing Cmpany, 1979.

[31] D. Basu, "A continuum-based model for analysis of laterally loaded piles in layered soils," *Geotechnique,* vol. 59, no. 2, pp. 127-140, 2009.

[32] A. Tsouvalas, "A three-dimensional vibroacoustic model for the prediction of underwater noise from offshore pile driving," *Journal of Sound and Vibration,* vol. 333, no. 8, pp. 2283-2311, 2014.

[33] N. Bazeos, "Static, seismic and stability analyses of a prototype wind turbine steel tower," *Engineering Structures,* vol. 24, p. 1015–1025, 2002.

[34] M. Hongwang, "Seismic analysis for wind turbines including SSI combining vertical and horizontal earthquake," in *15th World Conference on Earthquake Engineering*, Lisboa, 2012.

[35] E. Sapountzakis, "Nonlinear response of wind turbines under wind and seismic excitations with soil-Structure interaction," *Journal of Computational and Nonlinear Dynamics,* vol. 10, no. 4, pp. 041007-01-15, 2014.

[36] A. Kampitsis, "Seismic soil-pile-structure kinematic and inertial interaction - a new beam approach," *Soil Dynamics and Earthquake Engineering,* vol. 55, pp. 211-224, 2013.

[37] G. Alamo, "Dynamic soil-structure interaction in offshore wind turbines on monopiles in layered seabed based on real data," *Ocean Engineering,* vol. 156, pp. 14-24, 2018.

[38] G. Alamo, "Efficient numerical model for the computation of impedance functions of inclined pile groups in layered soils," *Engineering Structures,* vol. 126, pp. 379-390, 2016.

[39] R. D. Laora, "Insight on kinematic bending of flexible piles," *Soil Dynamics and Earthquake Engineering,* vol. 43, pp. 309-322, 2012.

[40] H. Zuo, "Dynamic analyses of operating offshore wind turbines including soil structure interaction," *Engineering Structures,* vol. 157, pp. 42-62, 2018.

[41] S. Kramer, Geotechnical eartquake engineering, Upper Saddle River: Prentice-Hall, 1996.

[42] N. Yoshida, Seismic Ground Response Analysis, Heidelberg: Springer Netherlands, 2015.

[43] A. Kaynia, K. Fan, S. Ahmad, G. Gazetas and E. Kausel, "Kinematic seismic response of single piles and pile groups," *Journal of Geotechnical Engineering,* vol. 117, no. 12, pp. 860-1879, 1991.

[44] A. Kaynia and E. Kausel, "Dynamic stiffnesses and seismic response of pile groups (Doctoral dissertation)," Deptartment of Civil Engineering MIT, Cambridge, Massachusetts, 1982.

[45] N. Makris and G. Gazetas, "Dynamic pile soil pile interaction. Part 2: Lateral and seismic response," *Earthquake engineering and structural dynamics vol. 21,* pp. 145-162, 1992.

[46] M. Kavvadas and G. Gazetas, "Kinematic seismic response and bending of free head piles in layered soil," *Geotechnique,* vol. 43, pp. 207-222, 1993.

[47] G. Madabhushi, Design of pile foundations in liquefiable soils, London: Imperial College Press, 2010.

[48] Roesset, "Soil amplification of earthquakes," *Numerical Methods in Geotechnical Engineering,* 1977.

[49] D. Boore, "Processing of strong-motion accelerograms: needs, options and consequences," *Soil Dynamics and Earthquake Engineering 25,* pp. 93-115, 2005.

[50] I. Towhata, Geotechnical Earthquake Engineering (Springer series in geomechanics and geoengineering), Berlin: Springer, 2008.

[51] W. Versteijlen, "Effective soil-stiffness validation: Shaker excitation of an in-situ monopile," *Soil Dynamics and Earthquake Engineering,* pp. 241-262, 2017.

[52] J. Roesset, "Dynamic stiffness of piles," *Numerical Methods in Ofshore Piling, Institution of Civil Engineers,* pp. 75-80, 1989.

[53] M. Shrikhande, Finite element method and computational structural dynamics, Delhi: PHI Learning Private Limited, 2014.

[54] J. Mendoza, "State-space representation for structural dynamics," Massachusetts Institute of Technology Press, Cambridge, 1996.

[55] G. Takács, Model Predictive Vibration Control, London: Spinger, 2012.

[56] W. Versteijlen, "Dynamic soil stiffness for foundation piles: Capturing 3D continuum effects in an effective, non-local 1D model," *International Journal of Solids and Structures 134,* p. 272–282, 2018.

[57] Sinotech, "Foundation FEED and detailed design of Formosa I offshore wind farm phase 2: Probability seismic hazard assesment report," Sinotech Engineering Consultants, Taipei City, 2017.

[58] A. Chopra, Dynamics of structure : Theory and applications to earthquake engineering, Upper Saddle River: Pearson/Prentice Hall, 2007.

[59] E.-M. Lourens, "System identification and modal testing," TUDelft lecture of the course OE44055 Load Identification and Monitoring of Structures, Delft, 2016.

[60] E. Chatzi, "Identification methods for structural systems," Eidgenossiche Technische Hochschule Zurich Lecture, Zurich, 2013.

[61] Y. Lu, "Seismic soil structure interaction in performance based design (Doctoral dissertation)," University of Nottingham, Nottingham , 2016.

[62] Badallo, "Frequencies extraction of a cantilever beam using finite element modelling," Eduacero, Vol. 2, Number 2, Madrid, Spain, 2013.

[63] Kwon, The finite element method using MATLAB, New York, USA: CRC Press LLC, 1997.

[64] Siemens-Gamesa, "Seismic Analysis Procedures for BHawC 7.3," Siemens Wind Power, The Hague, 2017.

[65] S. K. Duggal, Earthquake-Resistant, New Delhi, India: Oxford University Press, 2013.

[66] B. Hamilton, "Offshore Wind Market and Economic Analysis: Annual Market Assessment," Navigant Consulting, Inc., Burlington, MA, 2013.

[67] R. HE, "Vertical elastic dynamic impedance of a large diameter and thin-walled cylindrical shell type foundation," *Soil Dynamics and Earthquake Engineering, Volume 95,* pp. 138-152, 2017.

[68] A. Simone, "An introduction to the analysis of slender structures," Delft University of Technology, Delft, 2011.

[69] D. Hyawn, "Seismic fragility analysis of 5 MW offshore wind turbine," *Renewable Energy,* pp. 250-256, 2014.

[70] A. Duarte, "Incorporating time domain representation of impedance functions into nonlinear hybrid modelling," University of Toronto, Toronto, 2013.

[71] T. Letcher, Wind energy engineering: A handbook for onshore and offshore wind turbines, London: Academic Press, 2017.

[72] D. Kim, "A simplified method to predict fatigue damage of offshore riser subjected to vortex-induced vibration by adopting current index concept," *Ocean Engineering 157,* pp. 401-411, 2018.

[73] M. Kroon, "Design method for multifunctional reefs in a coastal environment," Delft Univeristy of Technology MSc Thesis Report, 2016, 2016.

[74] L. Padron, "Dynamic stiffness of deep foundations with inclined piles," *Earthquake engineering and structural dynamics Vol.39,* pp. 1343-1367, 2010.

[75] G. Wang, "Nonlinear analysis of a soil drilled pier system under static and dynamic axial loading," Pacific earthquake engineering research center, Berkeley, 2006.

[76] B. Friedland, "Control System Design - An Introduction to State-Space Methods," Dover Publications, New York, 1986.

[77] X. Karatzia, "Horizontal stiffness and damping of piles in inhomogeneous soil," *Journal of Geotechnical and Geoenvironmental Engineering, vol 143(4),* 2017.

[78] J. Wang, "Horizontal impedance of pile groups considering shear behavior," *Soils andFoundations, Volume 54(5),* pp. 927-937, 2014.

[79] X. Wang, "A review on recent advancements of substructures for offshore wind turbines," *Energy Conversion and Management 158,* pp. 103-119, 2018.

[80] F. Castelli, "Simplified Approach for the Seismic Response of a Pile Foundation," *Journal of Geotechnical and Geoenvironmental Engineering, Vol 135(10),* pp. 1440-1451, 2009.

[81] A. Markou, "Nonlinear soil-pile interaction for offshore wind turbines," *Wind Energy, vol. 21(7),* pp. 558-574, 2018.

[82] I. Lam, "Soil Structure Interaction of Bridges for Seismic Analysis," Multidisciplinary Center for Earthquake Engineering Research, New York, 2000.

[83] A. Pecker, "Earthquake Foundation Design," in *Advanced Earthquake Engineering Analysis. CISM International Centre for Mechanical Sciences, vol 494*, Vienna, Springer, 2007, pp. 33-42.

[84] J. Gutierrez, "A substructure method for earthquake analysis of structures including structure-soil interaction," *Earthquake Engineering and Structural Dynamics, Vol. 6,* pp. 51-

69, 1978.

[85] M. Li, "Influence of soilestructure interaction on seismic collapse resistance of super tall buildings," *Journal of Rock Mechanics and Geotechnical Engineering, vol. 6,* pp. 477-485, 2014.

[86] A. Boominathan, "Soil–Structure Interaction Analysis of Pile Foundations Subjected to Dynamic Loads," in *Geotechnics for Natural and Engineered Sustainable Technologies. Developments in Geotechnical Engineering*, Singapore, Springer, 2018, pp. 45-61.

[87] D. Pitilakis, "Soil structure interaction modeling using equivalent linear soil behavior in the substructure method (Doctoral dissertation)," Ecole Centrale Paris, Paris, 2006.

[88] C. Fu, "An Effective Substructure Analysis for Soil-Structure Interaction," in *5th International Conference on Civil Engineering and Transportation*, Guangzhou, 2015.

[89] Gazetas, "Seismic soil structure interaction: new evidence and emerging issues," *Geotechnical Earthquake Engineering and Soil Dynamics, ASCE, 2,* pp. 1119-1174, 1988.

[90] K. E. a. W. R., "The spring method for embedded foundations," *Nuclear Engineering and Design 48,* pp. 377-392, 1978.

[91] E. a. W. R. Kausel, "The spring method for embedded foundations," *Nuclear Engineering and Design 48,* pp. 377-392, 1978.

[92] D. Basu, "Analysis of laterally loaded piles in multi layered soil deposits," Purdue University, West Lafayette, 2008.

[93] M. Capatti, "Experimental and numerical study on the full scale behaviour of micropiles under lateral loading (Doctoral dissertation))," Universita Politecnica delle Marche, Ancona, 2017.

[94] L. Reese, Single piles and pile groups under lateral loading, Rotterdam: Balkema, 2001.

[95] K. Miura, "IISEE-UNESCO Earthquake Engineering Course," Hiroshima University, Hiroshima, 2011.

[96] J. Bardet, Experimental soil mechanics, Upper Saddle River: Prentice-Hall, 1997.

[97] D. Coduto, Foundation design: Principles and practices (2nd edition), Upper Saddle River: Prentice-Hall, 2001.

[98] G. Anoyatis, "Dynamic pile impedances for laterally–loaded piles using improved Tajimi and Winkler formulations," *Soil Dynamics and Earthquake Engineering vol.92,* pp. 279-297, 2017.

[99] I. Prowell, "Assessment of wind turbine seismic risk: existing literature and simple study of tower moment demand. Report SAND2009-1100," Sandia National Laboratories Albuquerque, New Mexico, 2009.

[100] Prowell, "Modeling the Influence of Soil Structure Interaction on the Seismic Response of a 5MW Wind Turbine," in *5th International Conference on Recent Advances in Geotechnical Earthwake Engineering and Soil Dynamics*, San Diego, California, 2010.

[101] J.-S. Wu, Analytical and Numerical Methods for Vibration Analyses, ProQuest Ebook Central: John Wiley & Sons, 2013.

[102] J. Häfele, "An improved two-steps soil structure interaction modeling method for dynamical analyses of offshore wind turbines," *Appliead Ocean Research,* vol. 55, pp. 141-150, 2016.

[103] S. Suhail, "Modeling and Analysis of Soil-Pile Interaction for Dynamic Loading-A Review," in *Soil Dynamics and Soil-Structure Interaction for Resilient Infrastructure*, Cham, Springer, 2017.

[104] E. Rovithis, "Dynamic stiffness and kinematic response of single piles in inhomogeneous

soil," *Bulletin of Earthquake Engineering,* pp. 1949-1972, 2011.

[105] M. Novak, "Dynamic stiffness and damping of piles," *Canadian Geotechnical Journal,* vol. 11, no. 4, pp. 574-598, 1974.

[106] G. Mylonakis, "Lateral Vibration and Internal Forces of Grouped Piles in Layered Soil," *Journal of Geotechnical and Geoenvironmental Engineering,* vol. 125, no. 1, pp. 16-25, 1999.

Appendix 1: Ground motion influencing a generic model

In order to determine how a prescribed ground motion influences a dynamic structural system when considering soil structure interaction. First, a simple mode considering 2 DOF is considered. Afterwards, the procedure is extrapolated to a more complex N DOF system.

Two degree of freedom system

For a 2 DOF system, the problem is visualized in the following figure. The mass in the right m_s represents the mass of the structure; meanwhile the mass in the left m_i represents the interface DOF of the system, located between the soil and the structure. This interface mass is attached to the ground considering a soil spring k_i (stiffness) and a soil dashpot c_i (damping). The ground motion is prescribed at the end of these elements, to consider the influence of the soil in the response of the system. Finally, the mass of the structure is excited by an external force F_e.

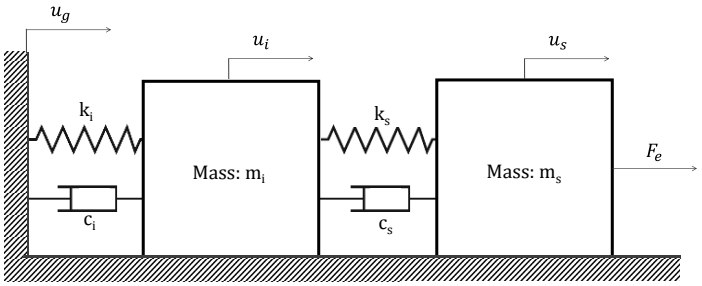

The dynamic behavior of the system can be estimated by writing the EOM of each DOF; for the structure:

$$m_s\ddot{u}_s + c_s(\dot{u}_s - \dot{u}_i) + k_s(u_s - u_i) = F_e \tag{0-1}$$

For the interface DOF:

$$-k_s u_s - c_s\dot{u}_s + m_i\ddot{u}_i + (c_s + c_i)\dot{u}_i + (k_s + k_i)u_i = c_i\dot{u}_g + k_i u_g \tag{0-2}$$

Writing these EOM in a matrix form:

$$\begin{bmatrix} m_s & 0 \\ 0 & m_i \end{bmatrix}\begin{bmatrix} \ddot{u}_s \\ \ddot{u}_i \end{bmatrix} + \begin{bmatrix} c_s & -c_s \\ -c_s & c_s + c_i \end{bmatrix}\begin{bmatrix} \dot{u}_s \\ \dot{u}_i \end{bmatrix} + \begin{bmatrix} k_s & -k_s \\ -k_s & k_s + k_i \end{bmatrix}\begin{bmatrix} u_s \\ u_i \end{bmatrix} = \begin{bmatrix} F_e \\ 0 \end{bmatrix} + \begin{bmatrix} 0 & 0 \\ 0 & c_i \end{bmatrix}\begin{bmatrix} 0 \\ \dot{u}_g \end{bmatrix} + \begin{bmatrix} 0 & 0 \\ 0 & k_i \end{bmatrix}\begin{bmatrix} 0 \\ u_g \end{bmatrix} \tag{0-3}$$

It is possible to isolate the structural terms from the interface/ground terms, meaning:

- Mass matrix: $\mathbf{M_s} = \begin{bmatrix} m_s & 0 \\ 0 & m_i \end{bmatrix}$
- Velocity vector: $\dot{\mathbf{u}} = \begin{bmatrix} \dot{u}_s \\ \dot{u}_i \end{bmatrix}$
- Structural damping matrix: $\mathbf{C_s} = \begin{bmatrix} c_s & -c_s \\ -c_s & c_s \end{bmatrix}$
- Acceleration vector: $\ddot{\mathbf{u}} = \begin{bmatrix} \ddot{u}_s \\ \ddot{u}_i \end{bmatrix}$
- Interface damping matrix: $\mathbf{C_i} = \begin{bmatrix} 0 & 0 \\ 0 & c_i \end{bmatrix}$
- Ground displacement vector: $\mathbf{u_i} = \begin{bmatrix} 0 \\ u_g \end{bmatrix}$
- Structural stiffness matrix: $\mathbf{K_s} = \begin{bmatrix} k_s & -k_s \\ -k_s & k_s \end{bmatrix}$
- Ground velocity vector: $\dot{\mathbf{u}}_\mathbf{i} = \begin{bmatrix} 0 \\ \dot{u}_g \end{bmatrix}$
- Interface stiffness matrix: $\mathbf{K_i} = \begin{bmatrix} 0 & 0 \\ 0 & k_i \end{bmatrix}$
- External forces vector: $\mathbf{f} = \begin{bmatrix} F_e \\ 0 \end{bmatrix}$
- Displacement vector: $\mathbf{u} = \begin{bmatrix} u_s \\ u_i \end{bmatrix}$

Writing eq. (2-6) using this format:

$$\mathbf{M_s}\,\ddot{\mathbf{u}} + (\mathbf{C_s} + \mathbf{C_i})\,\dot{\mathbf{u}} + (\mathbf{K_s} + \mathbf{K_i})\mathbf{u} = \mathbf{f} + \mathbf{C_i}\dot{\mathbf{u}}_\mathbf{i} + \mathbf{K_i}\mathbf{u_i}$$

Defining a load vector due to the ground motion acting on the structure through the interface DOF:

$$\mathbf{f_i} = \mathbf{C_i}(\dot{\mathbf{u}}_\mathbf{i} - \dot{\mathbf{u}}) + \mathbf{K_i}(\mathbf{u_i} - \mathbf{u})$$

Using this interface load vector:

$$\mathbf{M_s}\,\ddot{\mathbf{u}} + \mathbf{C_s}\,\dot{\mathbf{u}} + \mathbf{K_s}\mathbf{u} = \mathbf{f} - \mathbf{f_i}$$

Multiple degree of freedom system

This equation can be extrapolated for the general case, where the DOF corresponding to the structure are clearly differentiated from the DOF corresponding to the interface (soil structure interaction), meaning:

- Mass matrix: $\mathbf{M_s} = \begin{bmatrix} \mathbf{M_{ss}} & \mathbf{M_{si}} \\ \mathbf{M_{is}} & \mathbf{M_{ii}} \end{bmatrix}$
- Structural damping matrix: $\mathbf{C_s} = \begin{bmatrix} \mathbf{C_{ss}} & \mathbf{C_{si}} \\ \mathbf{C_{is}} & \mathbf{C_{ii}} \end{bmatrix}$
- Interface damping matrix: $\mathbf{C_i} = \begin{bmatrix} \mathbf{0} & \mathbf{0} \\ \mathbf{0} & \mathbf{C_{soil-ii}} \end{bmatrix}$
- Structural stiffness matrix: $\mathbf{K_s} = \begin{bmatrix} \mathbf{K_{ss}} & \mathbf{K_{si}} \\ \mathbf{K_{is}} & \mathbf{K_{ii}} \end{bmatrix}$
- Interface stiffness matrix: $\mathbf{K_i} = \begin{bmatrix} \mathbf{0} & \mathbf{0} \\ \mathbf{0} & \mathbf{K_{soil-ii}} \end{bmatrix}$
- Displacement vector: $\mathbf{u} = \begin{bmatrix} \mathbf{u_s} \\ \mathbf{u_i} \end{bmatrix}$
- Velocity vector: $\dot{\mathbf{u}} = \begin{bmatrix} \dot{\mathbf{u}}_\mathbf{s} \\ \dot{\mathbf{u}}_\mathbf{i} \end{bmatrix}$
- Acceleration vector: $\ddot{\mathbf{u}} = \begin{bmatrix} \ddot{\mathbf{u}}_\mathbf{s} \\ \ddot{\mathbf{u}}_\mathbf{i} \end{bmatrix}$
- Ground motion vector: $\mathbf{u_i} = \begin{bmatrix} \mathbf{0} \\ \mathbf{u_g} \end{bmatrix}$
- Ground velocity vector: $\dot{\mathbf{u}}_\mathbf{i} = \begin{bmatrix} \mathbf{0} \\ \dot{\mathbf{u}}_\mathbf{g} \end{bmatrix}$
- External forces vector: $\mathbf{f} = \begin{bmatrix} \mathbf{F_e} \\ \mathbf{0} \end{bmatrix}$
- Load vector: $\mathbf{f_i} = \mathbf{C_i}(\dot{\mathbf{u}}_\mathbf{i} - \dot{\mathbf{u}}) + \mathbf{K_i}(\mathbf{u_i} - \mathbf{u})$

The corresponding EOM reads exactly the same as:

$$\mathbf{M_s}\,\ddot{\mathbf{u}} + \mathbf{C_s}\,\dot{\mathbf{u}} + \mathbf{K_s}\mathbf{u} = \mathbf{f} - \mathbf{f_i}$$

This is the EOM of a system where the ground motion is applied considering the properties of the soil structure interaction. Some remarks:

- The ground motion acts on the structure through the soil spring and dashpot (which connect the structure to the ground). The spring is activated by the relative displacement between the DOF corresponding to the interface and the ground, meanwhile the dashpot is activated by the relative velocity.
- Even when the interface DOF is not being excited directly by the ground acceleration, does not receive the acceleration, the inertia force at this DOF is included since the mass of is considered in the response.

It is adequate to work with the ground velocities and displacements when considering soil structure interaction, even though the ground motion signal is commonly provided as acceleration.

Appendix 2: Kinematic and inertial interaction

Kinematic and inertial interaction

The kinematic interaction effect is the result from the stiffness difference between the pile and the surrounding soil. If the pile would not be installed, the soil particles would follow the pattern induced by the wave propagation (denominated as the free field motion). In the other hand, when the pile is installed, its flexural stiffness prevents it from following the free field motion, trying to modify the soil displacements at zones close to the pile shaft. Additionally, the motion of the soil surrounding the pile produces loads on it.

It is interesting to analyze the influence of the frequency component of the free field motion acting on the pile. The following figure [61].shows two cases, case a) shows a pile subjected to a high-frequency free field motion, whereas b) shows the same pile subjected to a low frequency free field motion.

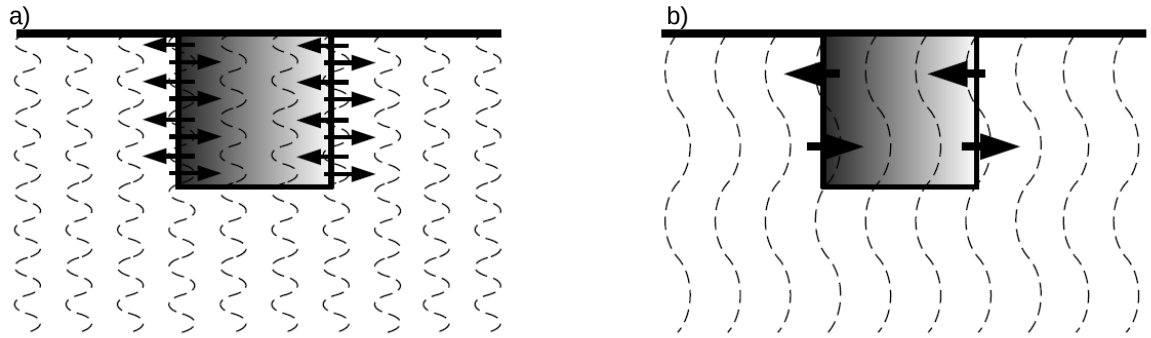

For case a), the kinematic load on the pile is cancelled out, leaving t unaffected by the motion. In case b) it is clear that the motion is not cancelling out, inducing the pile to rock and to translate. If the kinematic interaction motion is calculated at the pile head, a swaying (lateral) and a rocking (rotation) motion will be found, even when the free field motion is perfectly horizontal [61].

The kinematic interaction motion in a vertical pile, originated from a horizontal propagated free field motion depends on (basically) the predominant wavelength relative to the embedded length of the pile. For high frequency motions with wavelength considerable small relative to the length of the embedded pile, the contribution of the kinematic interaction motion can be neglected. In the other hand, if the embedded part of the pile is comparable to the wavelength of the free field motion, then should be taken into account.

The inertial interaction effect is related to the activation of the superstructure, originated from the kinematic interaction motion and the inertial forces developed within the structure. Two main features arise from this interaction. Firstly an elongation of the natural vibration period of the system analyzed, and the introduction of damping (both radiation and soil hysteretic damping) [61]. These two features are introduced to the system by including the frequency dependent dynamic impedances matrix.

Appendix 3: Free field motion step by step calculation

This Appendix contains the step by step procedure to obtain the free field motion for a given uniform soil profile.

The free field motion can be calculated by writing down the equation of motion (EOM) governing this shear wave propagation along the soil profile [41] [48]. For a small element like the one shown in he following figure the situation reads:

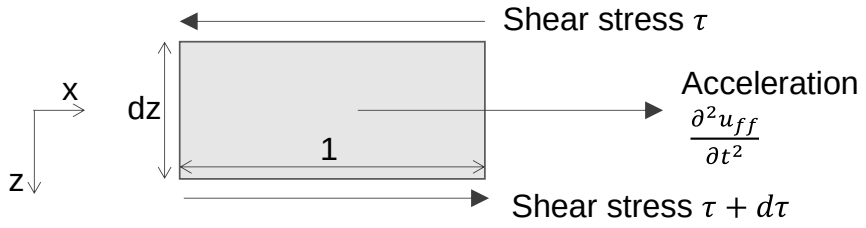

$$\rho \frac{\partial^2 u_{ff}}{\partial t^2} = \frac{\partial \tau}{\partial z}$$

Where u_{ff} is the horizontal displacement, ρ represents the mass density of the soil, τ is the shear stress in a horizontal plane at the top and bottom of the analyzed soil element. Note that lateral normal stresses are not included. This is due to the assumption of an idealized vertical propagation creating a constant stress in the x direction; therefore the normal stresses that are present at both sides of the element cancel each other.

The linear kinematic relation is defines the shear strain by:

$$\gamma = \frac{\partial u_{ff}}{\partial z}$$

A linear constitutive law including material dissipation η_s (Kelvin-Voigt model) can be written as:

$$\tau = G_s \gamma + \eta_s \frac{\partial \gamma}{\partial t}$$

Where the material dissipation depends on the damping ξ and on the frequency:

$$\eta_s = \frac{2 G_s \xi}{\omega}$$

It is possible to write the EOM of the displacement caused by the shear wave being propagated in the vertical direction by combining Eq. (2-4), Eq. (2-5) and Eq. (2-6).

$$\rho_s \frac{\partial^2 u_{ff}}{\partial t^2} = G_s \frac{\partial^2 u_{ff}}{\partial z^2} + \eta_s \frac{\partial^3 u_{ff}}{\partial z^2 \partial t}$$

Two boundary conditions are assumed for this problem:

1) Zero shear stress at the mudline (z=0):

$$\tau(0, t) = 0$$

2) Acceleration compatibility at soil bedrock interface (z=H):

$$\left. \frac{\partial^2 u_{ff}}{\partial t^2} \right|_{z=H} = a_g(t)$$

Assuming a harmonic solution for the lateral displacement, and a steady state regime:

$$u_{ff}(t) = U_{ff}(z, \omega) e^{i\omega t}$$

Considering this solution on the EOM previously defined in (2-7):

$$-\rho_s\omega^2 U_{ff}(z,\omega)e^{i\omega t} - G_s\frac{\partial^2 U_{ff}(z,\omega)}{\partial z^2}e^{i\omega t} - i\omega\eta_s\frac{\partial^2 U_{ff}(z,\omega)}{\partial z^2}e^{i\omega t} = 0$$

This can be re written as:

$$(G_s + i\omega\eta_s)\frac{\partial^2 U_{ff}(z,\omega)}{\partial z^2} + \rho_s\omega^2 U_{ff}(z,\omega) = 0$$

Defining a damped shear wave velocity:

$${c_s}^{*2} = \frac{G_s + i\omega\eta_s}{\rho_s}$$

The EOM can be rewritten as:

$$\frac{\partial^2 U_{ff}(z,\omega)}{\partial z^2} + \frac{\omega^2}{{c_s}^{*2}}U_{ff}(z,\omega) = 0$$

A general solution to this equation can be found:

$$U_{ff}(z,\omega) = B_1 e^{-i\frac{\omega}{{c_s}^*}z} + B_2 e^{i\frac{\omega}{{c_s}^*}z}$$

Applying this general solution into the boundary condition at the surface defined in equation (2-8):

$$G_s\frac{\partial U_{ff}(z,\omega)}{\partial z}\bigg|_{z=0} + i\omega\eta_s\frac{\partial U_{ff}(z,\omega)}{\partial z}\bigg|_{z=0} = 0$$

The boundary condition at the interface soil stratum-bedrock defined in equation (2-9):

$$-\omega^2 U_{ff}(H,\omega) = A_b \xrightarrow{yields} U_{ff}(H,\omega) = -\frac{A_b}{\omega^2}$$

Note that the ground motion at the bedrock is assumed to be:

$$a_g(t) = A_g e^{i\omega t}$$

This implies:

$$\frac{\partial U_{ff}(z,\omega)}{\partial z}\bigg|_{z=0} = 0$$

Replacing the general solution in the BC:

$$B_1 e^{-i\frac{\omega}{{c_s}^*}0} + B_2 e^{i\frac{\omega}{{c_s}^*}0} = 0 \xrightarrow{yields} B_1 = B_2$$

The BC rewritten considering the general solution:

$$B_1 e^{-i\frac{\omega}{{c_s}^*}H} + B_2 e^{i\frac{\omega}{{c_s}^*}H} = -\frac{A_g}{\omega^2}$$

Considering the exponential representation for the cosine function:

$$\cos(x) = \frac{e^{ix} + e^{-ix}}{2} \xrightarrow{yields} B_1 2\cos\left(\frac{\omega H}{{c_s}^*}\right) = -\frac{A_g}{\omega^2}$$

Leads to:

$$B_1 = -\frac{A_g}{2\omega^2}\frac{1}{\cos\left(\frac{\omega H}{{c_s}^*}\right)} = B_2$$

Therefore, the general solution can be written as:

$$U_{ff}(z,\omega) = -\frac{A_g}{2\omega^2}\frac{1}{\cos\left(\frac{\omega H}{{c_s}^*}\right)}e^{-i\frac{\omega}{{c_s}^*}z} - -\frac{A_g}{2\omega^2}\frac{1}{\cos\left(\frac{\omega H}{{c_s}^*}\right)}e^{i\frac{\omega}{{c_s}^*}z}$$

Meaning:

$$U_{ff}(z,\omega) = -\frac{A_g}{\omega^2}\frac{\cos\left(\frac{\omega z}{{c_s}^*}\right)}{\cos\left(\frac{\omega H}{{c_s}^*}\right)}$$

The ground motion (acceleration) at the bedrock can be written by:

$$A_g(\omega) = -\omega^2 U_g$$

Finally, the lateral displacement of the propagated shear wave, or free field ground motion (at every frequency and depth) can be found as a function of the ground motion (displacement) at the bedrock:

$$U_{ff}(z,\omega) = U_g(\omega)\frac{\cos\left(\frac{\omega z}{{c_s}^*}\right)}{\cos\left(\frac{\omega H}{{c_s}^*}\right)}$$

It is possible to determine the natural frequencies of the soil profile analyzed. When the denominator is equal to zero, resonances take place, meaning

$$\cos\left(\frac{\omega H}{{c_s}^*}\right) = 0$$

When considering no damping on the soil, this is accomplished for:

$$\omega_n = \frac{n\pi}{2H}\sqrt{\frac{G_s}{\rho_s}}$$

With n=1, 3, 5, 7…
Written in terms of the frequency:

$$f_n = \frac{n}{4H}\sqrt{\frac{G_s}{\rho_s}}$$

These frequencies are identified as the natural frequencies of the soil profile, and they determine the frequencies for which the complete soil profiles experiments resonance.

These calculations are applicable to calculate the free field motion along the soil profile considering only a single stratum. The same calculations can be performed for a multilayer soil profile, which are out of the scope of this work. However, this procedure can be can be consulted in the literature referred [17], [50].